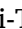




Overview of fundamental aspects of natural circulation loops[☆]

M. Hashemi-Tilehnoe^{a, }, M. Misale^{b, }, Seyyed Masoud Seyyedi^{c, d}, E. Palomo del Barrio^{a, e}, A. Marchitto^b, S.S. Rahim Hosseini^c, M. Sharifpur^{f, g}

^a Centre for Cooperative Research on Alternative Energies (CIC energiGUNE), Basque Research and Technology Alliance (BRTA), Alava Technology Park, Albert Einstein 48, 01510 Vitoria-Gasteiz, Spain

^b DIME Department of Mechanical, Energy, Management and Transportation Engineering, Thermal Division, University of Genoa, Via All'Opera Pia 15-a, (I), 16145 Genova, Italy

^c Department of Mechanical Engineering, Ali.C., Islamic Azad University, Aliabad Katoul, Iran

^d Energy Research Center, Aliabad Katoul Branch, Islamic Azad University, Aliabad Katoul, Iran

^e IKERBASQUE Basque Foundation for Science, Plaza Euskadi 5, 48009 Bilbao, Spain

^f School of Mechanical, Industrial and Aeronautical Engineering, University of the Witwatersrand, Private Bag 3, Wits 2050, South Africa

^g Department of Medical Research, China Medical University Hospital, China Medical University, Taichung, Taiwan

ARTICLE INFO

Keywords:

Natural circulation
Passive cooling
Instability analysis
Supercritical CO₂
Emergency cooling system

ABSTRACT

Natural Circulation Loops (NCLs) offer a passive method for heat transfer and eliminate the need for mechanical pumps. They play a critical role in energy applications such as solar heaters, geothermal power plants, emergency cooling systems, heat-driven refrigerators, heat exchangers, advanced nuclear reactors, and oscillating heat pumps. Technological advancements have opened opportunities to enhance NCL performance, focusing on cost reduction, energy efficiency, minimizing oscillations, and improving system reliability. Special attention is directed toward the dynamics of single-phase and two-phase flows, with investigations into the thermal-hydraulic performance of NCLs using various working fluids and configurations. This review evaluates experimental setups and simulation techniques, including the lattice Boltzmann method (LBM), computational fluid dynamics (CFD), and system codes, identifying the strengths and limitations of current modeling approaches. A particular focus is given to supercritical CO₂, heavy liquid metals, and molten salts as working fluids, underscoring their potential to enhance heat transfer efficiency while reducing operational risks compared to traditional fluids like water. Key trends and challenges in NCL design are explored, particularly concerning the improvement of safety and efficiency of next-generation passive thermal energy storage and cooling systems in solar power plants and advanced modular reactors. The insights from this review aim to guide future research in addressing the limitations of current technologies and furthering the development of robust and efficient passive safety systems.

1. Introduction

With increasing global demand for energy efficiency and reliability, the development of passive thermal management systems has gained significant attention. Among these, Natural Circulation Loops (NCLs) stand out as simple, reliable systems that operate without mechanical pumps, using buoyancy-driven flow for heat transport. Their application spans a wide range of fields, including solar thermal systems, nuclear reactor safety, geothermal energy, electronics cooling, and space technologies. NCLs exhibit complex thermofluidic behavior despite their conceptual simplicity, particularly under transient or high-power conditions. These behaviors include flow reversals, oscillations, and

stability thresholds, which are critical to their performance and reliability. Understanding and predicting these phenomena requires a solid grasp of fundamental principles, including momentum and energy balance, frictional losses, buoyancy dynamics, and thermal feedback mechanisms.

The crucial sections of a natural circulation system typically consist of the heater, a heat sink (cooler), and pipelines that create a closed loop with a working fluid to allow continuous circulation. The fluid circulates due to buoyancy forces generated by thermal density differences, which occur as heat transfers from the heating source to the cooling section, typically positioned higher than the heat source. One significant advantage of this system is that it operates without mechanical pumps, thereby lowering the risk of failure and minimizing both maintenance

[☆] This article is part of a special issue entitled: 'HD Oscillating Systems' published in Applied Thermal Engineering.

E-mail addresses: mhashemi@cicenergigune.com (M. Hashemi-Tilehnoe), mohsen.sharifpur@up.ac.za (M. Sharifpur).

<https://doi.org/10.1016/j.applthermaleng.2025.126936>

Received 19 November 2024; Received in revised form 19 May 2025; Accepted 23 May 2025

Available online 26 May 2025

1359-4311/© 2025 Elsevier Ltd. All rights are reserved, including those for text and data mining, AI training, and similar technologies.

Nomenclature	
\dot{m}	mass flow rate (kg/s)
C_p	specific heat ($Jkg^{-1}K^{-1}$)
$\frac{D}{Dt}$	material derivative operator
f	friction factor (–)
g	gravitational acceleration (ms^{-2})
Gr_m	modified Grashof number (–)
k	thermal conductivity ($Wm^{-1}K^{-1}$)
p	pressure (Pa)
P	power of heater (W)
Pr	Prandtl number (–)
q''	heat flux (Wm^{-2})
q'''	volumetric heat source (Wm^{-3})
Re	Reynolds number (–)
S_t	Stanton number (–)
T	temperature (K or °C)
U	overall heat transfer coefficient ($Wm^{-2}K^{-1}$)
\vec{V}	velocity vector ($m s^{-1}$)
V	Volume (m^3)
W	mass flow rate ($kg s^{-1}$)
z	vertical direction coordinate
Z	dimensionless vertical direction coordinate (–)
<i>Greek Letters</i>	
α	inclination angle (° – degree)
β	thermal expansion coefficient (K^{-1})
Δ	mass flow rate (kg/s)
ε	effectiveness (–)
θ	dimensionless temperature (–)
μ	dynamic viscosity (Pa.s)
π	pi number (–)
ρ	Density ($kg m^{-3}$)
σ	stability parameter
τ	dimensionless time
Φ	dissipation function
ω	dimensionless mass flow rate
<i>Acronyms</i>	
CNCL	Coupled Natural Circulation Loop
DBA	design basis accident
DHR	The hot helium rises up to the cooler
EH	Temperature Heater
ESM	Entropic Stability Map
FIHTD	Flow-induced heat transfer deterioration
HLM	Helium Liquid Metal
MSNCL	Molten Salt Natural Circulation Loop
N_{pch}	phase change number
LBE	Lead-Bismuth Eutectic
IED	Information Entropy Difference
IESA	Information Entropy Stability Analysis
RNC	reverse natural circulation
UPBEAT	Universal lead (Pb) bismuth (Bi) Eutectic Advanced Test loop
<i>Subscripts-superscripts</i>	
avg	Average
c	Cooler
cl	Cold leg
h	heater
H	heated
L	Cooled
hl	Hot leg
max	Maximum
ss	Steady state
t	total length/volume
–	Average

and operating expenses. NCLs can be categorized based on the type or phase of the working fluid. The performance of an NCL can be prone to instability during these transients, a subject that has been of ongoing interest to researchers [1]. The initial studies on the performance of NCLs date back to the 1960 s to 1980 s, with significant contributions from Keller (1966) [2], Welander (1967) [3], and Chen (1985) [4]. Further notable research includes the extensive work by Vijayan [5], and Misale and Tagliafico [6]. Zvirin and Greif [7] suggested an approximate technique for expecting the transient behavior of the system. Interactions between friction and buoyancy forces can destabilize the flow, resulting in oscillations and reversals. Consequently, system instability becomes a critical factor limiting the applications of NCLs [8]. From the other side, due to frequent velocity fluctuations, the flow regime in an unstable NCL often alternates among laminar, transitional, and turbulent states, making the laminar-turbulent transition impact more pronounced in oscillating NCLs [9]. Examining the dimensions of the heater, cooler, material properties, and the type of working fluid used in NCLs has garnered considerable attention from researchers. Corresponding to the recorded evidence and simulation data, the CFD model developed can be reliably applied to simulate the phenomenon of natural circulation. The reliability of the thermal-hydraulic passive safety systems, such as core makeup tanks, elevated tank NCL, sump reservoir natural circulation, along with uncertainty of calculations of thermal-hydraulic phenomena in the new generation of nuclear reactors like AP1000 and NuScale SMRs, as well as non-water cooled reactors (e. g. gas-cooled, liquid metal cooled, molten salt cooled, and fusion reactors) were comprehensively evaluated. These assessments ensure the safe operation and effective emergency response conditions under

various levels of defense in depth (DID) [10–13]. As we know, liquid metals and molten salts, recognized as high-temperature working fluids in fast nuclear reactors, accelerator-driven systems, molten salt reactors, and solar thermal energy storage systems. The key fundamental studies on NCL employing heavy liquid metals and molten salts have been extensively reviewed in prominent works by Borgohain et al. [14], Agbevanu et al. [15], Roper et al. [16], and D'Auria and Giorgio [17]. Researchers like Misale worked on mini-loops previously [18]. However, in recent years, researchers such as Seyyedi et al. [19] assessed the functioning of a rectangular mini NCL by Cu-water working fluid by considering the impacts of active parameters. In recent years, researchers have turned their attention to open NCL-based parabolic trough collectors. Researchers like Nakul and Arunachala [20] have demonstrated that the stability and consistency of solar heating systems can be improved by establishing an NCL for heat removal. In 2023, Nakul et al. [21] conducted an analytical-experimental stability analysis for a low aspect ratio NCL combined with a parabolic trough collector (PTC). The findings determined that using a single-phase high heat capacity NCL in PTCs shows promise as a replacement for conventional forced circulation receivers. Furthermore, the current characteristics of a supercritical NCL under a periodic power profile, despite its promise of attractive dynamics, have not been examined in open literature. In this context, Srivastava and Basu [22] examined the dynamic characteristics of a supercritical NCL under periodic excitation. Advances in computational and experimental techniques have brought new insights into NCL performance, yet a comprehensive review is needed to consolidate these findings. The use of secondary fluids such as CO₂ (instead of water) is another topic that warrants further research. This consideration can

even be extended to nanofluids. Thus, it is essential to explore whether other fluids can serve as better alternatives to water, while using secondary fluids other than water may have disadvantages. In summary, although natural circulation loops are conceptually simple, their real-world performance is governed by a set of complex and

interdependent physical mechanisms. This complexity has made NCLs a persistent challenge in thermal-fluid sciences, especially in high-stakes applications like nuclear safety or high-efficiency solar thermal systems. Several core challenges consistently appear in literature, regardless of working fluid, geometry, or scale:

Table 1

Summary of studies on NCLs in the past decades.

Author	Year	Experimental Facility	Analytical Approach	Numerical Approach	Direct Comparison with Experimental Data
Misale and Frogheri [23]	1999	L1 loop	No	Finite difference, RELAP5	Yes
Ambrosini and ferreri [24]	2003	1-D Loop	Yes	Finite difference	No
Mousavian et al. [25]	2004	L1 loop	No	Finite difference, RELAP5	Yes
Chatoorgoon et al. [26]	2005	NCL with SC-H2	No	CFD (Fluent), RELAP5	No
Vijayan et al. [27]	2007	BARC loop	Yes	Finite difference	No
Pilkhwil et al. [28]	2007	BARC loop	No	GENLOOP, RELAP5, CFD (Fluent)	No
Devia and Misale [29]	2012	L2 loop	No	CFD (Fluent)	Yes
Wang et al. [30]	2013	Water Loop	No	CFD (Fluent)	Yes
Naphade et al. [31]	2013	HANS-LBE	Yes	CFD (PHOENICS)	Yes
Sharma et al. [32]	2013	BARC Loop	Yes	NOLSTA Code	Yes
Kang et al. [33]	2013	liquid gallium NCL	Yes	CFD, MARS	Yes
Martelli et al. [34]	2014	L3 loop	Yes	CFD (Fluent), RELAP5	Yes
Lu et al. [35]	2014	TALL facility-LMNCL	Yes	TRACE, MATLAB	Yes
Yadav et al. [36]	2015	Loop with exchangers	Yes	CFD (ANSYS (FLUENT) 14.5)	No
Kudariyayar et al. [37]	2016	BARC loop	No	CFD (Fluent)	Yes
Luzzi et al. [38]	2016	L2 loop	Yes	CFD (OpenFOAM)	Yes
Kudariyayar et al. [39]	2016	MSNCL	Yes	CFD	Yes
Krishnani and Basu [40]	2016	Water	Yes	CFD	No
Srivastava et al. [41]	2016	MSNCL	Yes	CFD, in house code	Yes
K.S Sarkar and Basu [42]	2017	Supercritical CO2 loop	No	CFD (Fluent), RELAP5	Yes
Shin et al. [43]	2017	HELIOS MSNCL	Yes	MARS-LBE	Yes
Nadella et al. [44]	2017	Water	Yes	1D Modeling – SiPhN/LSA	Yes
Yue et al. [45]	2017	KYLIN-II, LBE	Yes	CFD (Fluent)	Yes
Inampudi et al. [46]	2018	Loop with exchangers	No	CFD (Fluent), OpenFOAM	Yes
Braz Filho et al. [47]	2018	Test Loop	Yes	RELAP5/3D	Yes
Yadav et al [48]	2018	NCL with end Heat Exchangers	Yes	CFD (Fluent), RELAP5	No
Seyyedi et al [49].	2019	AKIAU-R-1P loop	Yes	CFD (Fluent), RELAP5	Yes
Hashemi-Tilehnoee et al. [1]	2019	AKIAU-R-1P loop	Yes	Fluent and RELAP5	Yes
Akhil Dass and Gedupudi [50]	2019	1-D Loop	Yes	ANSYS Fluent 16.1	No
Li et al. [51]	2019	NCL With Rod Bundles	Yes	RELAP5	Yes
Dipankar N. Basu [52]	2019	Test Loop	Yes	Numerical model	No
Chouhan et al. [53]	2019	MSNCL	Yes	OpenFoam	Yes
Liu et al. [54]	2020	MK1 PB-FHR	Yes	RELAP5-3D	No
Tlili et al. [55]	2020	AKIAU-R-1P	Yes	MATLAB	No
Raveesh et al. [56]	2020	Loop with orifice	No	ANSYS FLUENT 19.0	Yes
Misale et al. [57]	2020	Loops with a small inner diameter	Yes	Experimental analysis	No
Srivastava et al. [58]	2020	Supercritical loop	Yes	Finite-Difference Method	No
Hariyanto et al. [59]	2020	Two NCLs with a vertical height	Yes	Experimental and simulation approach – CFD (COMSOL Multiphysics)	Yes
Yun et al. [60]	2020	FINCLS	Yes	Lumped component method	Yes
Battistini et al. [61]	2021	DYNASTY experimental facility	Yes	OpenFOAM	No
Seyyedi et al. [19]	2021	AKIAU-R-1P	Yes	CFD (Fluent), RELAP5	No
Misale et al. [62]	2021	Two parallel NCL	Yes	Experimental Study	No
Elton et al. [63]	2021	Mini loop	Yes	CFD (OpenFOAM)	Yes
Das and Gedupudi [64]	2021	Mini loop	No	CFD (Fluent), ANSYS CFX	Yes
Jinshah B.S et al. [65]	2021	SPNCL	No	Experimental	Yes
Geng et al. [9]	2021	toroidal loop	Yes	CFD – ANSYS Fluent	No
Schriener et al. [66]	2021	LBE NCL	Yes	Numerical code	Yes
Hariyanto et al. [67]	2022	VHHC Loop	Yes	CFD – COMSOL Multiphysics	Yes
Dass and Gedupudi [68]	2022	Coupled Natural Circulation Loop	Yes	CFD (ANSYS FLUENT 16.1)	No
Cai et al. [69]	2022	PKL Facility Reverse NC	Yes	CFD-RELAP, CATHARE, ATHLET, TRACE	Yes
Gao et al. [70]	2023	1U CubeSat	Yes	CFD	No
Sahu et al. [71]	2023	NCL	Yes	Experimental	Yes
Bozkr et al. [72]	2023	SPNCL	Yes	CFD (COMSOL Multiphysics)	No
Bocanegra et al. [73]	2023	Square NCL	Yes	Numerical – Lattice Boltzmann Method	No
Subramaniyan et al. [74]	2024	CNCL	Yes	Fourier series based 1-D model	No
Angelo et al. [75]	2024	VHVC Loop	Yes	CFD – Ansys Fluent	Yes
Boopalan et al. [76]	2024	VHHC SCO ₂ Loop	Yes	Numerical – CFD Analysis	No
Li et al. [77]	2024	UPBEAT	Yes	Numerical Analysis	Yes

- Instability and oscillatory behavior.
- Laminar-turbulent transition in buoyancy-driven Flow.
- Multiphase and supercritical behavior.
- Limited predictive capability of numerical models.
- Lack of systematic design guidelines.
- Underexplored integration with emerging systems.

By synthesizing these challenges, this review seeks to clarify where the current limitations lie (like loop orientation, fluid choice, and geometry) and to guide the development of more robust modeling approaches, experimental campaigns, and design methodologies for future passive heat transfer systems based on advanced NCL-based technologies.

So, this review is intended to serve both experienced researchers and new entrants to the field. By presenting a layered structure-tarting from basic principles, followed by classification, instability analysis, and then advanced topics. We aim to build a coherent picture of how NCLs are currently understood, modeled, and applied. To provide a consolidated perspective on the development of NCL studies, Table 1 presents a curated list of representative experimental and numerical investigations from the past three decades. The works are categorized based on the type of loop, analytical or numerical approach, and whether experimental validation was performed. This table is not merely a list; instead, it reflects key methodological trends, such as the early reliance on 1D lumped models, the progressive shift toward CFD tools (e.g., Fluent, OpenFOAM), and the ongoing challenge of achieving direct correlation between simulations and experiments. Particular attention is drawn to the dominant use of water-based loops until the recent surge in studies involving supercritical CO₂, molten salts, and liquid metals. The increasing complexity of loop geometries, including multi-loop and coupled systems. The use of codes like RELAP5, TRACE, and MARS, particularly in nuclear applications, and the emerging use of LBM or other codes in academic research. Readers should interpret this table not as a comprehensive database, but as a strategic sampling of influential work that highlights shifts in both technology and research priorities in the field of natural circulation.

From the data in Table 1, several insights emerge:

- Model diversity: Even for similar experimental setups, different modeling approaches yield varying results, underscoring the need for model validation and benchmarking datasets.
- Reliability of CFD tools: While tools like Fluent and COMSOL are popular, quantitative agreement with experimental data is still inconsistent. Full-loop simulations with transient and multiphase capabilities remain challenging.
- Gap in Multiphysics studies: Only a few studies integrate thermal, hydraulic, and structural behaviors, a key requirement for next-generation NCL-based systems.
- Need for generalized design principles: Most studies are case-specific. Very few papers provide general insights or dimensionless groups (e.g., modified Grashof or Stanton numbers) that could aid future design.

These observations reinforce the need for more systematic investigations, better reporting of operating conditions, and cross-validation between tools to build a true predictive framework for NCLs.

2. Classification of natural circulation loops

Fig. 1 illustrates instances of NCL prototypes with a detailed highlighting of their purposes. Specifically, the figure shows the schematic of an NC solar water heater [78]. This configuration features water-saturated porous media as the working fluid. NCL for multichannel vertical systems with non-uniform heat inputs [79]. This system, depicted in a 2-D schematic, consists of two vertical legs with small sources of heating and cooling at the ends. Annular loop with a heated lower semi-circular section and a top section with fixed wall temperature [44]. This model emphasizes the use of external cladding to maintain a constant wall temperature. NCL with finite-length tubes and different thermal boundary conditions [80]. This configuration features heat sources equipped with finite-length tubes, imposing various thermal boundary conditions.

In the following, the main applications of NCLs in the industry are briefly presented. The extensive use of this technology has led researchers to focus more on improving the performance of NCLs in recent

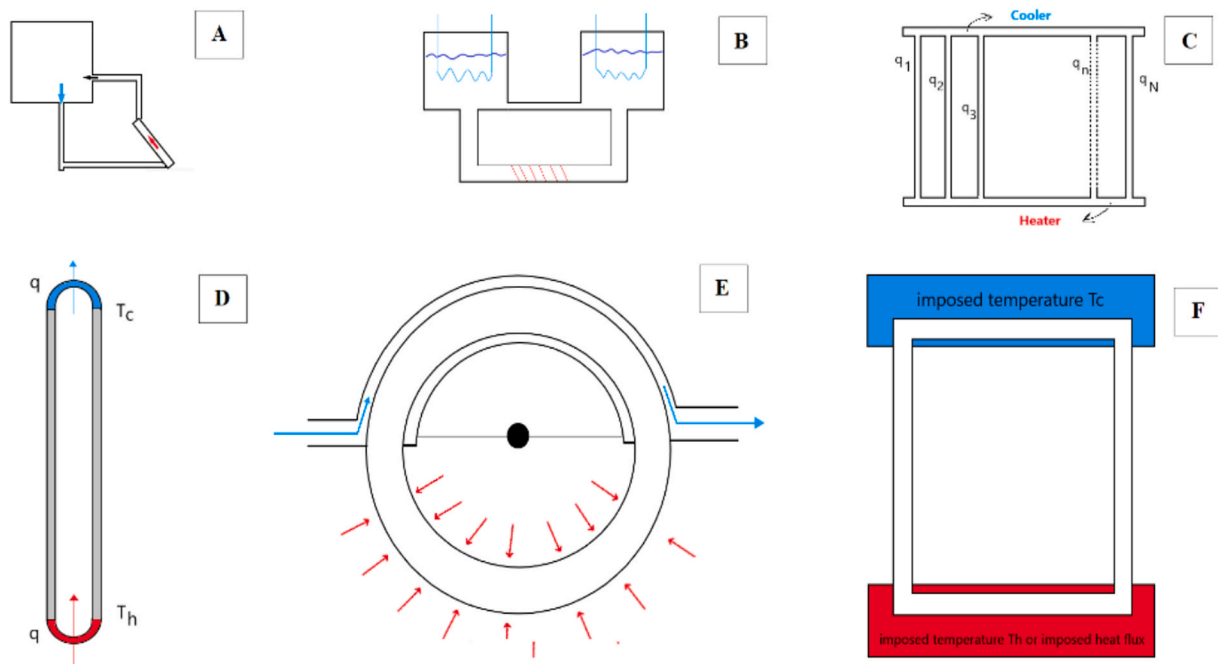


Fig. 1. Schematic arrangement of the natural circulation solar heater (A), A unique and novel feature of the loop [B] parallel-channel configuration with nonuniform sources for heating [C], two vertical legs with point sources of heat and sink [D], toroidal geometries of identical dimensions [E], heater has been replaced by finite length pipe[F] [81]. Copyright © Institute of Research Engineers and Doctors.

years. Various factors can influence this performance, including the material of the pipes, the dimensions, and positioning of the cooler and heater, or the type of working fluid. Fig. 2 provides a summary of the main industrial applications of NCLs.

The NCLs are generally divided into four main categories.

- HHHH (Horizontal Heater-Horizontal Cooler): This structure consists of both the cooler and heater positioned horizontally. It is often used in applications where space constraints require a more compact design.
- VHVC (Vertical Heater-Vertical Cooler): In this setup, both the heater and cooler are oriented vertically. This arrangement can enhance natural circulation due to the significant vertical height difference, leading to better thermal performance.
- HHVC (Horizontal Heater-Vertical Cooler): Here, the heater is placed horizontally, and the cooler is vertical. This combination can be beneficial in systems where the cooler needs to dissipate heat more effectively over a vertical surface.
- VHHH (Vertical Heater-Horizontal Cooler): In this configuration, the heater is vertical, and the cooler is horizontal. This setup is suitable for applications where vertical space for the heater is available, and the horizontal cooler can effectively manage heat removal.

Fig. 3 shows configurations of the four main types of NCLs. These configurations are tailored to specific industrial applications, including solar energy systems, nuclear reactors, geothermal energy extraction, and electronic equipment cooling, to optimize their thermal management and efficiency.

In addition to the four configurations mentioned above, NCLs can also be categorized into several other types. Detailed descriptions of these additional categories are provided below:

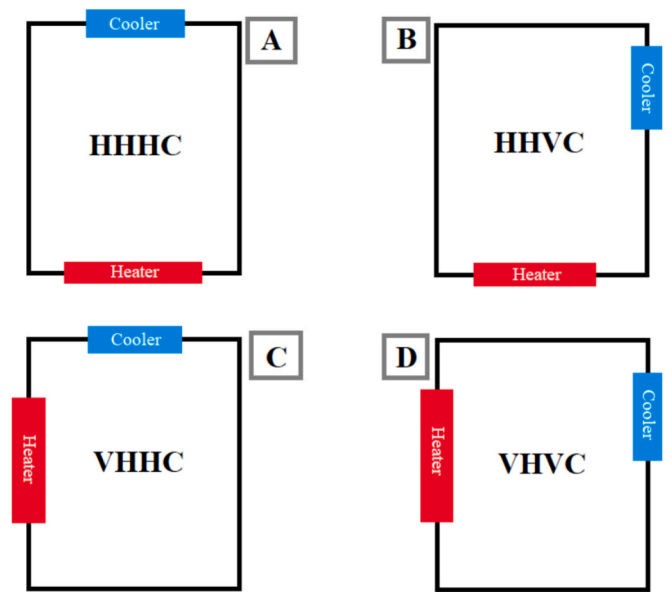


Fig. 3. Configurations of NCLs, including HHHH (A), HHVC (B), VHHH (C), and VHVC (D).

- Inclined Heater Inclined Cooler (IHIC): Can be unstable depending on the degree of inclination and the positioning. The work by Dass and Gedupudi [64] highlights that inclined configurations can experience heat transfer coefficient jumps and hysteresis, similar to cavity systems.
- Mixed Heater and Cooler: A combination where either the heater or cooler are positioned differently (e.g., one horizontal and one

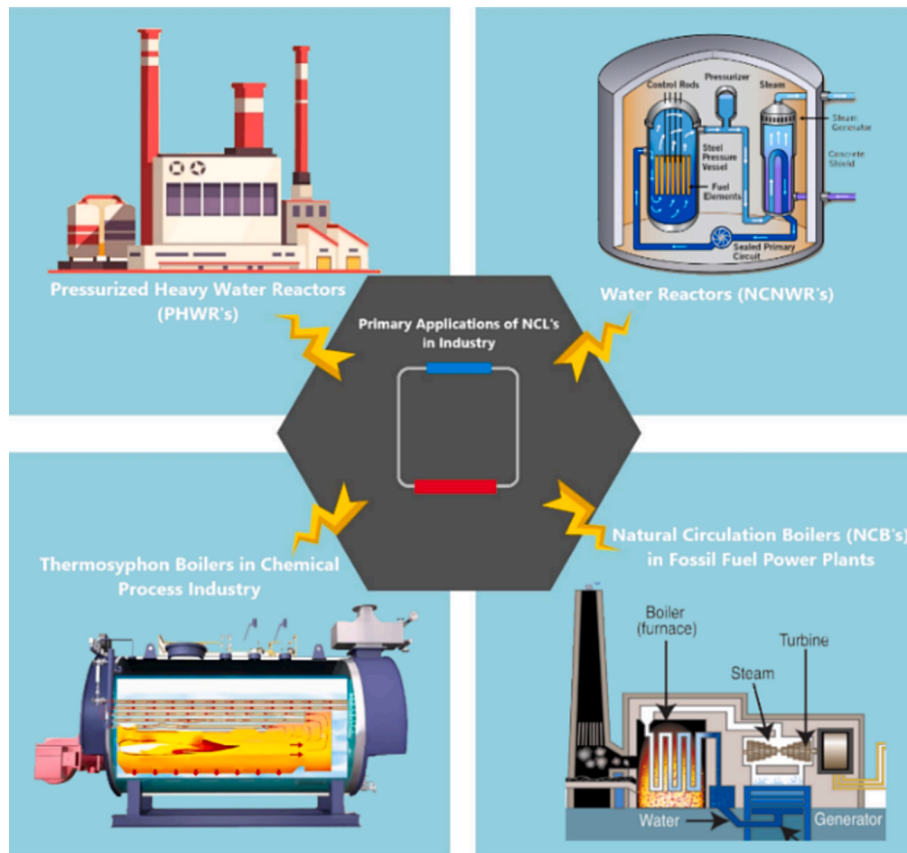


Fig. 2. The primary application of NCLs in the industry.

vertical). Varies are widely based on specific configurations and operational conditions. Mixed configurations can offer a balance between stability and spatial constraints.

- **Parabolic Trough Collector-Based NCL (PTC-NCL):** Generally, stable and provide enhanced thermal performance due to the concentrated solar input. Recent studies, like those by Nakul et al [20], have shown promising results in using PTC-NCL for solar thermal applications.

2.1. Current industry Preferences for using NCLs

The industry typically prefers configurations that offer a balance of stability, efficiency, and ease of integration into existing systems. The VHVC configuration is among the most stable and widely used, especially in nuclear power plant applications because of its reliability and predictability. The PTC-NCL configuration is gaining traction in the renewable energy sector for its ability to enhance thermal efficiency using solar energy. The next generation of parabolic collectors based on NCLs is considered a recent area of study among scientists. Based on the studies by Balasubramanian et al. [82], it was determined that initial radiation and geometrical configuration apply a substantial impression on the required period to start the flow circulation and the appearance of startup oscillations. Table 2 gives a brief overview of the phase of NCLs:

2.2. General Explanation of conservation equations in NCLs

The conservation equations perform a fundamental function in the analysis and design of NCLs. These equations cover three main parameters:

- **Conservation of Mass Equation:** This equation says that the fluid mass within the loop should be constant. In other words, the amount of fluid entering a section of the system must equal the amount of outlet fluid. This principle is crucial in the design and simulation of flow systems.
- **Conservation of Momentum Equation:** This equation deals with the forces acting on the flowing fluid. These forces include pressure forces, gravitational forces, and frictional forces. The conservation of momentum equation explains how changes in pressure and velocity of the fluid occur along the loop.
- **Conservation of Energy Equation:** This equation addresses the changes in energy within the system. The conservation of energy equation describes how thermal energy is transferred and transformed within the system.

Table 3 presents the fundamental equations used for analyzing NCLs, originating from the basic conservation laws. These equations are essential for understanding the dynamics and performance of NCLs under various operating conditions.

The governing equations are continuously and simultaneously solved in CFD simulations to predict the precise thermodynamic and hydraulic behavior of the NCL. Overall, the analysis of conservation equations is essential for designing and optimizing NCLs, as they help us understand the stability and performance under various operational conditions.

Table 2
Regime of working fluids in NCLs.

Type	Applications	Advantages	Instabilities
Single-phase	Domestic water heating systems, solar power plants, cooling systems like liquid metal cooled nuclear reactors	Simple and low-cost, easy maintenance	Less than two-phase; due to temperature differences
Two-phase	Nuclear power plants, industrial air conditioning systems, petrochemical industries	High efficiency in heat transfer, high heat transfer capability with small volume	More than single-phase; includes dynamic and thermal instabilities

3. Instability of NCLs: The main challenge for researchers

Studies on the dynamic behavior of NCLs under conditions such as startup, shutdown, and step power increases are rare. Additionally, nearly all studies have examined NCLs with operating pressure controlled by a tank (or pressurizer) that adjusts the mass inventory within the loop. However, there is a lack of numerical models for NCLs with fixed mass and without a tank, where the operating pressure varies. These loops are simpler in design, as they do not require a pressurizer, making them suitable for applications such as waste heat recovery systems, solar thermal systems, and similar technologies [44]. Table 4 presents scientific works conducted by researchers in the field of stability analysis of NCLs from the beginning to the present.

Analyzing the function of various geometrical factors at the designing stage is crucial [104]. CFD simulations provide excellent results for NCL configurations including VHVC, VHHC, and HHVC. Only in HHHC no stable flow mode exists, and the continuous transition from laminar to turbulent flow leads to deviations in results when using purely laminar or turbulent models compared to experimental data. During transient flow initiation, when the heater is activated, heat transfers from the heat source to the heat sink. Initially, the stream of the fluid is nearly stagnant, then heating causes fluid near the surface to rise and move toward the center, facilitating heat transfer through both conduction and natural convection. Continuous heating creates a “hot plug” that spreads axially along both sides of the heater (Fig. 4).

An NCL with a shorter height and smaller diameter exhibits better efficiency, transferring more input power to the heat sink. However, due to reduced buoyancy, the fluid has a lower velocity. An extended heater enhances heat exchange from the wall boundary to the fluid and stabilizes the circulation loop. Additionally, better thermal conductive wall materials effectively reduce large thermal gradients within the loop [37]. In newer studies, such as those by Srivastava and Basu [22], it has also been stated that the HHHC configuration is generally considered the most unstable orientation.

3.1. Thermo-hydraulic behaviors and stability analysis of single-phase NCLs

Most researchers have focused on large-scale systems optimization and analysis of their stability. In contrast, only a limited number of studies focus on NC in small-scale devices, primarily concerning two-phase flow where single-phase NCLs frequently demonstrate instability. Various thermo-hydraulic behaviors can occur in a single-phase NCL, such as steady state, neutrally stable, neutrally unstable, and unstable conditions. Fig. 5 provides a summary of these four general behaviors of NCLs. The thermal-hydraulic behavior of an NCL varies with several constraints such as the impact of thermal conductivity of the wall, heater power and inclination, heater and cooler orientation, loop stabilization by local pressure drop or nano-fluids, and geometric dimensions (mini loops). Instability arises from the interplay between buoyancy forces due to density differences and friction in the loop. Thermal dissipation and viscous dissipation appear to face any variation in mass flow rate. Indeed, any increase in flow rate results in increased friction and reduced buoyancy force. These opposing consequences might not be in phase, which could lead to overcompensation and eventually result in growing oscillations. Additionally, flow fluctuations are primarily caused by the formation of cold and hot density pockets

Table 3
Equations for NCL analysis (expression from the conservation laws).

Equations	Mathematical Formulation	Description	Refs.
Continuity	$\frac{\partial \rho}{\partial t} + \nabla \cdot (\rho \vec{V}) = 0$	conservation of mass in the system	[49]
Momentum	$\rho \left(\frac{\partial \vec{V}}{\partial t} + (\vec{V} \cdot \nabla) \vec{V} \right) = -\nabla p + \rho \vec{g}$	Navier–Stokes equation for incompressible flow	[83]
Energy	$\rho C_p \frac{DT}{Dt} \nabla \cdot (k \nabla T) + \beta T \frac{Dp}{Dt} + \mu \phi + q''$	conservation of energy, accounting for conductive and convective heat transfer as well as internal heat sources.	[49]
Modified Grashof Number	$Gr_m = \frac{g \beta \Delta T_{avg} D^2 H}{\nu^2} \cos \alpha$	Considers the mean temperature difference between the legs and loop inclination.	[84]
Reynolds Number	$Re_{ss} = \frac{4 \dot{m}}{\pi D \mu}$	Measures the ratio of inertial forces to viscous forces in the flow.	[85]
Modified Stanton Number	$St_m = \frac{4 Nu}{Re_{ss} Pr}$	The effects of heat sink temperature	[49]
Buoyancy vs. Friction Balance	$\rho g \beta T dx = \frac{n^2}{2p} \sum (f_i \frac{L_i}{D_i} + k_i) \frac{1}{A_i^2}$	Balances buoyancy force with friction in the loop	[57]
Heater Energy Balance	$\frac{\dot{m}}{\rho A_H} \frac{\partial T}{\partial x} = \frac{q}{c \cdot \rho A_H L_H}$	Energy balance in the heater	[57]
Adiabatic Condition	$\frac{\dot{m}}{\rho A_{leg}} \frac{\partial T}{\partial x} = 0$	Heat balance for an adiabatic condition at vertical legs	[57]
Cooler Energy Balance	$\frac{\dot{m}}{\rho A_{leg}} \frac{\partial T}{\partial x} = -\frac{U L_L (T - T_{sink})}{c \cdot \rho A_L}$	Energy balance at the cooler	[57]
Temperature Difference	$T_h - T_c = \frac{q}{c \cdot \dot{m}} = \frac{q}{c \cdot \rho A_H \cdot w}$	Relation between mean flow velocity and temperature difference between hot and cold legs	[57]
Mass Flow Rate	$\dot{m} = \frac{q}{c \cdot (T_h - T_c)}$	Formula for mass flow rate	[57]
Friction Factor	$f_i = \frac{64}{Re_{ss,i}}$	Relation of friction factor with Reynolds number	[57]
Integrated Buoyancy vs. Friction	$\int T dx = \frac{\dot{m}^2}{2 \cdot \rho^2 \cdot g \cdot \beta \cdot 0} \sum \frac{64}{Re_{ss,i}} \left(\frac{L_i}{D_i} \right) \frac{1}{A_i^2}$	Simplified form considering uniform diameter along the loop	[57]
Relationship of Temperature Difference	$T_h - T_c \propto \sqrt{\frac{128 \cdot q \cdot L / D}{\pi \cdot D^3 \cdot H \cdot g}} \cdot \sqrt{\frac{k}{(c \cdot \rho)^2 \cdot \beta}} \cdot Pr$	Relationship of temperature difference with fluid parameters (Prandtl number)	[57]
Reynolds Number	$Re_{ss} = \sqrt{\frac{16}{1284} \frac{4 \cdot q \cdot D \cdot H \cdot \rho^2 \cdot (\beta \cdot g)}{\mu^3 \cdot c \cdot \rho \cdot \pi \cdot N_G}} = 0.178 \cdot \sqrt{\frac{Gr}{Ng}}$	Reynolds number considering friction in NCL	[57]

that amplify over time within the system. Moreover, observing the initial transient flows with various orientations concluded that an NCL with a horizontal heater has a more oscillatory flow initiation than one with a vertical heater. Only the HHHC loop exhibited unstable behavior [81].

In the stability analysis of NCLs, stability maps are generated, clearly delineating the stable and unstable boundaries. In the nonlinear stability analysis, time-dependent equations are solved numerically using the finite difference method, which can encounter numerical instability issues. Notable studies in this area include the works of Vijayan et al. [28], Mousavian et al [25], and Hashemi-Tilehnoee et al. [49]. Misale [105] carried out an experimental investigation into how power steps affect the thermo-hydraulic behavior of NCLs. The most common dynamic instability is density wave oscillations, which occur due to buoyant driving forces influenced by pressure losses and the fluid density and temperature distribution. Under specific restrictions in the NCL, these fluctuations can grow over time, causing issues like flow reversal that significantly impact system reliability [63,95]. Bocanegra et al. [106] investigated the thermohydraulic behavior of NCLs with three altered working fluids. The working fluids used included deionized water (DW), FC-43, and an aqueous glycol solution in parallel NCLs (in a horizontal heater-horizontal cooler configuration). As shown in Fig. 6, an experimental setup consisting of three parallel NCLs was employed to evaluate the thermal-hydraulic performance of different working fluids.

The results suggest that thermal performance is significantly influenced by the properties of the working fluid, allowing effective cooling across various heat loads. The 1D model accurately describes the thermohydraulic performance of parallel NCLs for all tested fluids. Originally developed for a single loop, this model remains applicable due to negligible interaction effects in the complex NCL circuit (characterized by small internal diameters, parallel connections, and different working fluids). Krishnani and Basu [40] examined a three-dimensional

mathematical model of an NCL to systematically evaluate the pertinency of the Boussinesq approximation. Observations indicated that the loop demonstrates unstable behavior with increasing heating power and cooler temperature due to a decreasing in frictional resistances. The character of the unstable response can be significantly influenced by the sink temperature. They also emphasized that simulations using the Boussinesq approximation take considerably longer to capture the initiation of flow, and the relevant discrepancy with the other model is enhanced with heating power. The dynamical NCL system behavior is unstable for the considered power levels. The flow undergoes continuous reversal, as indicated by changes in the sign of the temperature difference through the heat source. At lower power levels, the temperature oscillations remain consistent. In contrast, with increasing energy, two distinct oscillation modes are discernible: frequent flow reversals and periods of oscillation around an average value, ultimately leading to reversing the flow. Those phenomena can be described by considering that an intensification in flow rate caused enhanced friction and a reduction in the overall buoyant force [105].

3.2. A comprehensive stability analysis framework for NCLs

The reliability of natural circulation loops is fundamentally limited by their tendency to exhibit oscillatory or reversing flow under certain conditions. To improve system stability without active control mechanisms, researchers have investigated a range of passive stabilization techniques, often integrated directly into the loop geometry. These include orifice plates, loop inclination optimization, non-circular cross-sections, and directional valves such as Tesla valves. Several studies have shown that loop inclination affects buoyancy-driven flow development and oscillation onset. For example, vertical heater–horizontal cooler (VHHC) configurations often display improved stability

Table 4
Summary of stability analyses for NCLs (HHHC configuration).

Publication date	Category	Inclination of the Loop (θ) / loop orifice (β)	Fluid	Input power	Consideration remarks
Welander (1967) [2]	Theoretical	–	Water	–	Stability is influenced by friction factors and buoyant forces.
Vijayan et al. (1995) [80]	Computational	–	Water	Up to 2 kW	The transition occurs at a lower power than observed experimentally.
Misale and Frogheri (1999) [23]	Experimental	$\beta = 6, 10, 14$ mm	Water	300–900 W	Smaller orifice shows lower oscillation
Misale and Frogheri (2001) [86]	Experimental	$\beta = 20, 40$ mm	Water	500—3400 W	Effect of orifice pressure drop
Chatoorgoon (2001) [87]	Computational	–	SCW	–	Flow-power curve with stability.
Cammarata et al. (2003) [88]	Theoretical	–	Water	–	Effect of diameter, aspect ratio, and heat input.
Mousavian et al. (2004) [25]	Experimental & Numerical	–	Water	100–1000 W	Stability map with RELAP5 simulation. No flow reversal was reported.
Chatoorgoon (2005) [89]	Computational	–	SCW, SCCO ₂ , SC-H ₂	1.1–1.8 MW	Flow-power curve and stability.
Misale et al. (2007) [18]	Experimental	$\alpha = 0^\circ, 30^\circ, 75^\circ$	Distilled water	2.5 – 25 W	Effect of the heater and cooler orientations. Recognizing stability zones and flow oscillations.
Vijayan et al. (2007) [27]	Experimental and theoretical	–	Water	0 – 1250 W	Effect of loop inclination and heating power.
Nayak et al. (2008) [90]	Experimental	–	Water – Al ₂ O ₃ , CuO, TiO ₂ nanofluid	100 – 600 W	Influence of operating procedure on stability threshold
Jain and Rizwan-Uddin (2008) [91]	Computational	–	Supercritical CO ₂	0.4–2 MW	Effect of inlet condition and flow-power curve.
Misale et al. (2011) [92]	Numerical and Experimental	–	Water and FC43	0.1 – 2.5 kW	By increasing the heat sink temperature, the circulation frequency smoothly increased, meaning that the fluid flowed faster inside the loop.
Swapnalee and Vijayan (2011) [93]	Theoretical and analytical	–	Water	225 – 3507 W	Stability analysis reported in the literature for single-phase loops is either for laminar or turbulent flows.
Misale et al. (2012) [84]	Experimental	$\alpha = 0^\circ$ and 75°	distilled water and Al ₂ O ₃	10–50 W	Stability analysis with varying inclination angles.
Basu et al. (2012) [94]	Experimental	–	Water	1000–5000 W	analysis of single-phase NCL, with constant heat flux heating and convective cooling.
Krishnani and Basu (2016) [40]	Computational	–	Water	0.5 – 2.5 kW	systematic appraisal of the viability of employing Boussinesq approximation during transient simulation of single-phase NCLs
Sarkar and Basu (2017) [42]	Computational	$\theta = 30^\circ, 60^\circ$ (XY and YZ plane)	Supercritical CO ₂	200–3000 W	Loop inclination affects stability. No flow reversal was reported.
Yadav et al. (2017) [48]	Computational	$\theta = 0^\circ, 30^\circ, 45^\circ$ (XY, YZ plane)	Supercritical CO ₂	End heat exchangers	Detailed analysis of loop inclination effects.
Krishnani and Basu (2017) [95]	Computational and Numerical	$\alpha = 15^\circ, 30^\circ, 45^\circ$ (XY plane)	Water	0.5 – 2.5 kW	Steady-state and heat transfer analysis.
Inampudi et al. (2018) [46]	Computational	$\theta = 0^\circ$ to 60° (YZ plane), 0° to 90° (XY plane)	Water and Supercritical CO ₂	End heat exchangers	Entropy generation is influenced by loop height and inclination.
Sadhu et al. (2018) [96]	Experiment	–	air-cooled supercritical CO ₂	0 – 0.5 kW	Effects of important operating parameters on the performance and safety of the loop are studied.
Nadella et al. (2018) [44]	Theoretical and analytical	–	Water	end heat exchangers	Non-linear analysis is performed with a 1D model to further validate the prediction of SiPhN/LSA.
Saha et al. (2018) [97]	Numerical	$\theta = 0^\circ$	Water	65–182 W	Heater power is a critical factor in influencing the dynamics of the system
Deng et al. (2019) [98]	Experimental and Computational	–	Supercritical CO ₂	1000 – 10000 W/m ²	Flow behavior with heat load is studied.
Seyyedi et al. (2019) [49]	Experimental and Analytical	$\theta = 0^\circ, 45^\circ, 75^\circ$ (YZ plane)	Water	250–1500 W	Flow rate reduced with inclination angle. Lower threshold identified.
Cheng et al. (2019) [99]	Experimental and theoretical	–	Distilled water	end heat exchangers	By fine-tuning the geometrical factors within the constraints of the 1D mathematical model, the system can achieve optimal flow conditions for the heater power and temperature difference.
Misale et al. (2020) [57]	Experimental analysis	–	distilled water	20 – 140 W	Optimizing both the heat sink temperature and the heat input is critical to maximizing the thermal efficiency of NCL systems
Tlili et al. (2020) [55]	Experimental	$\alpha = 0^\circ, 45^\circ, 75^\circ$ (XY plane)	hybrid nanofluid (Al ₂ O ₃ -Cu and water)	200–500 W	Stability is influenced by the inclination angle. Upper and lower thresholds were identified.
Elton et al. (2020) [100]	Experimental	–	Water	0 – 300 W	The loop geometry plays a crucial role in determining the stability and predictability of oscillatory behaviors in NCL systems
Raveesh et al. (2020) [56]	Computational	$\theta = 10^\circ, 20^\circ, 30^\circ$ (XY), $\beta = 0.5$	Water	500 W	Both the inclusion of an orifice and tilting the NCL result in a steady-state flow, but at a much lower flow rate. The system stabilizes, but the circulation is less effective due to increased resistance or disrupted buoyancy forces

(continued on next page)

Table 4 (continued)

Publication date	Category	Inclination of the Loop (θ) / loop orifice (β)	Fluid	Input power	Consideration remarks
Das and Gedupudi (2021) [64]	Computational	$\theta = 0^\circ$ to 90° (XY plane)	Air	$Ra = 1.6 \times 10^5$ to 6.4×10^5	Stability of mini loop under varying conditions.
Elton et al. (2021) [63]	Experimental	$\beta = 0.5, 0.6, 0.7, 0.9$	Water	150–1100 W	Stability and lower threshold identified.
Srivastava and Basu (2022) [101]	Numerical	$\theta = 0^\circ, 30^\circ, 45^\circ, 60^\circ$	Supercritical CO ₂	10–2500 W	Static and dynamical stability analysis of supercritical CO ₂ .
Nakul and Arunachala (2022) [20]	Numerical	$\beta = 0.5$ and $0.25, \theta = 15, 30$ and 45°	Dowtherm A	1 and 2.63 kW	The validated CFD model predicts bidirectional pulsating flow. To maintain stable and efficient operation, instability restraining techniques such as flow restrictors, loop tilt adjustments, or optimized control systems are essential to prevent or mitigate these instabilities.
Sahu et al. 2023 [71]	Experimental	$\theta = 0^\circ, 15^\circ, 30^\circ$ and 60°	Water and nanoparticles	200, 400, 600 and 800 W	This combination of Al ₂ O ₃ + MWCNT + TVP1 hybrid nano-oil enhanced heat transfer efficiency and minimized system irreversibility makes it an excellent choice for optimizing thermal systems
Srivastava et al. [102]	Experimental and analytical analysis	–	molten salt (NaNO ₃ + KNO ₃)	1–3 kW	Local pressure losses increase the lower threshold of instability
Nakul and Arunachala U C (2024) [103]	Numerical	$\beta = (0.7), (\theta = 4^\circ)$	Therminol VP 1	500 – 3600 W	Transient and steady-state analysis with Loop inclination
Srivastava and basu (2024) [22]	Numerical 1-D Loop	–	CO ₂	250 – 1600 W	As the system operates near a transition regime small irregularities begin to appear in the system's profile which shows increasing sensitivity to disturbances as it approaches the critical transition point.



Fig. 4. Cross-sectional view of temperature contour and velocity vector (a) at heater (b) at cooler [37]. Copyright © 2015 Elsevier Masson SAS.

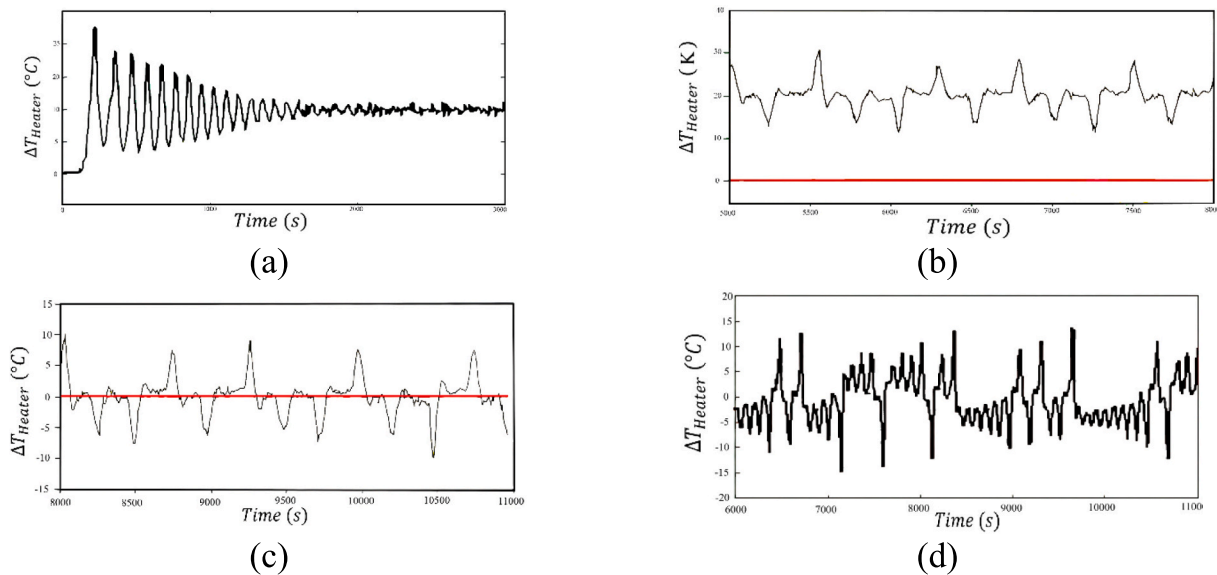


Fig. 5. Four dynamic behaviors of NCLs: (a) stable, (b) neutral stable, (c) neutral unstable, and (d) unstable [81]. Copyright © Institute of Research Engineers and Doctors.

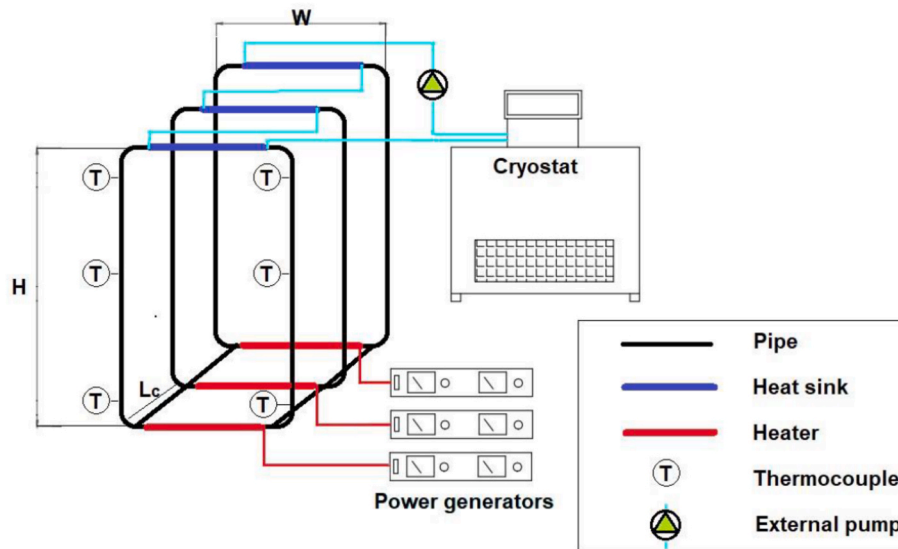


Fig. 6. Sketch of the experimental setup [106].Creative Commons Attribution 3.0 license, Published under license by IOP Publishing Ltd.

compared to horizontal heater–horizontal cooler (HHHC) setups. Adjusting the heater angle or using inclined loops can reduce the effective height difference or change the thermal stratification pattern, thereby reducing the likelihood of flow reversal. Seyyedi et al. [49] investigated the instability behavior of NCLs at three different angles: 0, 45, and 75 degrees, with various power steps. Based on the information

presented in this article, a comprehensive overview of the stability analysis for NCLs is provided. This analysis involves deriving dimensionless governing equations from fundamental conservation laws, specifically focusing on both momentum and energy equations. The equations address various factors, including buoyancy and friction effects and their dependency on the Reynolds number, to accurately model

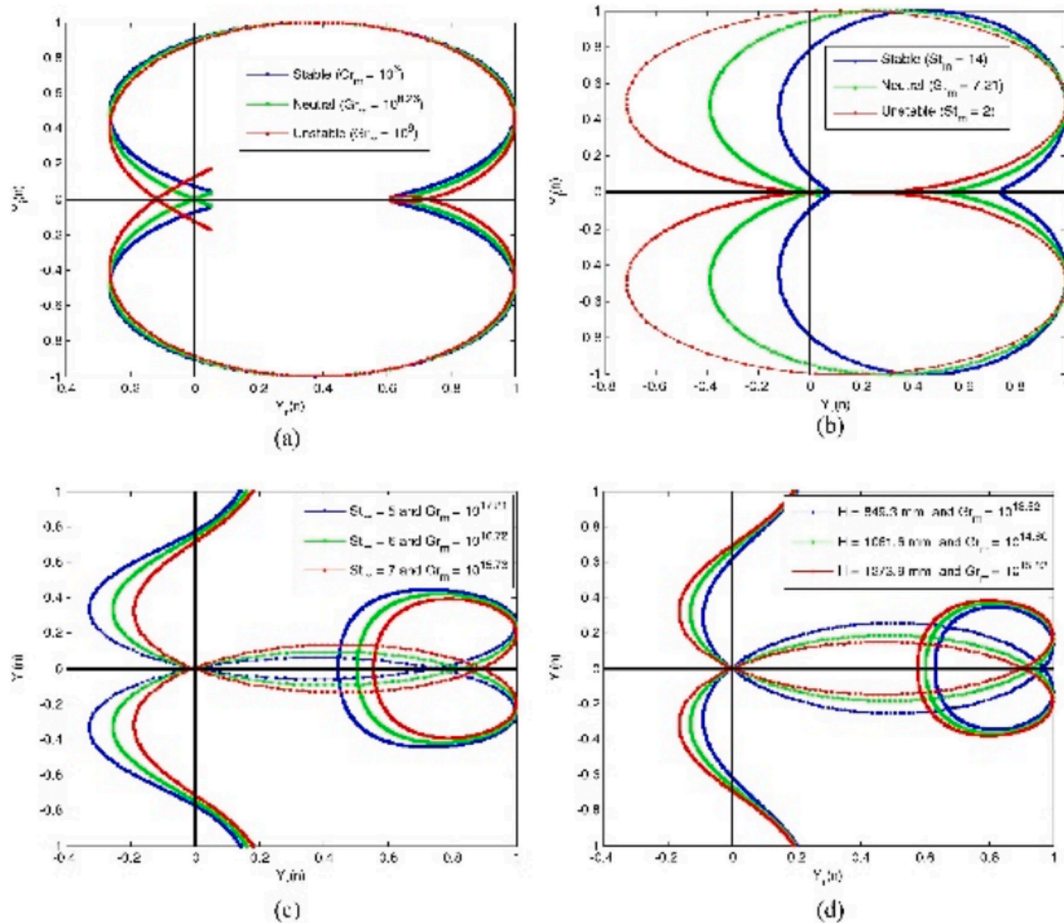


Fig. 7. Nyquist stability criterion plot; (a) changed modes in the different Gr_m , (b) changed modes in the different St_m , (c) neutral mode for unlike BCs, (d) neutral mode for different H . [49]. Copyright © 2018 with permission from Elsevier.

the behavior of NCLs. The article also highlights the transitions between laminar and turbulent flow regimes. A key aspect of the analysis is the use of a continuous friction factor equation, which is adapted for all flow regimes to ensure accurate predictions across different conditions. Furthermore, the stability analysis involves solving these governing equations to determine the complete behavior of the NCLs. Non-transient solutions provide insights into the system equilibrium conditions, while transient solutions offer an understanding of the system response to perturbations over time. The direct numerical solution of the nonlinear governing equations is commonly used to perform nonlinear stability analysis. Fig. 7 illustrates the application of the Nyquist stability criterion to assess the stability of the NCL. This figure shows plots for stable, neutral, and unstable modes using the Nyquist criterion. The Nyquist stability criterion is used to evaluate the system response to different heater powers and cooler temperatures, as expressed through the modified Grashof and Stanton numbers.

Fig. 7(a) shows Nyquist plot for a fixed modified Stanton number ($St_m = 10$) and varying Grashof numbers ($Gr_m = 10^6, 10^{8.26}, 10^9$) to show the system transitioning between stable, neutral, and unstable states. In the neutral state, the plot passes through the origin. In the stable mode, the origin is inside the curve, indicating no real positive roots, while in the unstable mode, the origin lies outside, signaling at least one real positive root. Fig. 7(b) Shows Nyquist plots for a constant Grashof number ($Gr_m = 10^8$) while varying the Stanton numbers. It indicates that increasing the Stanton number shifts the system toward stable behavior. Fig. 7(c) analyzes boundary conditions (varying Stanton numbers) and their impact on system stability. Fig. 7(d) Explores the effect of loop geometry (changing loop height) on stability. Both boundary conditions and geometric variations pass through the Nyquist origin at neutral stability. Saha et al. [97] analyzed the dynamical stability and instability behaviors of NCL systems. Their study revealed that the dynamic of the system can be categorized into three distinct regimes based on heater power. The system demonstrates stable steady-state behavior at heater power levels below 625 W. As power increases, the system transitions to an oscillatory flow regime up to 742 W. Beyond this point, flow reversal occurs within the loop. The resulting temperature difference creates a density difference, which drives fluid flow by balancing buoyancy and friction forces. The numerical analysis revealed that dynamical behavior can be classified into three distinct groups: stable steady-state, stable oscillatory flow, and flow reversal. While the heating power is within the oscillation range, the magnitude of oscillations for both the mass flow rate and the temperature difference is enhanced with rising heater power. In 2021, Akhil Das et al. [64] noted

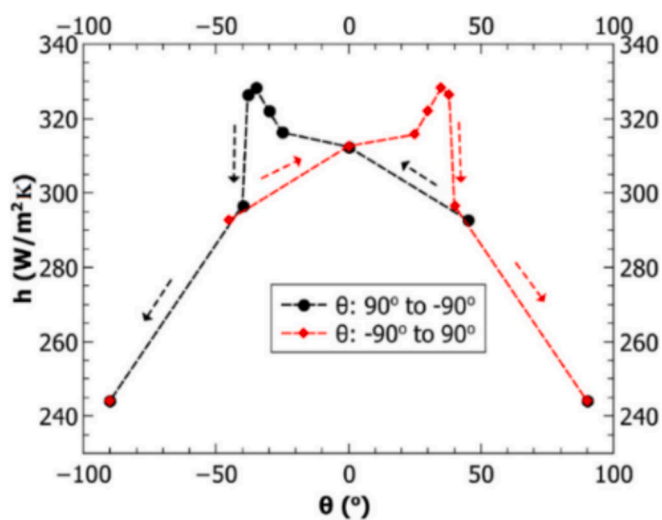


Fig. 8. The effect of inclination on the cooler heat transfer coefficient [64]. Copyright © 2020 with permission from Elsevier.

that, based on the available data. Fig. 8 illustrates the impact of inclined NCL on heat removal capability, highlighting the significant increase in the heat transfer coefficient and the related hysteresis behavior for the incline angle. The figure highlights that the reversal of flow direction is the primary cause of the heat transfer coefficient spike in NCL systems.

Regarding instability and its significance, it is worth reviewing the summary of studies by Goyal et al. [107]. In their study, a rectangular NCL was simulated to analyze both small and large perturbations, highlighting the significance of nonlinear stability analysis. Identifying the subcritical Hopf bifurcation and examining the effects of superior perturbations across different parameter spaces were the main objectives. The findings highlight that the tested conditions are risky for real-world NCL applications, as oscillations cannot be eliminated from practical systems. To ensure stability in practical applications, the system must remain stable for both small and large oscillations. This can be achieved by operating the system properly away from the stability boundary. In 2017, a new method was evaluated by Cammi et al. [108] against experimental data on natural circulation, utilizing a signal analysis approach grounded in information entropy to evaluate the stable condition of dynamical systems. Observer bias can affect the clustering of stability regimes in dynamic behavior analysis. The Information Entropy Signal Analysis (IESA) method addresses this by establishing a clear threshold for identifying dynamic behaviors, using sinusoidal signals that match the data points of experimental or numerical data. In this method, linear model signals show negative Information Entropy Deviation (IED) during stable transients, positive IED in nonstable regions (diverging signals), and zero IED for sinusoidal signals with constant amplitude. The IESA method effectively distinguishes between stable and unstable states, allowing an accurate assessment of signal convergence or divergence. To assess the stability characteristics of the L2 facility, different approaches have been employed, including both linear and nonlinear methods. Fig. 9 (a) and (b) offer a visual comparison between these methods and the semi-analytical stability map, providing insights into the accuracy and differences in stability predictions across various models.

In Fig. 9 (a), the linear Entropy Signal Model (ESM) is presented, derived from temperature perturbations at the heat sink to align with the information entropy analysis and the semi-analytical stability map. Stable conditions are indicated by regions with negative Information Entropy Deviation (IED) values (blue areas), while unstable conditions are marked by positive values (red areas). The line of iso-entropic, representing a bounded sinusoidal signal, delineates the transition between stable and unstable regions, closely matching the transition line of the semi-analytical approach. Fig. 9(b) illustrates the nonlinear ESM, calculated from temperature measurements at the cooler inlet for consistency with experimental data and linear signals. Regions showing negative IED values indicate stability, while instability is represented by positive or near-zero IED values (red areas), which include a negative bias observed in the temperature records. Adding orifices or local flow restrictions has been one of the simplest and most widely adopted methods to suppress oscillations. The orifice introduces a fixed pressure drop that increases flow resistance and dampens velocity fluctuations. Experiments by Elton et al. [63,100] demonstrated that the placement and size of these orifices significantly shift the instability threshold and effectively enlarging the stable operating regime. Fig. 10 demonstrates that the loop without an orifice became unstable above 100 W, while orifice configurations of $\beta = 0.9, 0.77,$ and 0.64 exhibited instability at higher power levels of 175 W, 210 W, and 325 W, respectively. The stability thresholds for the orifice configurations showed significant increases of 75 %, 110 %, and 225 % compared to the loop without an orifice, indicating improved stability at higher power levels. In the third operating procedure, the system remained stable at power levels below 185 W for $\beta = 0.9$, with the threshold ranging from 185 W to 200 W, as shown in the power distribution in Fig. 10(c).

Geng et al. [9] demonstrated several secondary flow phenomena to

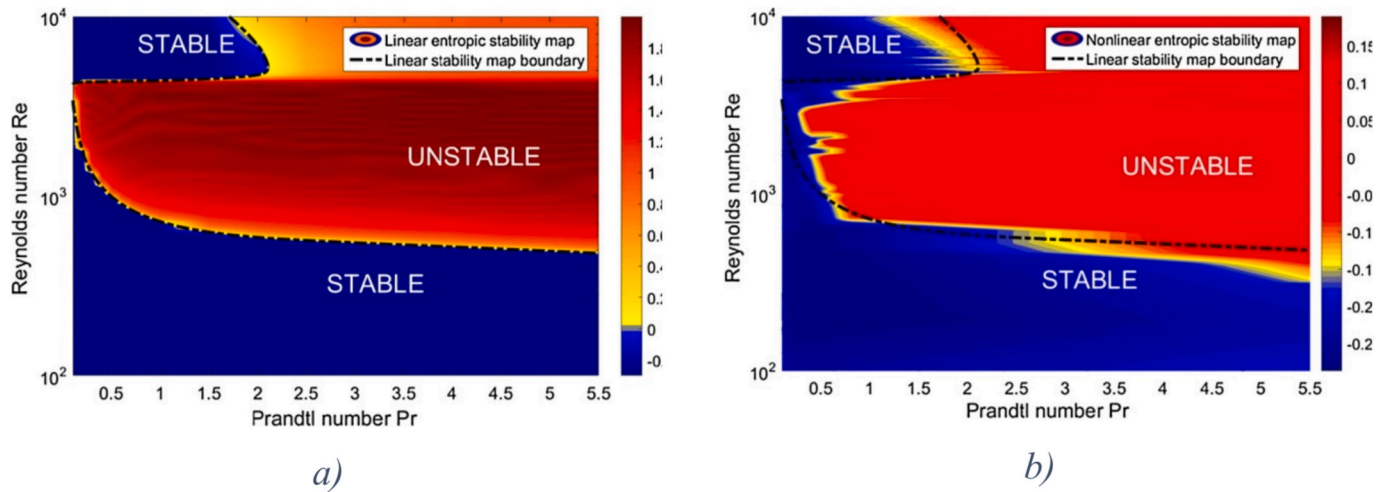


Fig. 9. (a) Entropy Signal Model of the L2 facility obtained with the a) linear method, b) nonlinear approach, and the semi-analytical method [108]. Copyright © 2017 with permission from Elsevier.

illustrate spatial non-uniformity. From the data shown in Fig. 11, it can be inferred that the NCL exhibits complicated flow field features.

A more recent innovation involves the use of Tesla valves, no-moving-part structures that create direction-dependent hydraulic resistance. Wahidi et al. [109] explored their integration into supercritical CO₂ NCLs, showing that such valves can significantly reduce flow reversal and dampen thermal oscillations. Fig. 12 shows the temperature and pressure field asymmetry under forward and reverse flow conditions.

In 2023, Bocanegra et al. [73] studied a single-phase NCL using the LBM. They developed a 2D-LBM utilizing dual distribution functions to simulate a quadrangle configuration NCL with constant temperatures at both the heat source and cooler in HHC loop. The average Nu is comparable to the experimental relationship for Re less than 200.

Fig. 13(a) illustrates the convergence of the loop to a steady state, displaying the ΔT_{avg} between the adiabatic vertical legs at various time-step iterations. At higher Re_{ss} and Ra values, the duration from rest to the onset of natural convection was reduced, leading to a decrease in the ΔT_{avg} between the legs. This pattern is in agreement with the conclusions of Cheng et al. [110], although an increase in the absolute ΔT_{avg} was reported in their work. Additionally, the transient behavior is associated with the previous conclusions of Garibaldi and Misale [111] for mini loops with small inner diameters where it is understood that the amplitude of fluctuations increases with higher heating power. A phase diagram in Fig. 13(b) illustrates the simultaneous convergence of velocity and temperature difference. Especially, a greater phase difference between the oscillations of temperature and velocity was observed at higher Re [73].

4. The impacts of sink temperature on the behavior of NCLs

One of the extremely important aspects in studying the structure of NCLs is certainly the assessment of the effects of the sink temperature. Stability maps are generally plotted based on the operational variables. In NCLs, the primary operational parameters are the values of heater power and the coolant flow rate in the cooler. In 2020, Devia and Misale [29] presented an experimental and numerical study focused on the thermal-hydraulic performance of an NCL, using Ansys Fluent. These types of systems are used in many engineering applications for thermal energy transfer. Unfortunately, under certain conditions, the system exhibits undesirable characteristics such as flow instability, including amplified oscillations due to reversing flow. The numerical analysis accurately estimates the amplitude and frequency of temperature oscillations and pressure difference fluctuations. Despite this minor

discrepancy, CFD results provide valuable insights, including flow velocity, local fluid speed, pressure drop, and other key data.

Fig. 14 shows a comparison of the temperature difference (a) and pressure difference (b) in the heater, aimed at comparing numerical results and experimental tests. The results indicated that mathematical modeling accurately forecasts the frequency and amplitude of pressure drops and temperature oscillations. However, it falls short of predicting the quantity of oscillations relating to consecutive flow reversals. In addition, whole tubes contribute significantly to the net immediate heat transfer, with the “adiabatic” sections accounting for up to 25 % of the total [29].

4.1. Analysis of an NCL with a horizontal adiabatic plate

In a study by Dai et al. [112], a numerical analysis of heat transfer was conducted on an NCL embedded within a horizontal adiabatic plate, with counterflowing hot and cold air at the bottom and top, respectively (see Fig. 15).

Findings reveal that, for an identical lateral length, the heat transfer rate of the NCL is lower than that of a copper fin. With an increase in both the size and temperature difference between the heating and cooling air, the heat transfer rate of the NCL becomes significantly higher, transferring up to 60 % more heat compared to a copper fin with a 50 mm lateral length. It is worth noting that a single-phase NCL may alternatively be replaced by a heat pipe or a two-phase NCL. The high latent heat and significant density difference between the liquid and gas phases during condensation and evaporation processes are expected to result in more efficient heat transfer enhancement. In Fig. 16, the normalized immediate temperature field along the loop is presented at different time intervals (17240 s – 18000 s) during a mass flow rate inversion. Each colored strip illustrates the temperature distribution within the loop, which has been cut and stretched for clarity. The first strip clearly shows the hot plug in the heater section and the cold plug in the cooler section. The subsequent strips illustrate the movement of the hot plug rising toward the cooler and the cold plug descending toward the heater [38].

5. Considering fluids other than water for increasing heat transfer of NCL

The selection of fluids other than water in NCLs has been a topic of much discussion among researchers over the past decade. For example, CO₂ is a natural working fluid that is non-flammable and non-toxic, making it a safe alternative to traditional HCFCs, CFCs, ammonia, and

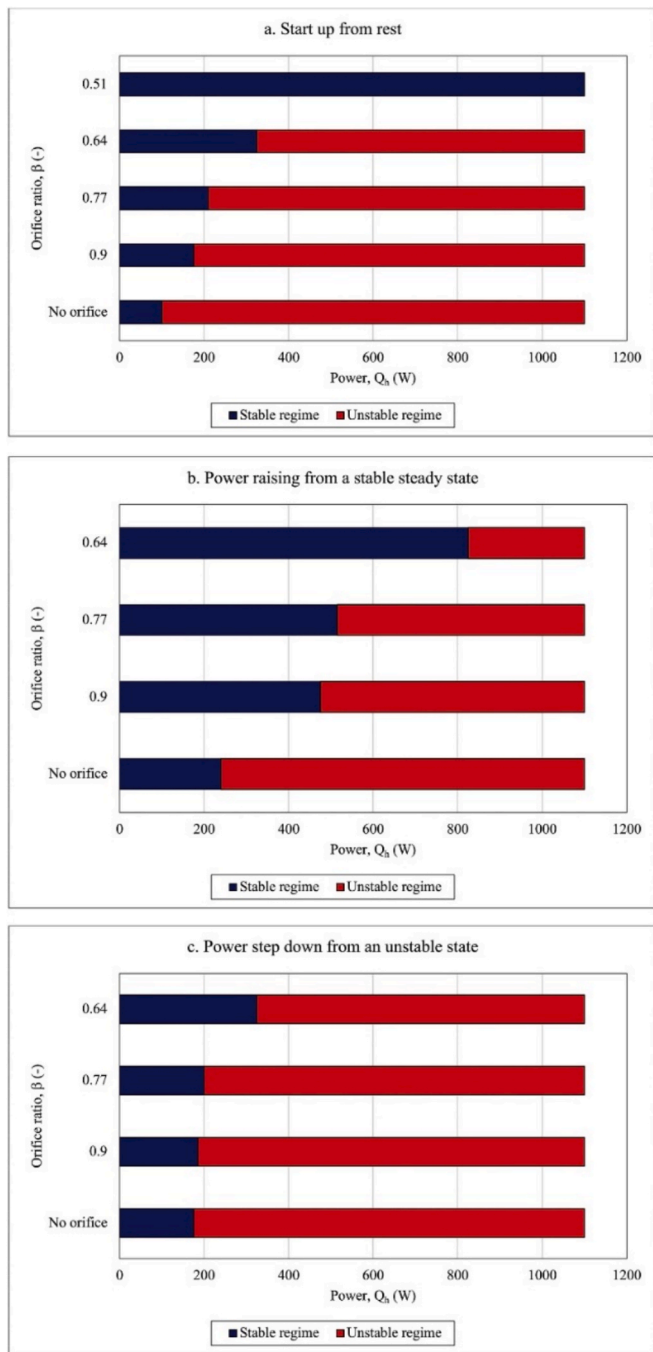


Fig. 10. Diagram of stability regime for startup from rest (a) power raising from a stable steady state (b) and power step down from an unstable state (c) [63]. Copyright © 2021 with permission from Elsevier.

hydrocarbons in various applications [83]. For more details, you can refer to Fig. 17. This figure illustrates the carbon cycle, highlighting the significant role of CO₂ in natural processes. This image is included to emphasize the importance of understanding CO₂ dynamics in the context of NCLs. The study of NCLs with alternative working fluids such as CO₂ is crucial for improving energy efficiency and reducing environmental impacts. By exploring the behavior of CO₂ within these systems, researchers can develop more sustainable and effective solutions for heat transfer applications, thereby contributing to the broader goal of managing carbon emissions and mitigating climate change. This figure serves as a reminder of the interconnectedness of natural and engineered systems and the potential benefits of integrating CO₂ into

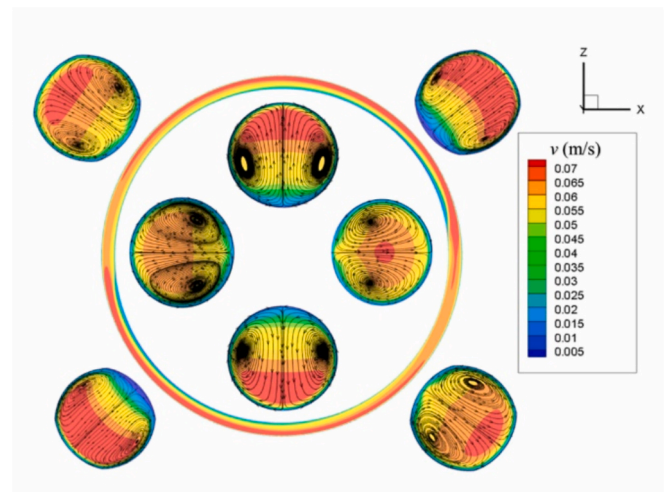


Fig. 11. Spiraling streamlines of eight angular sections for toroidal loop [9]. Copyright © 2023 Korean Nuclear Society. Published by Elsevier B.V.

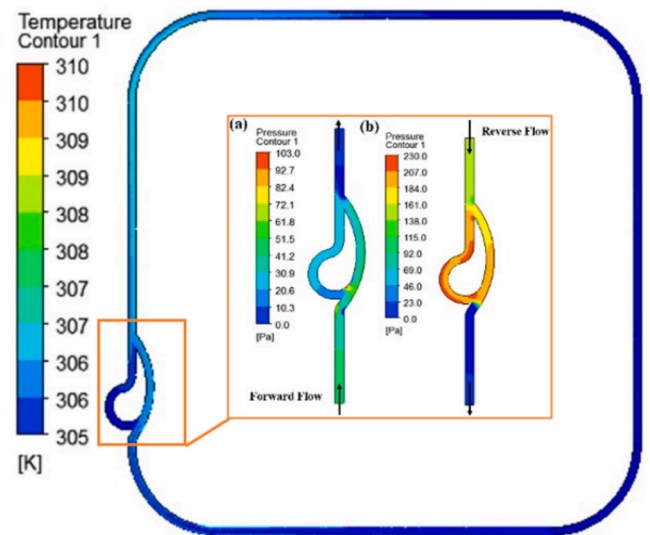


Fig. 12. Temperature contour for SCO₂ NCL with the contour of the pressure for (a) forward and (b) reverse flow [109]. Copyright © 2020 with permission from Elsevier.

NCL designs. At present, fossil fuels account for 82 % of global energy production. Heat transfer devices are essential for enhancing the efficiency of power generation systems and minimizing environmental impacts. Among these devices, NCLs stand out due to their simplicity and safety. Single-phase NCLs are widely used across various industries, with the temperature range varying significantly depending on the specific application [76].

The physical characteristics of water are reasonably well-known, and considerable variations in parameters such as density or various derivatives can be expected within the pressure range encountered in typical applications [114]. In addition, the operating temperature range is limited when using water as a working fluid. On the other hand, employing air as the working fluid allows for a broader range of temperature variations within the heat exchanger. Air is also a more suitable fluid for low-capacity open systems. However, there has yet to be a study in the open literature that focuses on air-cooled NCLs [96]. A summary of the advantages and disadvantages of the two working fluids, water and carbon dioxide, is also provided in Fig. 18. This image compares the characteristics of two important fluids used in NCL (water and CO₂).

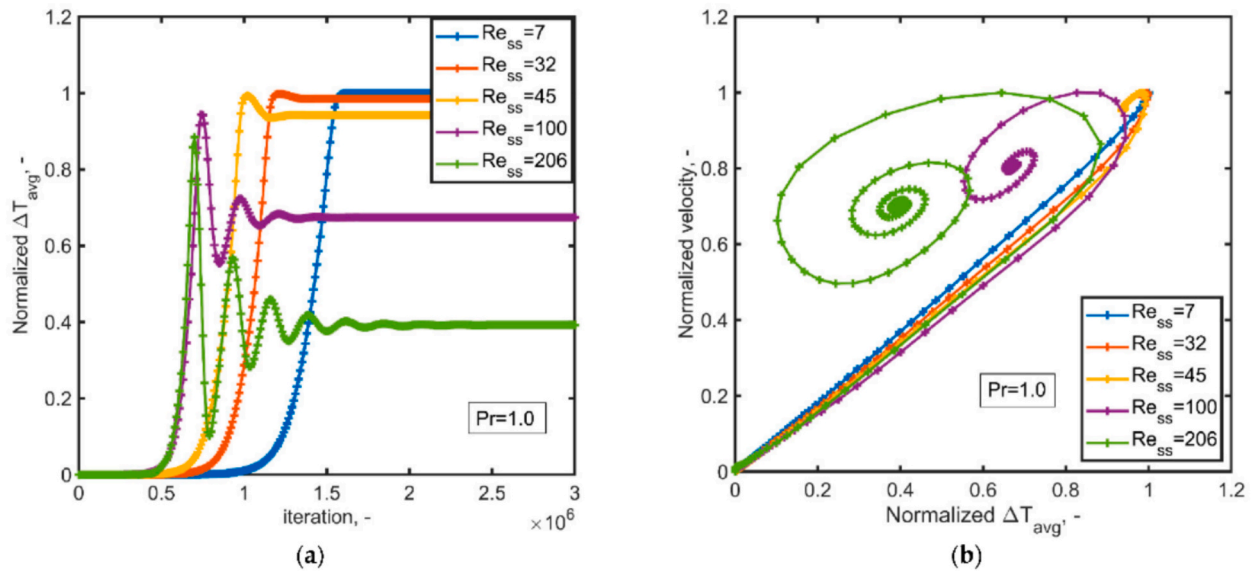


Fig. 13. The transient response of the NCL, simulated using LBM for different Re and a Pr of 1.0, is presented as follows: (a) the ΔT_{avg} versus time, and (b) the phase diagram of normalized velocity versus normalized ΔT_{avg} [73] Copyright: © 2023 by the authors. Licensee MDPI, Basel, Switzerland.

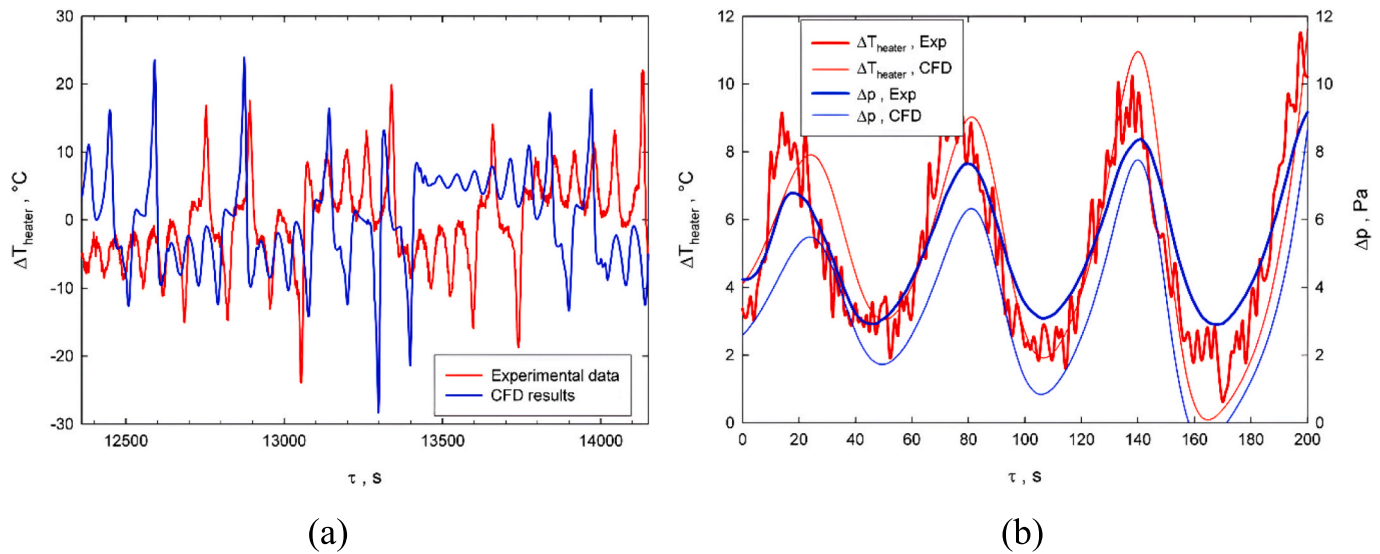


Fig. 14. Comparison between CFD results and experimental data (a) Temperature differences at the heater, (b) Pressure difference at the heater [29]. Copyright © 2012 Elsevier Masson SAS.

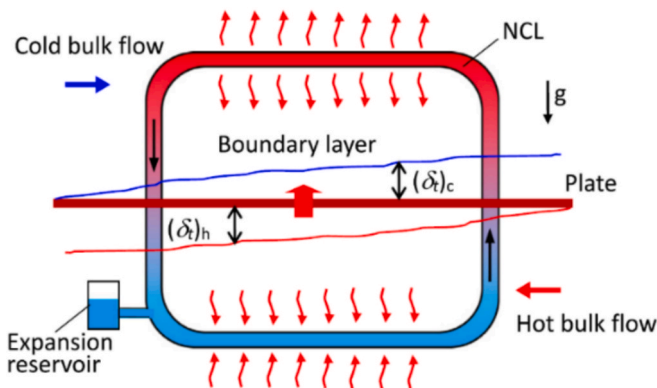


Fig. 15. Schematic of counter-current heat exchanger with a flat plate [112] Copyright © 2020 Elsevier Ltd.

Each fluid has unique properties that affect the performance of the system. The advantages and disadvantages of each fluid in terms of thermal conductivity, safety, and heat storage capabilities are examined. This comparison helps you better understand the differences and similarities between the two fluids and make informed choices for specific applications.

5.1. An overview of major research conducted on CO₂-based NCLs

According to the literature, the behavior and thermo-physical properties of supercritical CO₂ are dependent on the temperature (Fig. 19). So, the instability mechanism in these loops remains more challenging. It is noteworthy that CO₂-based NCLs are used in various applications, such as material preparation [115], chemical extraction [116], new-generation nuclear reactors [117], cryogenic refrigeration [118], heat pump systems [119], as well as waste heat recovery.

For subcritical CO₂, significant changes in physical properties and

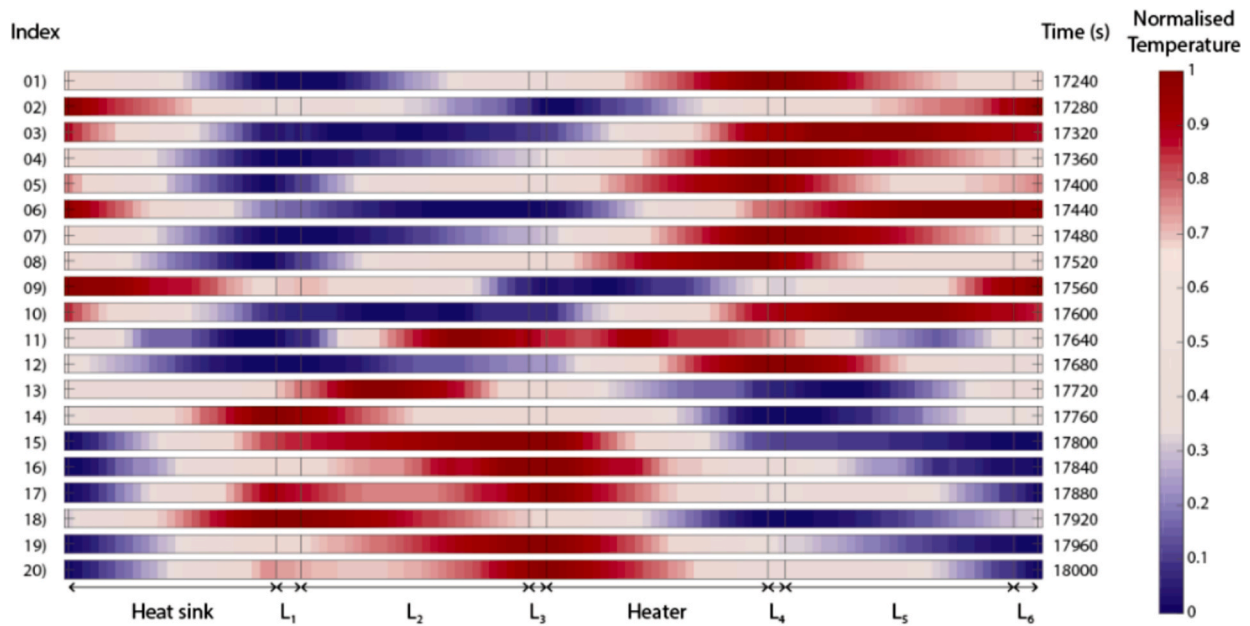


Fig. 16. The normalized temperature field, hot and cold plug movements in the loop [38].Copyright © 2016 Elsevier Ltd.

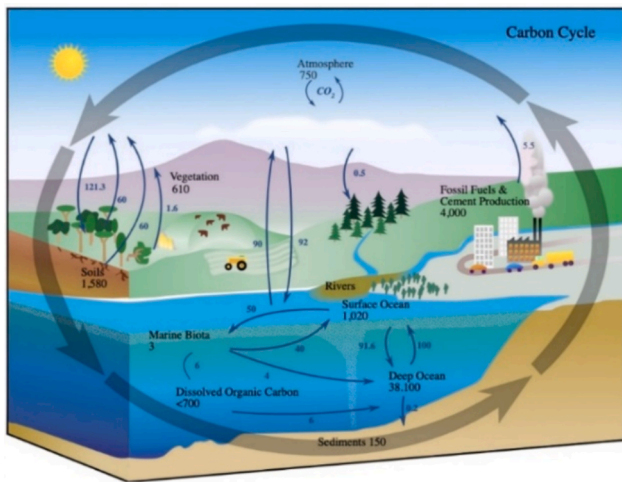


Fig. 17. CO₂ natural cycle [113] Copyright © 2004, food and agriculture organization (FAO) of the United Nations.

transfer coefficients result in turbulence and instability. However, extensive research has been conducted on subcritical NCLs (Misale et al. [18], Mousavian et al. [26], Garibaldi and Misale [111], Vijayan et al. [121], Kumar and Gopal [122]), but the results obtained for subcritical NCLs cannot be applied to supercritical NCLs [120]. Fig. 20 depicts the density difference between water and CO₂ as a function of temperature and pressure. Positive (in blue) values indicate that CO₂ has a lower density than water, which leads to CO₂ buoyancy, and negative (in red) values indicate that CO₂ has a higher density than water, leading to sinking potential.

Chen et al. [83] concluded that the viscosity of supercritical CO₂ is very low, making the flow highly sensitive to minor changes in applied forces, with temperature variations having a significant effect as well. Swapnalee et al. [124] mentioned that instability is observed in the NCL with supercritical water, while instability with supercritical CO₂ is not observed. The effect of pressure was found to reduce the unstable region. At higher pressures, instability occurs at very low inlet temperatures. Fig. 21 (a) shows the phase diagram of pure water and CO₂.

The concept of the Widom line has gained prominence in the supercritical phase. When a fluid crosses this line, it experiences a significant dynamical crossover in its properties [76]. Based on the Widom line, CO₂ is categorized into two regions (Fig. 21(b)).

5.2. Comparative heat transfer analysis in NCLs using water and CO₂

In the research by Kumar et al. [126], it was found that while water possesses excellent heat transfer characteristics, it necessitates larger diameter pipes than CO₂ to achieve optimal heat transfer processes. It is important to note that the operating pressure for CO₂ is significantly higher than that of the other fluids examined. Additionally, because of low critical temperature, the CO₂-based loop operates close to the critical point. Deng et al. [98] conducted precise tests on the flow transition characteristics of the supercritical CO₂-based closed NCL system. They discovered that a decrease in heating intensity leads to a rapid decline in the flow temperature curve within the loop. If the cooler temperature drops into the critical point region, the flow quickly becomes unstable, regardless of temperature changes in the heater. Additionally, the heater control transition responds relatively slowly to reductions in heat flow but exhibits a rapid response during heat flow surges. The reverse flow in the pipe causes turbulence, which has led some researchers to focus on this topic in their studies. Fig. 22 specifically addresses this issue.

To better explain reverse flow, Battisini et al. [61] concluded that fluid particles closer to the vertical wall become warmer during reverse flow and are driven upward by buoyant forces, in contrast to the downward flow in the cooler central region. Opposing flow circulation of a descending central region of cooler fluid and an ascending cylindrical boundary of warmer fluid creates turbulence, evidenced by the turbulent directions of fluid particles at the boundary between ascending and descending flows (Fig. 22).

To further discuss the flow behavior of the supercritical CO₂ loop, the pressure difference in the flow field is shown in Fig. 23. In the beginning, a vertical pressure difference is created in the adiabatic legs for wall cases then it begins to oscillate. After some time, when the flow reaches a steady state (either periodic repetitive flow or stable unidirectional flow), the pressure difference also stabilizes with relatively smaller oscillations. As the heating wall temperature increases, the rectangular circulation loop becomes unstable. This allows the supercritical CO₂ natural convection loop to achieve higher flow speeds with lower losses.

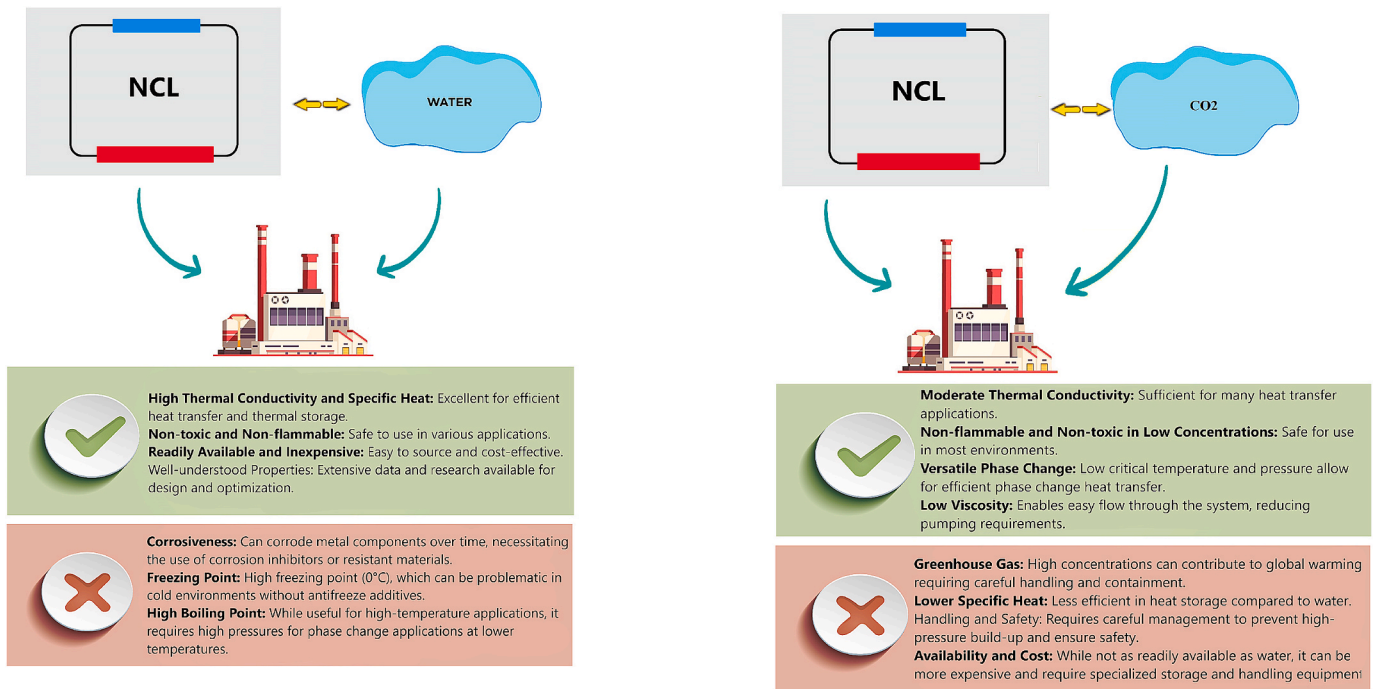


Fig. 18. Comparison between water and carbon dioxide as working fluids.

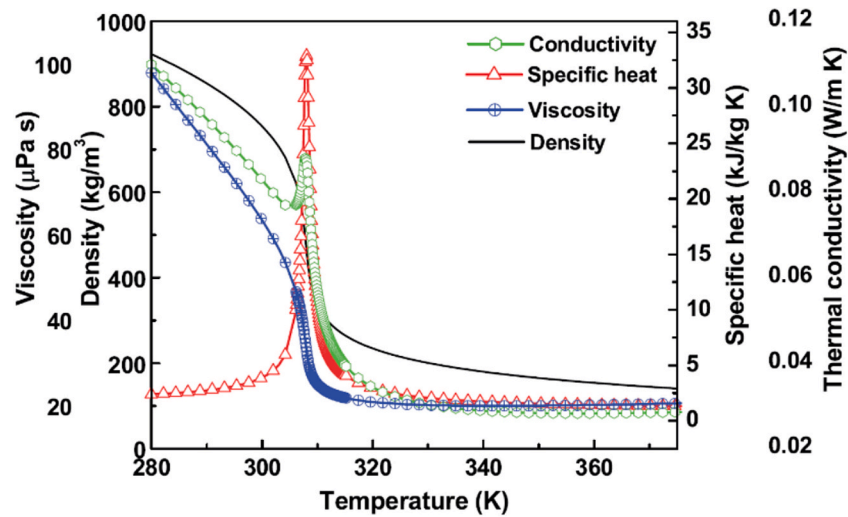


Fig. 19. Characteristic of CO₂ at 1116.1 Psi [120]. Copyright © 2015 Elsevier B.V.

Consequently, greater efficiency in heat and mass transfer processes can be attained, offering a significant advantage over traditional fluid flow systems [83]. The CO₂-based NCL was tested in the XY plane as well as in the YZ plane at angles of 0 and 45 degrees. The effect of inclination on the fluid loop temperature (at the center of the left leg) is visible at an inclination angle of 45 degrees. Tilting the loop in the YZ plane reduces the effective height of the loop, which decreases the buoyancy effect and increases the loop temperature. At an inclination angle of 30 degrees, there is no significant change in the loop fluid temperature compared to a 0-degree inclination angle [48].

Fig. 24 (a) and (b) compare the heat removal capability of subcritical and supercritical CO₂ with water. The results demonstrate that at the same isothermal wall temperatures for both the source and sink, CO₂ achieves a heat transfer rate roughly seven times higher than water. For instance, at 50 bars, carbon dioxide has a 15 times lower viscosity, and 100 times greater volumetric expansion coefficient compared to water.

As expected, CO₂ flow in the loop is highly turbulent, while water remains laminar. This difference is attributed to the relative viscosity and density of the fluids, which significantly impact the Re [127]. Fig. 25 (a, b) presents temperature contour plots (in K) for water and CO₂ (at 100 bar) with TC = 315 K and TH = 331 K, respectively, at the center of the source, riser, sink, and downcomer. The isotherms display uneven temperature distribution and variations in velocity within the pipe at specific cross-sections.

In 2015, Sarkar et al. [42] experimentally tested water, CO₂, and R134a for possible application in supercritical regions. The results revealed that each supercritical fluid undergoes significant changes in thermodynamic and transfer properties near the pseudo-critical temperature. This study also showed that the CO₂-based loop requires the least mass inventory. At higher power levels, R134a requires less mass inventory than water while maintaining similar maximum temperature levels, making it a potential fluid option, if its chemical stability is

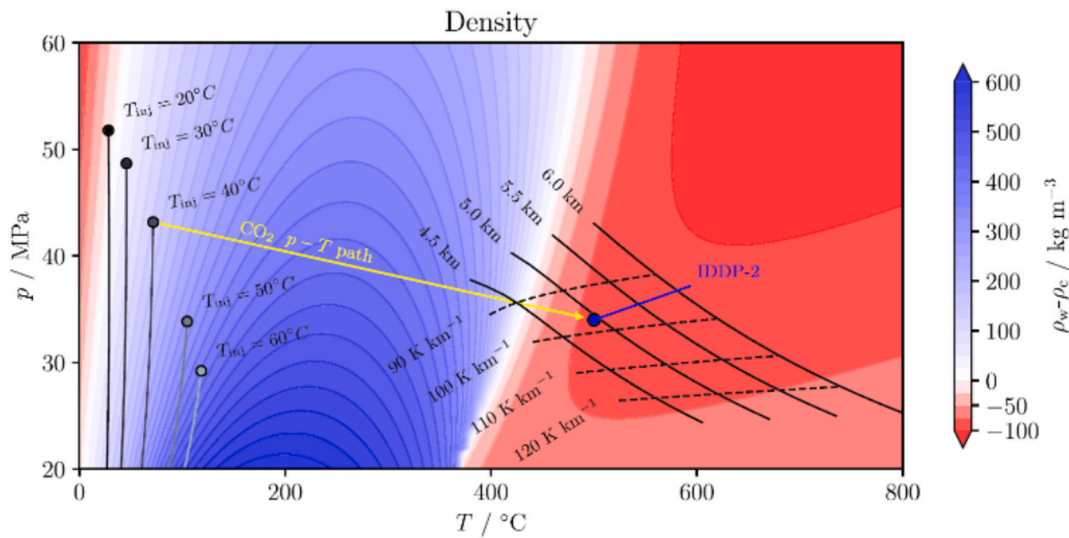


Fig. 20. Density difference between water and CO₂ as a function of pressure (up to 60 MPa) and temperature (up to 800 °C). [123] Copyright ©2020. The Authors.

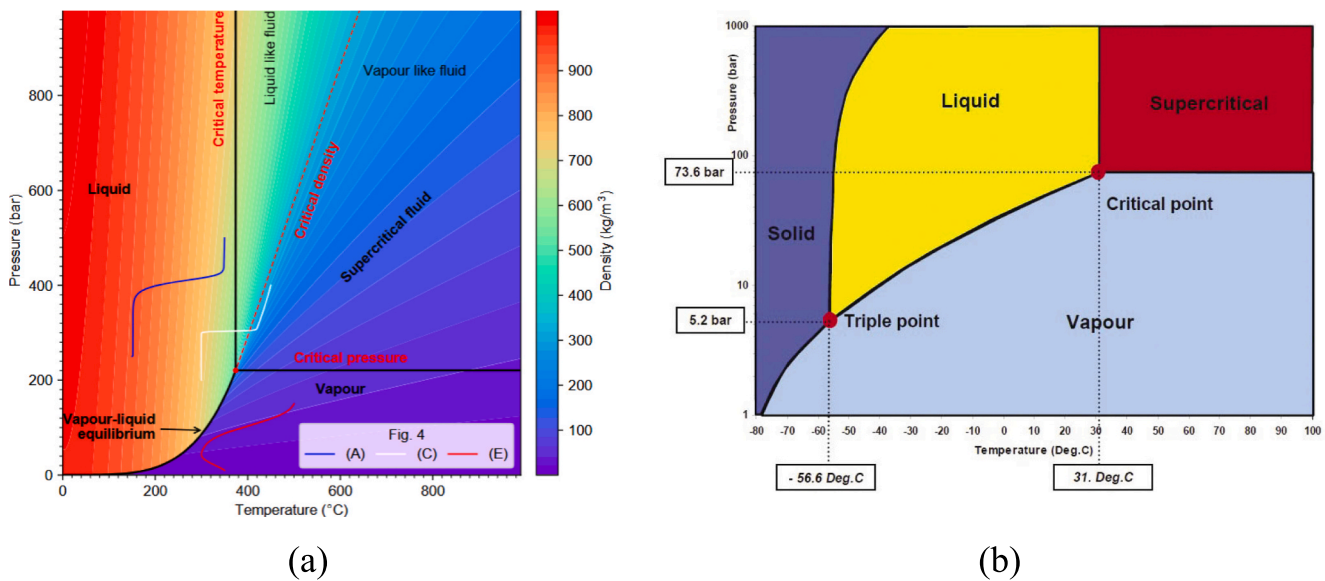


Fig. 21. (a) Phase diagram and density of pure water and (b) Phase diagram of CO₂. [125], Copyright © 2020 Authors.

maintained. Additionally, for a given loop geometry, liquid CO₂ delivers a heat transfer rate that is seven times higher than water. Kumar Rai et al [128] numerically analyzed the impact of geometrical and operational parameters on dynamic and Ledinegg instability in a supercritical water NCL. They explored that a smaller loop diameter is more stable in terms of power compared to a larger loop diameter. The loop height plays a critical role in determining the stability thresholds in natural circulation systems, with increased height contributing to more pronounced flow instabilities. The stability of NCLs is influenced by various factors, including power levels. Fig. 26 illustrates the marginal stability boundary of Ledinegg instability where the power increases within the lower power range, and the likelihood of experiencing Ledinegg instability initially rises. However, at higher power ranges, the system becomes more stable with increasing power. Consequently, there are two distinct stability thresholds, one in the lower power range and another in the higher power range, providing critical insights into the design and operation of supercritical water NCLs.

Reducing system pressure enlarges the unstable region, while Ledinegg instability disappears above a specific enthalpy input of 450.00 kJ/

kg. Smaller loop diameters require higher enthalpy for stability. At low enthalpy and high pressure, Ledinegg stability is achieved. The stability region decreases near the critical point but expands beyond it. Fig. 27 illustrates the fluid dynamics within the NCL, emphasizing density stratification and local recirculation phenomena by Srivastava and Basu [101]. The fluid rises along the heater wall and descends in the cooler section, creating strong density stratification, with lighter fluid accumulating in the upper part of the channel. This behavior is essential for understanding the thermal and flow characteristics within the vertical loop.

Such a study aims to identify a generalized criterion for the early identification of flow-induced heat transfer deterioration in a rectangular sCO₂-based NCL, with a special emphasis on the role of vertical inclination. Bhopalan et al. [76] conducted numerical investigations on the supercritical CO₂-based NCL with a three-dimensional rectangular cross-section in different operational regimes. They revealed that the average temperature of the NCL was maintained near the Widom line, far from the Widom line (higher buoyancy region), and very far from the Widom line (very supercritical region). Findings show that in all areas,

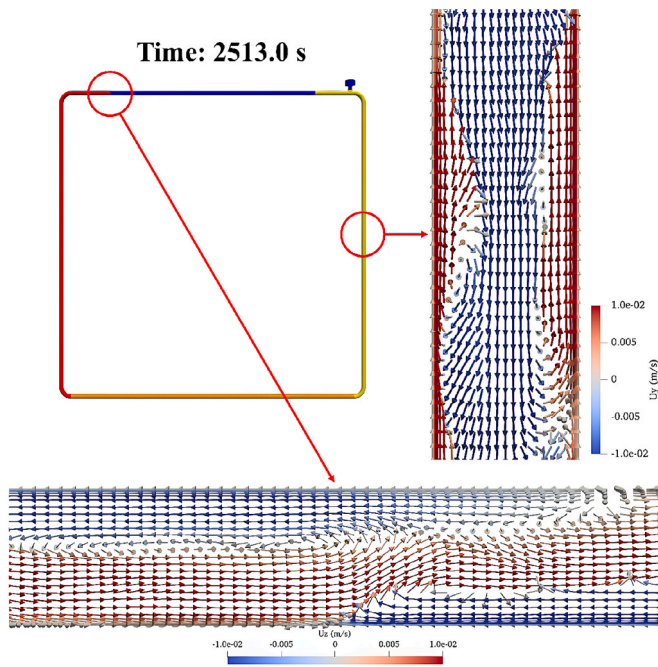


Fig. 22. Flow reversal behavior [61]. Copyright © 2021 Authors.

with increasing pressure, both the heat transfer rate and the mass flow rate increase. The maximum heat transfer rate is observed at 14 MPa in all regions. Although the near pseudo-critical region shows efficient heat transfer capability, the higher buoyancy region exhibits excellent heat transfer rates. The rate of changes in density difference, mass flow rate, and average velocity in a natural circulation loop with supercritical fluid is another important aspect covered in Fig. 28.

Fig. 28 (a) shows the relationship between the average loop velocity and the density difference caused by increasing pressure, which helps to understand the flow behavior in the supercritical NCL system. The study found that the higher buoyancy region (HBR) exhibits the highest velocity due to a greater density difference in the loop. In the near pseudo-critical region (NPCR) and HBR, the fluid crosses the Widom line, transitioning from a liquid to a gas state, causing significant density variations within the loop. While NPCR must maintain a near pseudo-critical state with a smaller temperature difference than HBR, a larger density difference does not impact the mass flow rate. NPCR transfers more mass than HBR because of its higher average loop density.

However, the greater speed in HBR enhances heat convection, resulting in a higher heat transfer rate in the supercritical NCL. Fig. 28(b) illustrates that the average density of the loop mirrors the pattern of the mass flow rate. As a result, the deeply supercritical region exhibits the lowest average fluid density at any given pressure, leading to a reduced system mass flow rate. In supercritical NCL is driven by buoyancy, which is generated by the density difference along the loop. Thus, the density difference is key in determining supercritical NCL performance.

5.3. A look at research on NCLs based on helium

Here, it is worth looking at the studies by Világi et al. [129] on the experimental model of the NCL based on helium fluid in a real environment (Fig. 29). The presented research investigates hydraulic and thermodynamic processes in a large-scale natural circulation loop (NCL) through various measurements. It was observed that the temperature distribution in the electrical heater (EH) followed a linear pattern, while in the decay heat removal (DHR) cooler, it displayed a logarithmic distribution.

In continuous with the helium NCL, Vach and Knížat [130] conducted a numerical analysis of unsteady helium flow in an NCL, with applications in nuclear safety systems, which was experimentally validated. Their model incorporates boundary conditions based on various scenarios that simulate the performance of the physical system. Furci et al. [131] conducted experimental and numerical study aimed at controlling the transient early boiling crisis caused by step-change thermal load pulses in a helium NCL with dynamic initial conditions. The simulations revealed that while the maximum transient quality during the initial stages depends on the initial conditions, the time-averaged cumulative local quality remains constant, regardless of diameter, position, or initial conditions (Fig. 30). This insight allows for predicting the onset of a boiling crisis in such systems, provided the mass flow rate evolution can be estimated beforehand, such as through dynamic modeling, as demonstrated in the referenced study.

5.4. Liquid metal and molten salt; high-temperature fluids in NCL

Given that heavy liquid metal cooling technology in the new generation of advanced nuclear reactors has not yet fully matured, it is worth examining this area. Liquid metals, such as sodium, lead, lead-bismuth eutectic (LBE), and others, are prized for their excellent thermal conductivity, high boiling point, low vapor pressure, chemical stability at high temperatures, and relatively low melting points compared to pure metals. In nuclear reactors, liquid metals are used

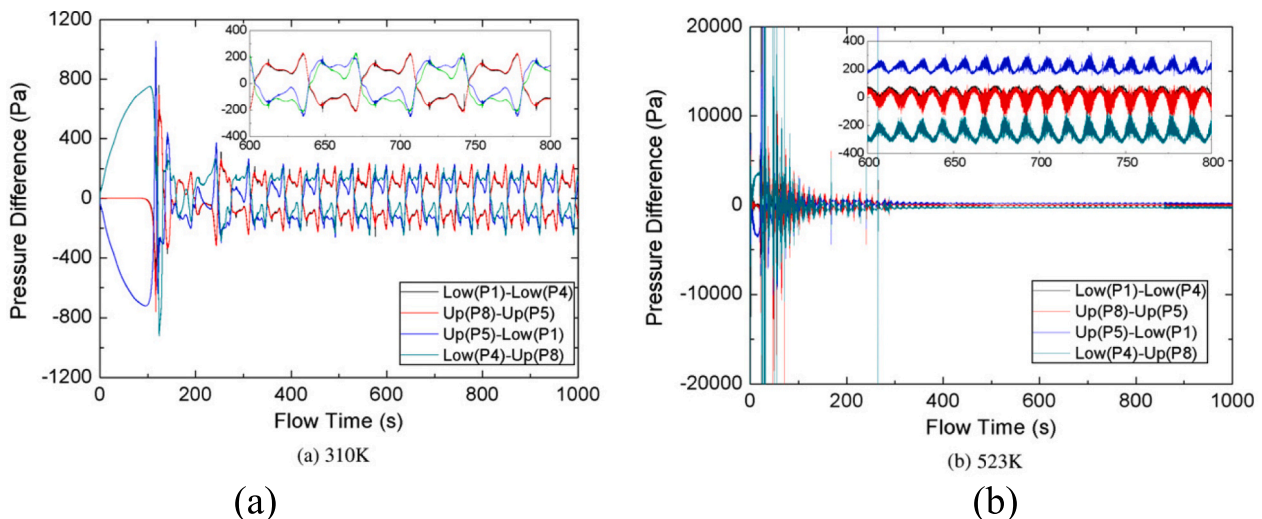


Fig. 23. Variations of pressure differences in the circulation loop at different heat source temperatures [83]. Copyright © 2010 Elsevier Ltd.

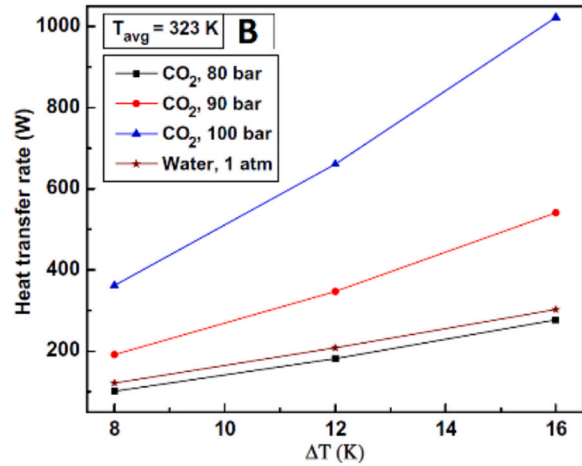
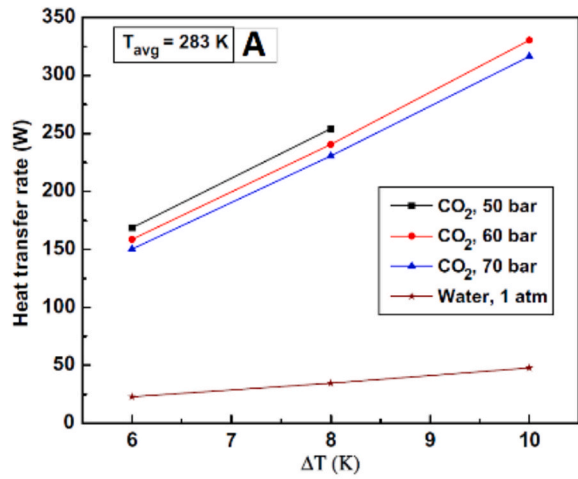


Fig. 24. Heat transfer rate versus ΔT for CO_2 and water [127]. Copyright © 2012 Elsevier Ltd.

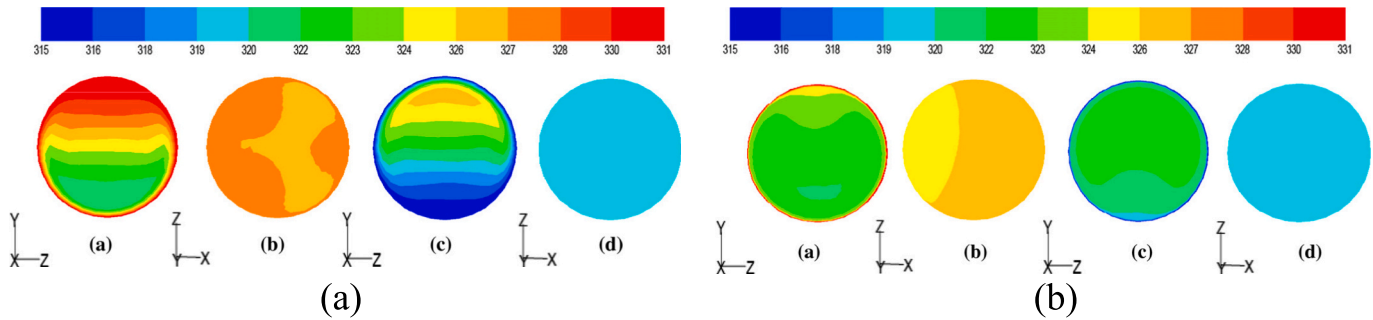


Fig. 25. Temperature contour plot for (a) water and (b) CO_2 at the center of (a) source, (b) riser, (c) sink, and (d) downcomer [127]. Copyright © 2012 Elsevier Ltd.

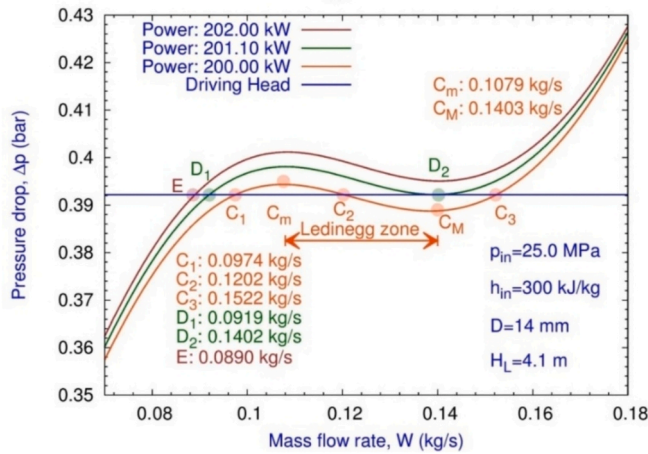


Fig. 26. Low and high-power marginal stability boundary of Ledinegg instability in a SCWNCL [128]. Copyright © 2020 Elsevier B.V.

primarily as coolants. For instance, sodium and LBE are favored in fast neutron reactors because they can efficiently transfer heat from the reactor core to the heat exchangers without moderating (slowing down) the neutrons. However, the corrosivity of structural materials and the problem of producing activated products are the challenges. The mentioned advantages besides thermal stratification and flow mixing can impact the performance of liquid metal natural circulation to be used in advanced thermal systems [15]. On the other hand, molten salt, typically fluorides or chlorides of lithium, beryllium, and zirconium are also attractive alternatives to be used with fertile thorium in molten salt

reactors as fuel-based coolants, sensible heat storage medium in solar power plants, and as working fluid in natural circulation loops. However, compromising thermal stability in accident conditions, chemical stability, and corrosion effects are the main challenges of advanced systems that use molten salts [53]. Li et al. [77] study also showed that the use of lead–bismuth in natural circulation can maintain thermal stability; however, temperature fluctuations and corrosion remain major challenges. Regarding the impact of heater and cooler orientation on the performance of molten salt-based natural circulation loops, it has been observed that the VHHC configuration offers better thermal performance, although thermal inertia effects are more pronounced. Overall, the VHHC configuration can be suitable for optimizing passive heat removal in emergency conditions [132]. However, in the event of heater failure, molten salt may solidify and block the circulation path, posing a significant safety challenge [133]. Hariyanto et al. [67] conducted a CFD analysis of an NCL by COMSOL in a molten salt ($\text{NaNO}_3 + \text{KNO}_3$) loop featuring a VHHC configuration. This study aimed to analyze the transient and steady-state behavior of the natural circulation system in a molten salt loop with a vertical heater and horizontal cooler using computational fluid dynamics. Fig. 31 shows the temperature distribution contours at the heater outlet of a molten salt-based natural circulation loop within the power range of 1600 to 1700 W.

The temperature distribution results on the heater output showed that the molten salt NCL with a VHHC demonstrated good flow stability without flow reversal.

Metallic alloys can be utilized in NCLs at higher temperatures, allowing for greater heat flux. Consequently, NC in liquid metal reactors is favored for lower operational, and maintenance costs [8]. Further research has also been conducted on asymmetric liquid metal NCLs.

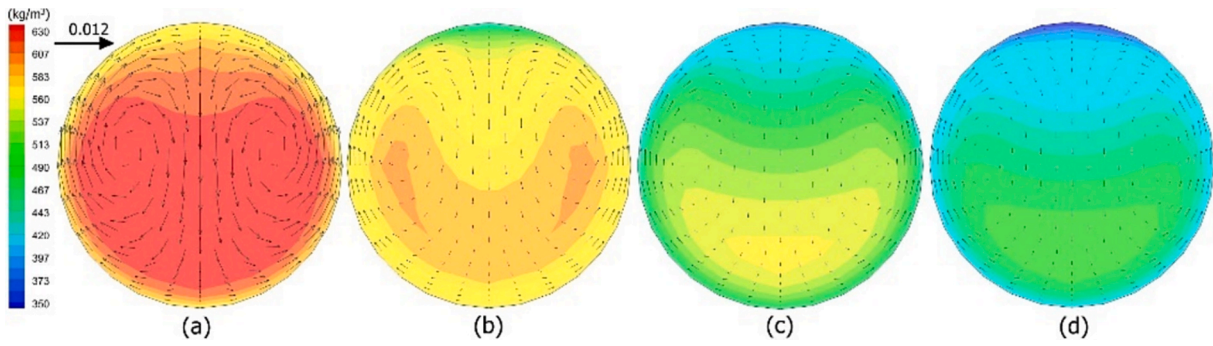


Fig. 27. Density contours and velocity vectors at different locations of the heater of the vertical supercritical [101]. Copyright © 2022 Elsevier B.V.

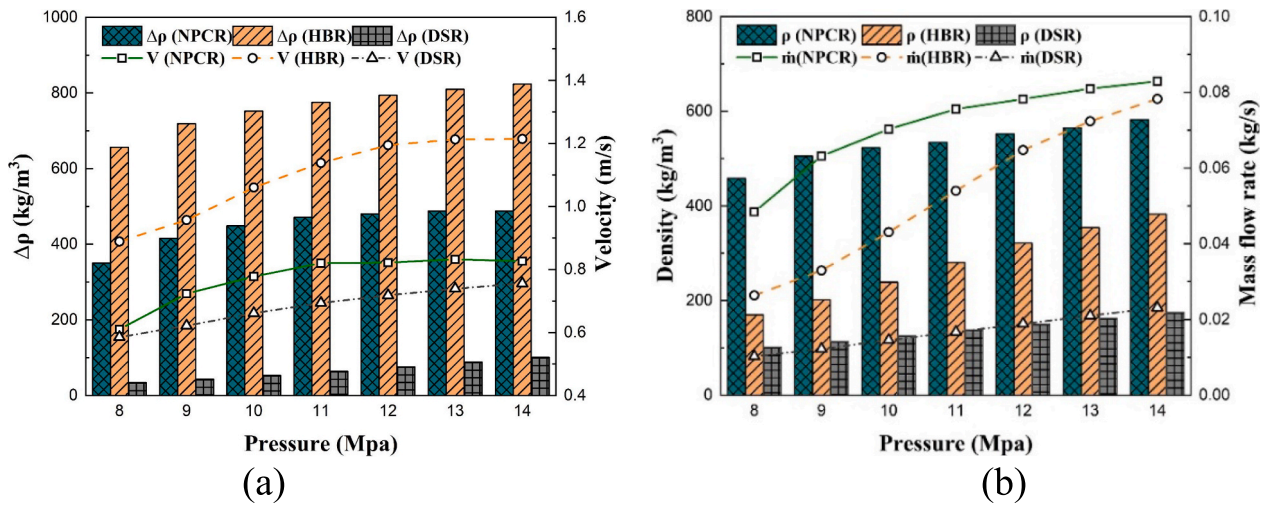


Fig. 28. Variation in density difference and loop average velocity for different pressure and operating region (a), Variation in loop average density and loop average mass flow rate for different pressure and operating region (b) [76]. Copyright © 2024 Elsevier Ltd.

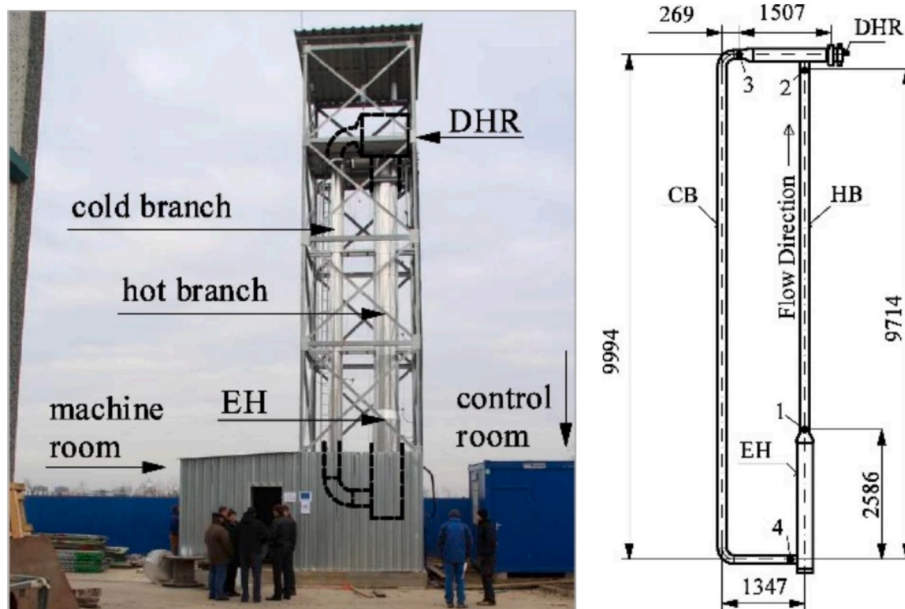


Fig. 29. Experimental high-pressure and high-temperature natural circulation helium loop (left) and Sketch of the experimental setup sizing (right) [129]. Copyright © 2020 Elsevier Ltd.

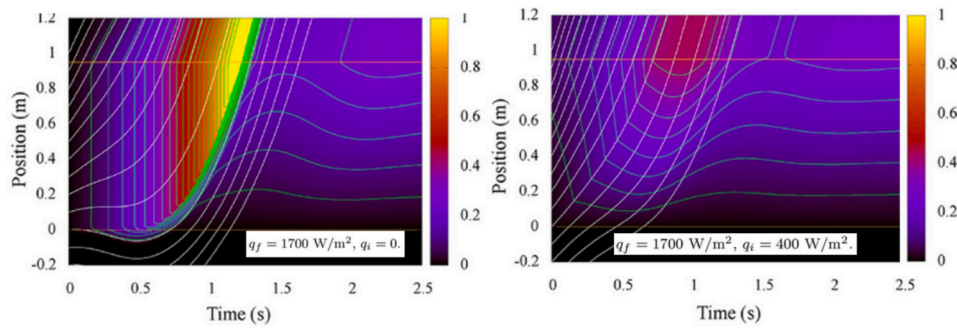


Fig. 30. Thermodynamic quality for non-static initial condition. White lines: particle trajectories; green lines: level contours of quality [131]. Copyright © 2018 Elsevier Ltd.

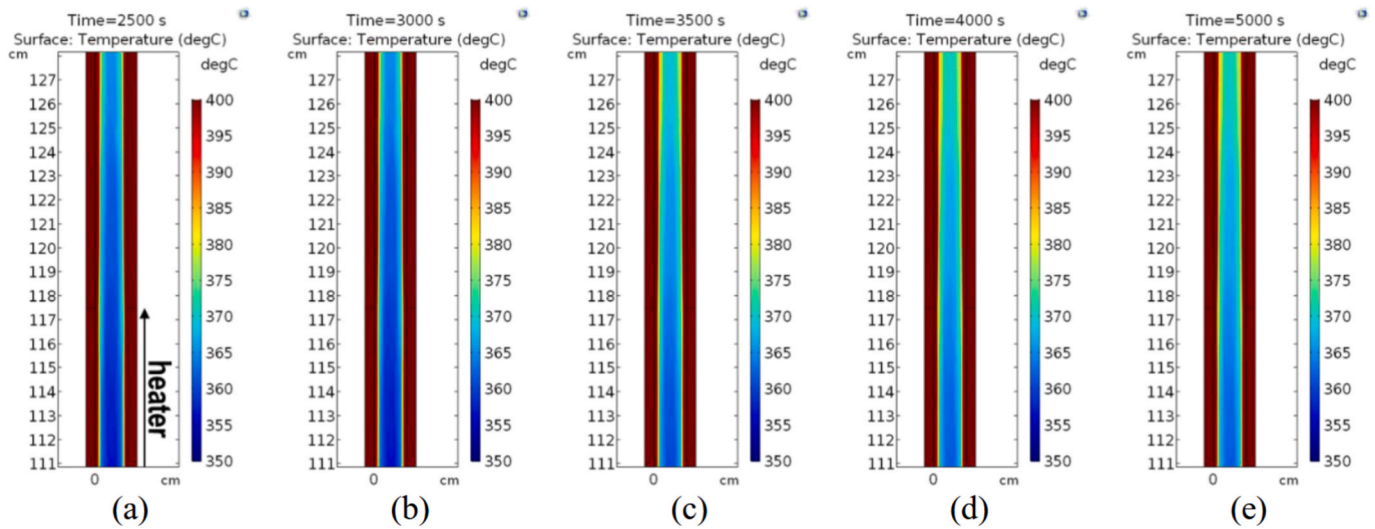


Fig. 31. Heater output temperature distribution in the case of step-up power from 1600 W to 1700 W at different running time [67]. Copyright: © 2022 by the authors.

6. Impact of nanoparticles to improve instability of NCLs

Certainly, this has been one of the key questions for researchers in recent years. Generally, the use of NCLs with advanced heat transfer fluids like nanofluids can be beneficial for various industrial applications to improve heat transfer performance and stability. The concept of nanofluids was first introduced by Choi [134]. Nanofluids are stable colloidal suspensions formed by dispersing nanoparticles (hydrophilic such as metal oxides or hydrophobic like CNT and graphene) into base fluids like water, oil, ethylene glycol, and others. These nanoparticles greatly influence the thermal properties of base fluids, particularly their thermal conductivity and viscosity. Nanofluids are employed as efficient working media in various applications, including heat pipes [135], heat exchangers [136], car radiators [137], solar energy systems [138], and electronic chips, owing to their excellent thermal performance, uniform dispersion, and stability. Nayak et al. [90,139] have experimentally investigated the stability of a rectangular single-phase NCL by adding nanoparticles to the fluid. The findings demonstrate a notable improvement in flow rate and enhanced stability, even at low levels of nanoparticle concentration. Misale et al. [84] evaluated the performance of a mini NCL using Al_2O_3 /water nanofluid, focusing on the effects of sink temperature and loop inclination. They observed that performance enhanced with increasing sink temperature but diminished as the inclination angle rose. Other researchers like Hu et al. [140], Doganay and Turgut [141], Koca et al. [142], Thomas and Sobhan [143], Bejjam et al. [144], and Ghorbanali and Talebi [145] numerically and experimentally examined the NCL performance using nanofluids

and determined that NCL performance improved with nanofluids. They studied the pressure drop oscillation across a section of horizontal unheated piping over time. The flow remained stable with the addition of nanoparticles at varying concentrations, unlike with water. Sahu et al. [71] highlighted that, despite the increasing interest in the application of hybrid and ternary nanofluids in single-phase NCL systems, research on this topic remains limited in the current literature. It was further highlighted that the increase in mass flow rate observed in single-phase NCL systems with water-based hybrid nanofluids is strongly influenced by the shape of the nanoparticles and the input power [129,130]. Likewise, a similar effect was observed in SPNCL systems when ternary hybrid nanofluids containing dissimilar particles were used [146]. Many researchers have used water as the working fluid for SPNCL where the serious problem in the use of nanofluids is sedimentation [147–150]. However, deposition (fouling) is the main limitation in the engineering application of nanofluids. Bocanegra et al. [148] provided a review article on the literature regarding the gravitational deposition of nanofluids. The literature review revealed that gravitational deposition is a significant challenge in utilizing nanofluids. To overcome nanofluid deposition challenges, systematically collecting experimental data is essential, with consideration given to various nanoparticles, base fluids, and commonly used additives. Liu et al. [151] investigated the sedimentation and aggregation kinetics of titanium dioxide (TiO_2) nanoparticles with varying material properties such as crystallinity, morphology, and chemical composition. However, differences in chemical composition, particularly the concentrations of impurities like silicon and phosphorus in the raw materials, influence the surface

charge, which in turn affects the sedimentation and aggregation of TiO_2 nanoparticles in the aqueous phase. An ideal nanofluid is a suspension of uniformly dispersed and highly stable nanoparticles. However, due to the large specific surface area and high surface energy of nanoparticles, they can easily aggregate and settle in the base liquid, affecting the heat transfer characteristics of nanofluids [152]. The stability of nanofluids depends on preparation methods, namely the one-step method [153,154] or the two-step method [155–161]. Additionally, in studies conducted on NCL with nanofluids, researchers are advised to pay attention to the effects of the position of heat sources. Nayak et al. [90], demonstrated that nanofluids in NCLs, commonly used in process and nuclear industries, suppress flow instabilities and increase buoyancy-driven flow rates. Their experiments with Al_2O_3 , CuO , and TiO_2 nanofluids showed that higher nanoparticle concentrations enhance flow rates, with TiO_2 and Al_2O_3 being particularly effective. Even at low concentrations (0.5 wt%), these nanofluids outperformed water. Single-phase NC flow depends on the fluid thermal expansion, specific heat, and viscosity, with fluid temperature being the most critical factor, while pressure has minimal impact on incompressible fluids [162]. Misale et al. [84] compared the thermo-hydraulic performance of a mini NCL using distilled water – Al_2O_3 nanofluid. The study confirmed that the loop remained stable with both fluids. The average temperature was similar for both water and nanofluid. A slight improvement was observed with nanofluid at a 75-degree loop inclination. The study also noted that increasing the loop inclination reduced thermal performance while raising the sink temperature. Misale et al. [147] conducted a long-term experimental study on the sedimentation of Al_2O_3 -water nanofluids at different volume concentrations. They used a simple experimental setup with a thin test cavity filled with nanofluid, equipped with laser diode-photodiode pairs to measure absorbance and local volume concentration. Fig. 32 presents data for a 1.0 % volume concentration over time. They found that the experimentally estimated sedimentation velocity was higher than that predicted by Stokes law, indicating that the dynamics of nanoparticle clusters play a crucial role in settling behavior. As the initial volume concentration increased, a higher sediment bed formed, but the overall sedimentation trends remained similar across all tested concentrations [147].

Bejjam et al. [144] experimentally examined the impact of particle concentration, input power, and cold inlet temperature on the performance of an NCL using water-based nanofluids such as SiO_2 , CuO , and Al_2O_3 . The researchers found that when using nanofluid in an NCL, the system reached a steady state faster than when using water. Additionally, the average Nusselt number increased as both particle concentration and input power increased. However, since nanofluids have a higher viscosity and density than water, the loop operating with

nanofluids experienced a greater pressure drop compared to water. Tlili et al. [55] investigated the impact of using a hybrid nanofluid ($\text{Cu-Al}_2\text{O}_3$ -water) in an NCL on the temperature distribution, Reynolds number, and mass flow rate. The results showed that adding copper nanoparticles to an alumina-based nanofluid enhances stability and thermophysical properties, especially thermal conductivity. Additionally, from a cost perspective, the hybrid nanofluid proved to be a more economical option compared to alumina-only nanofluids. Ghorbanali and Talebi [145] also numerically studied the stability and thermal performance of water, TiO_2 -water, and Al_2O_3 -water as working fluids in NCL. The study found that the thermal performance improves with the use of nanofluids and increased input power where the best one was using Al_2O_3 -water (4 wt%). In another work, Sahu et al [146] studied an inclined VHHC NCL water-based tri-hybrid nanofluids ($\text{Al}_2\text{O}_3 + \text{Cu} + \text{CNT}$, $\text{Al}_2\text{O}_3 + \text{Cu} + \text{graphene}$, $\text{Al}_2\text{O}_3 + \text{CNT} + \text{graphene}$, $\text{Cu} + \text{CNT} + \text{graphene}$). The results revealed that trihybrid nanofluids enhance fluid stability by reducing mass flow rate oscillations compared to pure water. These nanofluids allow the system to reach a steady state more quickly at the same input power. Additionally, loop inclination improves steady-state effectiveness and total entropy generation rate but decreases the mass flow rate. Conversely, increasing the aspect ratio reduces steady-state effectiveness and entropy generation while boosting the mass flow rate at a given input power. Fig. 33 depicts the transient variation of the total entropy generation rate at 500 W input power. The utilization of trihybrid nanofluids attributes the reduction in heater wall temperature to the enhancement in effectiveness, which consequentially diminishes the entropy generation rate.

In the study by Sahu et al. [71], the energy-exergy performance of a single-phase NCL was explored using mono and hybrid nano oils. The results showed that hybrid nano oils with spherical nanoparticles had better energy efficiency, resulting in higher heat exchanger effectiveness and lower total entropy generation rate. The $\text{Al}_2\text{O}_3 + \text{MWCNT} + \text{Therminol VP1}$ hybrid nano oil demonstrated the best performance in terms of both energy and exergy, showing superior heat transfer capabilities and reduced thermodynamic losses compared to other tested oils.

7. Two-phase NCLs; higher heat transfer and minimizing instability

Two-phase NCLs are essential for enhancing system stability and optimizing heat transfer, particularly in power systems and nuclear reactors. These loops efficiently transport heat between cold and hot regions by using natural fluid circulation in both vapor and liquid phases. The design and operation of two-phase NCL systems focus on optimizing

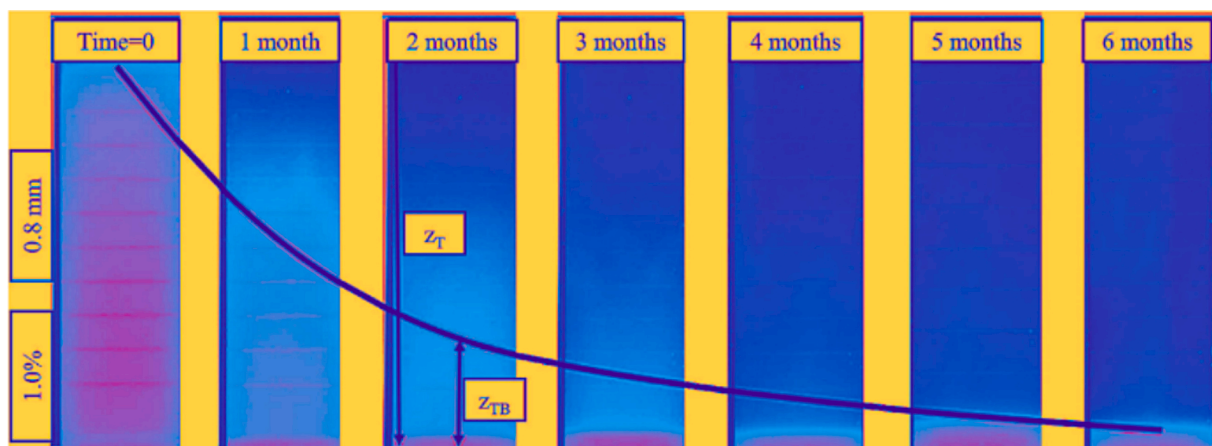


Fig. 32. Stability test result of water aluminum oxide nanofluid as a function of time. In digital photography, the red channel was extracted from the red–green–blue (RGB) image to increase contrast. Clearer zones indicate the presence of nanoparticles, while darker zones indicate their absence [147]. Copyright © 2023 International Research and Training Centre on Erosion and Sedimentation/the World Association for Sedimentation and Erosion Research. Published by Elsevier B.V.

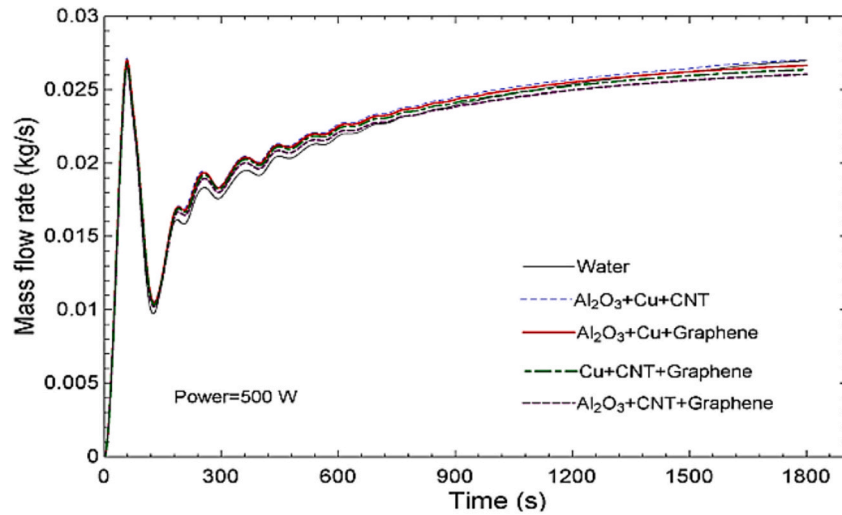


Fig. 33. Transient variation of total entropy generation rate at 500 W input power [146] Copyright © 2021 American Institute of Chemical Engineers.

geometry and heat input to maximize flow rates while minimizing instabilities. Analytical and numerical models predict loop behavior, considering variables such as pressure drop, subcooling, and heating power. Stability analysis is vital to ensure reliable operation, with adjustments in parameters like riser and heated section lengths improving performance and reducing entropy production [163]. Song [164] analyzed the optimal design of a two-phase NCL with a rectangular configuration, focusing on geometry and heat input with and without subcooling. By modifying the aspect ratio and adjusting volume distribution between the hot and cold sections maximum flow velocity was identified. The study also demonstrated that using a simplified pressure drop approximation ruled out the possibility of multiple solutions, suggesting a low risk of static flow instability, though density wave instability could still occur. Goudarzi and Talebi [165] performed a linear stability analysis to investigate the stability behavior of a two-channel two-phase NCL. The stability of the low-pressure two-channel NCL is sensitive to temperature and input power. Increasing heating power in the low-power region makes the system more stable, while in the high-power region, the system becomes less stable. Increasing the subcooling input makes the system more unstable. Additionally, Goudarzi and Talebi [166] aimed to improve the performance of two-phase NCLs by reducing entropy production. Increasing the riser length expands and shifts the stable region while decreasing entropy generation. Peng et al. [167] utilized the CATHARE code to analyze the pressurizer characteristics in a two-phase NC system. They found that pressure drop oscillations between the loop and the pressurizer could trigger flow instability in the system. D'Auria and Galassi [168] investigated the instabilities in two-phase NCL under typical PWR conditions, focusing on U-tube flooding dynamics and condensation. Using the RELAP5 system code, they identified system parameters influencing oscillation characteristics. Their study revealed that the instabilities stem from siphon condensation, which is regulated by the flooding occurring in the ascending legs of the U-tubes. Lisowski et al. [169] examined how boiling affects two-phase NCL behavior, highlighting that hydrostatic pressure shifts the boiling boundary to various riser sections, influencing flow regime and system performance. At low steam production, void growth in horizontal sections creates a stable, stratified regime. However, if boiling occurs in vertical sections, bubble coalescence forms large cavities, impacting stability. High steam production prevents cavity accumulation, ensuring stable two-phase flow. For safety-critical applications, natural circulation water loops, especially with steam venting, offer effective heat removal with simplicity and extended operation time. To better understand the behavior of two-phase NCLs, Franken et al. [170] conducted experiments using deionized water, tap

water, and artificial seawater to study two-phase NCL behavior, focusing on stability across different heat flux levels. The mass flow rates across all fluids were similar, but seawater stabilized flow fluctuations due to the lack of bubble coalescence, preventing slug formation. Seawater also had smaller bubble departure diameters, likely due to local salt accumulation increasing wettability and limiting bubble growth. The slower mass diffusion compared to thermal diffusion in seawater is believed to be a key factor in this behavior, resembling boiling in binary mixtures where the process is diffusion limited. Li et al. [171] examined flow instability in a two-phase NCL with parallel steam generators, crucial for the passive residual heat removal system in small integrated pressurized water reactors. They focused on the single-failure criterion during station blackout accidents, analyzing only half of the passive systems. Their RELAP5 model showed that low power post-blackout prevents full steam conversion, resulting in a two-phase fluid between the OTSG outlet and the condenser. The condensed water reenters the OTSG feed-water

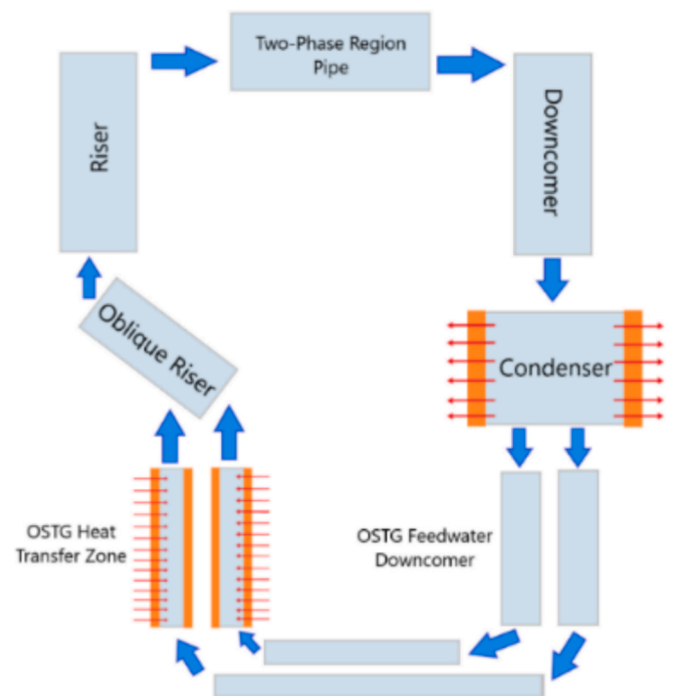


Fig. 34. The system diagram of the Two-Phase NCL [171]. Copyright © 2024 Xi'an Jiaotong University.

downcomer for reheating by the primary loop (Fig. 34).

Abbati et al. [172] investigated two-phase flow instability in a multi-loop natural circulation system, comprising two NCLs and one forced circulation loop. Their experiments revealed that high heating power directly contributes to flow instability. They identified an optimal inlet temperature that can eliminate instability; increasing the heating section entrance temperature can either stabilize or destabilize the system. Elevated system pressure also stabilizes the flow, allowing for more heating power without destabilization, while reduced pressure can lead to instability. Additionally, increasing the heat sink temperature significantly amplifies flow instability, with continuous increases resulting in exponential growth of oscillation amplitudes. Lim et al. [173] experimentally investigated a two-phase NCL as a passive containment cooling system. Their findings revealed the presence of both falling film and plug flow in the riser, validating the two-phase flow regime map despite some flow instability. The experimental heat transfer coefficient was found to be lower than Chen’s correlation but higher than the Dittus-Boelter correlation, indicating that two-phase natural convection offers superior heat transfer performance compared to single-phase forced convection. Adinarayana et al. [174] analyzed two-phase NCLs and developed numerical models based on the Homogeneous Equilibrium Model (HEM) and Drift Flux Model (DFM). Their study on vertical and horizontal configurations of Coupled-Two-Phase NCLs revealed that DFM provided more accurate predictions than HEM. Key findings included the impact of heater-cooler orientation and coupling configuration on system dynamics. The study showed that increasing heater flux positively affects the primary loop flow, but the secondary loop flow increases to a certain flux threshold before declining. Parameters like loop diameter (SF = 1.51), ambient temperature (SF = 1.35), and aspect ratio were influential, with the aspect ratio showing a more significant effect on the primary loop than the secondary (Fig. 35). The study also noted that while initial conditions such as forced circulation and working fluid temperature did not affect the steady-state flow, they played a critical role during the transient phase.

8. Importance of computer codes in NCL simulation

As computer hardware continues to improve, researchers are increasingly focusing on numerical simulations. Many studies compare experimental and numerical results. Key challenges in modeling NCL performance include low-flow natural circulation, which often involves not fully developed and multidimensional nature, as well as flow

instability and critical heat flux during oscillations. Beyond industrial applications of NCLs, single-phase NCLs offer an opportunity to validate the capabilities of thermal-hydraulic system codes like CATHARE, ATHLET, RELAP, and CFD codes like Ansys Fluent in simple systems [49]. Mangal et al. [175] evaluated RELAP5 system code effectiveness in simulating NC behavior in high-pressure NCLs and parallel channel configurations. While the code can accurately simulate single-phase NCL performance under stable flow conditions, it struggles with oscillation predictions, resulting in mismatched stability maps compared to experimental data. Stability was significantly influenced by initial conditions, wall thickness, heat loss, and power supply methods. The semi-empirical nature of RELAP5 constitutive relations also contributes to discrepancies, as they are more suitable for fully developed flows, which may not apply in test facilities. In 2013, Wang et al. [30] presented a paper aimed at evaluating the capability of Fluent CFD software to simulate the behavior of the NC. They obtained reasonable thermal-hydraulic characteristics including thermal stratification, density-driven flow, and secondary flow patterns. They found good agreement between the numerical outputs in comparison with experimental data from Misale et al. [18] and Kumar et al. [176]. Sharma et al. [32] utilized the NOLSTA code, which is designed to predict the steady-state mass flow rate and heater outlet temperature in closed-loop natural circulation thermosiphons using supercritical CO₂. This code also performs stability analyses for both open and closed-loop natural circulation under supercritical conditions and allows for the evaluation of a single-phase NCL with closed-loop boundary conditions. It considers factors such as the heat capacity of the pipe wall, the overall heat transfer coefficient for the cooler, and the internal heat transfer coefficient using empirical correlations. Additionally, NOLSTA iteratively adjusts the heater inlet temperature to align with a steady-state mass flow rate corresponding to the specified power, effectively simulating experimental outcomes. The stability maps for supercritical CO₂ at 8.1 and 9.1 MPa with HHC orientation are illustrated in Fig. 36. While NOLSTA predicts a significantly large unstable zone, the predictions align qualitatively with experimental observations, indicating instability over a range of power levels, with distinct lower and upper stable zones, and no predicted instability at higher secondary flows. The code identifies instability near the pseudo-critical region, where the fluid’s volumetric expansion coefficient is high, and it also shows the power required to achieve an average loop temperature equal to the pseudo-critical temperature for both pressures. Although one-dimensional codes typically produce larger unstable zones, the thermal capacitance of the wall plays a strong stabilizing role in the stability behavior of

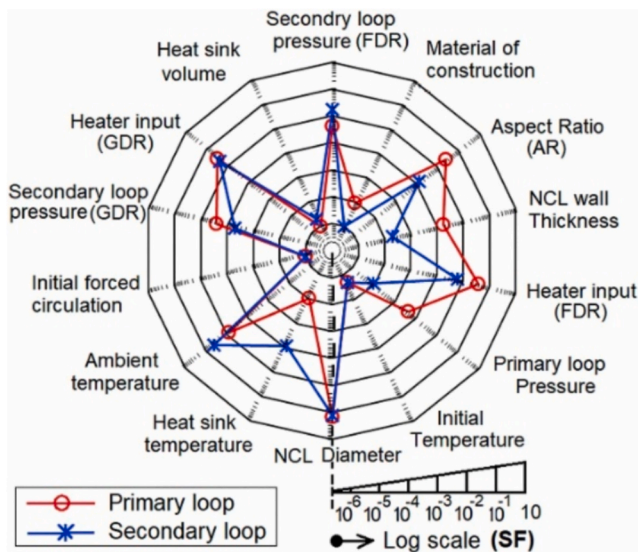


Fig. 35. Sensitivity factors (SF) of all the geometrical and operating parameters for primary and secondary loops [174]. Copyright © 2023 Elsevier Masson SAS.

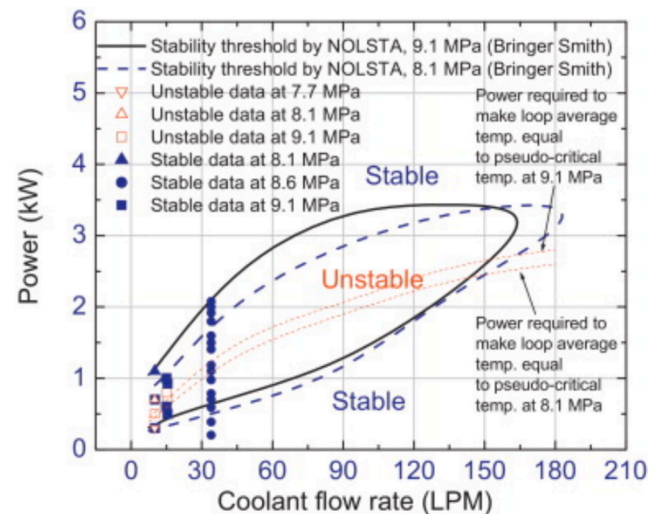


Fig. 36. Stability maps for supercritical CO₂ NCL with HHC orientation at different pressures [32]. Copyright © 2013 Elsevier B.V.

single-phase natural circulation loops. CFD codes, such as Fluent and STAR-CCM+, are well-suited for modeling 3D flows, thermal stratification, and natural circulation, making them valuable for high-fidelity local flow analysis. However, they require high computational resources and lack fully developed models for two-phase flow phenomena, which limit their accuracy in complex multiphase scenarios. In contrast, system codes like RELAP5 and TRACE are validated for system-level simulations and offer lower computational costs but cannot fully resolve 3D transient behaviors. The coupled CFD and system code approach aims to leverage the strengths of both, enhancing prediction accuracy while addressing individual shortcomings.

Hashemi-Tilehnoee et al. [1] simulated the dynamic behavior of a rectangular single-phase NCL featuring an asymmetric heater (Fig. 37). The computational demands for transient simulations in a 3D CFD model are substantial, even with relatively simple geometries, owing to the large number of cells and the very small-time steps dictated by the Courant-Friedrichs-Lewy conditions. Furthermore, CFD is essential for assessing three-dimensional effects like the movement of the Hot Pocket that cannot be determined from temperature measurements taken at limited locations.

Bozkır et al. [72] evaluated local Nusselt number variations along the heating section of an NCL by comparing numerical results with well-established correlations for hydrodynamically and thermally developing flow, such as those by Shah and London [177], Shah [178], and Siegel et al. [179] (Fig. 38). Initially, the numerical results aligned with Shah's correlations. However, Nu began to increase as $Gz^{-1} < 0.004$ dropped below 0.004 (Gz^{-1} is inverse of Graetz number), explained by Mayer and Orts [180] through the influence of natural convection. With higher Grashof and lower Reynolds numbers, Nu decreased until the flow was fully developed, then increased under natural convection effects. In comparison to Shah and London, Nu from COMSOL analyses was 96 % higher and 71 % higher at $Gz^{-1} = 0.028$, while ANSYS CFX results showed 92 % and 68 % improvements, respectively. This study found natural convection became more significant with increasing heat flux and tube diameter, shortening the thermal entrance length and raising Nu values by up to 38 % compared to [180] experimental results.

Bocanegra and Misale [181] studied the development of a 2D model of a square NCL, focuses on utilizing the LBM to model and analyze the behavior of a natural circulation loop (NCL) with different working fluids. The implementation of the model was carried out using C++

alongside the PALABOS library (a parallel solver for the Lattice Boltzmann method) [182]. Unlike traditional computational fluid dynamics (CFD) methods that solve macroscopic equations like the Navier-Stokes equations, LBM operates on a mesoscopic scale, making it highly parallelizable and effective in handling complex flow problems. The study found that the Prandtl number significantly affects both transient and steady-state behavior. The paper reports that fluids with lower Prandtl numbers exhibited more dampened oscillations and faster convergence to steady-state conditions. This implies that fluids with lower Prandtl numbers are more efficient in stabilizing the flow in NCL systems.

9. Research gaps and unexplored areas

Research on NCLs has mainly concentrated on terrestrial applications like nuclear reactors and solar energy systems. However, there is significant untapped potential for using NCLs in thermal control systems for spacecraft and other aerospace applications, an area that remains relatively under-explored in current studies. This system has not yet been extensively researched, especially for thermal control in micro spacecraft. While loop heat coolers have been studied as a promising solution for spacecraft thermal management, the supercritical CO_2 -NCL stands out for its potential to optimize performance, volume, mass, and energy consumption [215–216]. Therefore, it's crucial to conduct detailed studies on the performance of NCLs, focusing on flow behavior, heat transfer rates, and other characteristics, to fully understand their application in various gravitational environments [70]. As depicted in Fig. 39, heat from solar radiation or high-power payloads is transferred via supercritical CO_2 circulation and eventually dissipated into the cold cosmic environment.

Misale et al. [57] introduced a novel approach utilizing a quaternary NCL system (Fig. 40). While most studies focus on rectangular or circular NCLs, this experiment explored more complex loop configurations in parallel. The results revealed that both single and connected NCLs displayed stable behavior throughout the tests. Additionally, the temperature difference between the hot and cold legs exhibited a nonlinear increase as power was raised, a trend observed in both single and connected loops. Connecting the heated sections had minimal effect on NCL stability and performance, with only slight changes in the average temperature difference (T_{avg}) between the hot and cold legs. Stability and thermal performance improved with higher heat sink temperatures but decreased as power in the heated section increased.

9.1. Unaddressed research areas in aerospace

In aerospace, several NCL research areas remain underexplored. Key gaps include understanding NCL behavior in microgravity and developing high-temperature materials for space applications. NCLs could be valuable in future lunar and Martian bases, but compact, lightweight systems that meet strict space and weight requirements are needed. Further studies should focus on integrating NCLs with spacecraft thermal control systems and assessing their reliability in extreme space conditions like radiation and vacuum environments. The NCL with supercritical CO_2 was found to be highly suitable for micro spacecraft, where space, weight, and energy consumption are strictly limited. The absence of mechanical pumps enhances system reliability and reduces power needs, making the design an attractive option for space missions.

9.2. Underexplored topics in NCL research

Furthermore, certain topics within NCL research have not been thoroughly investigated. The integration of NCLs with other cooling technologies in hybrid systems is an area with limited research, despite the potential to enhance both efficiency and safety. Detailed studies on advanced fluid dynamics, especially under transient conditions and complex geometries, are scarce, and comprehensive models to accurately predict two-phase flow behavior in NCLs are still needed. The

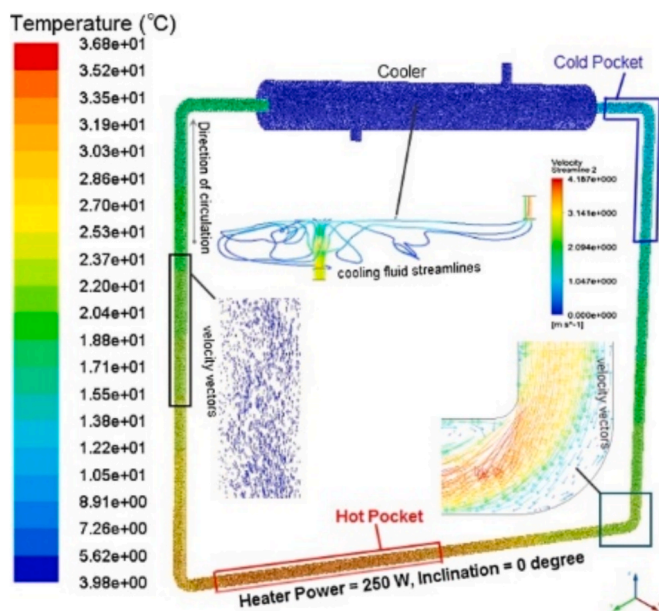


Fig. 37. Modeling the AKIAU-R-1P NCL in the 3D computational domain [1]. Copyright © 2019 Elsevier Ltd.

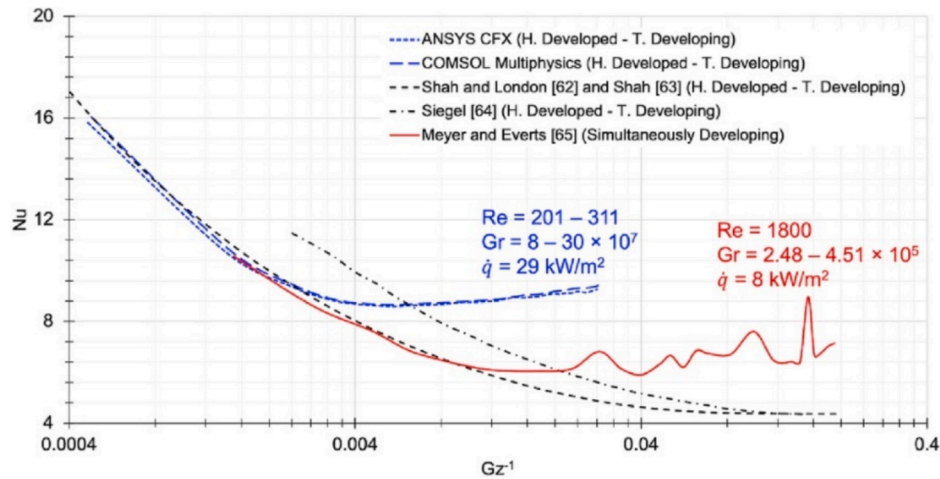


Fig. 38. Comparing the results of ANSYS CFX, and COMSOL with Shah and London [177], Shah [178] and Siegel [179] correlations. [72]. Copyright © 2023 Elsevier Ltd.

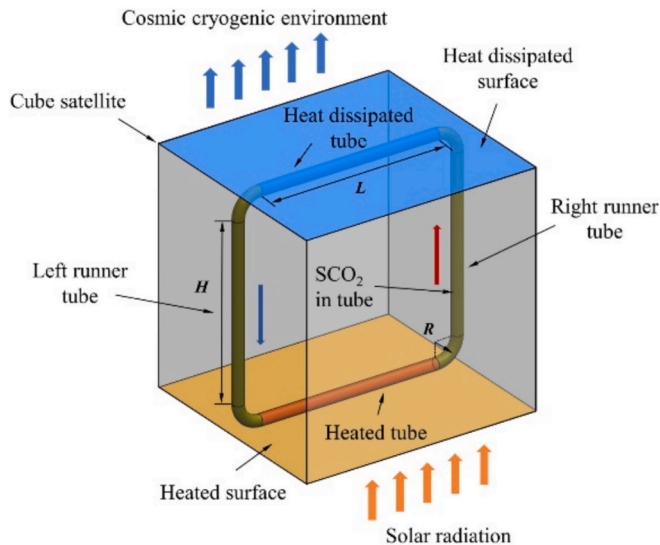


Fig. 39. The schematic diagram of NCL in the 1U CubeSat for thermal control. [70] Copyright © 2023 Elsevier Ltd.

impact of nanofluids on the thermal–hydraulic performance of NCLs is an emerging area that requires more exploration. Similarly, the effects of non-uniform heat flux distributions on NCL performance and stability are not well understood and warrant more research. Finally, long-term studies on material compatibility and corrosion in different working fluids are essential to ensure the durability of NCL systems.

10. Conclusion

Natural Circulation Loops (NCLs) offer a passive, robust means of heat transport for diverse energy systems, from nuclear reactors to solar thermal collectors. The main advantages of NCLs include increased reliability, lower maintenance costs, and enhanced energy efficiency. However, challenges such as flow oscillations, transitions between laminar and turbulent regimes, and sensitivity to boundary conditions can significantly impact their stability and overall performance. One of the most significant advancements in improving NCL efficiency is the exploration of alternative working fluids such as supercritical CO₂, liquid metals, and molten salts. Supercritical CO₂ offers high thermal conductivity and density, making it an attractive option for cooling systems, but its behavior near the critical point can lead to severe

instabilities. Studies have shown that at 50 bar, Supercritical CO₂ can provide up to seven times the heat transfer rate of water, but its unpredictable density variations require precise control of operating conditions. Liquid metals exhibit extremely high thermal conductivity and heat capacity, making them suitable for high-temperature heat removal in advanced nuclear reactors and some industrial heat transfer systems like solar power plants. However, they pose significant challenges, including severe corrosion and deposition of activated materials, requiring the development of protective coatings and corrosion-resistant materials. Molten salts, particularly fluoride and chloride-based mixtures, provide excellent thermal stability (up to 700 °C) and are widely considered for solar thermal storage and nuclear cooling applications. Nevertheless, molten salts can experience solidification in the event of system failure, which can block circulation pathways and pose operational risks. Besides the HHHC configuration well-known parameters to be used in water fluid NCL, recent studies suggest that the VHHC configuration improves the stability of molten salt-based NCLs making it a promising candidate for specific passive cooling systems. Passive stabilization techniques (e.g., orifice plates, Tesla valves, geometric tuning) offer targeted improvements but lack scalability. To further enhance the performance and stability of NCLs, researchers have explored nanofluids, which improve heat transfer and minimize flow instabilities. Adding nanoparticles such as Al₂O₃, CuO, and TiO₂ to base fluids has been shown to increase heat transfer rates and reduce thermal and hydrodynamic instabilities. Experimental studies indicate that a 12.8 % increase in mass flow rate can be achieved by increasing nanoparticle concentration, although challenges such as sedimentation and long-term changes in fluid properties remain. Hybrid nanofluids, which combine multiple nanoparticle types, have been proposed as a potential solution, but their full impact on NCL behavior requires further investigation. From the point of view of phase regime, two-phase NCLs can significantly improve heat transfer efficiency but introduce complex instabilities such as flow reversals, pressure oscillations, and density wave instability. In supercritical CO₂-based NCLs, rapid variations in density and viscosity can lead to extreme fluctuations and limit system reliability. Similarly, in liquid–metal-based NCLs, turbulent mixing and stratification effects can further complicate heat transfer processes. Researchers have used advanced numerical modeling techniques with commercial codes and software like Ansys Fluent, COMSOL, OpenFOAM, RELAP, PHOENIX, MARS, TRACE, and CATHARE to analyze these behaviors, yet significant challenges remain in predicting the full range of instabilities and there is no unified modeling framework capable of capturing all relevant behaviors across flow regimes and working fluids. The issues are the inaccurate prediction of unstable flows, high computational costs, failure to correctly capture flow

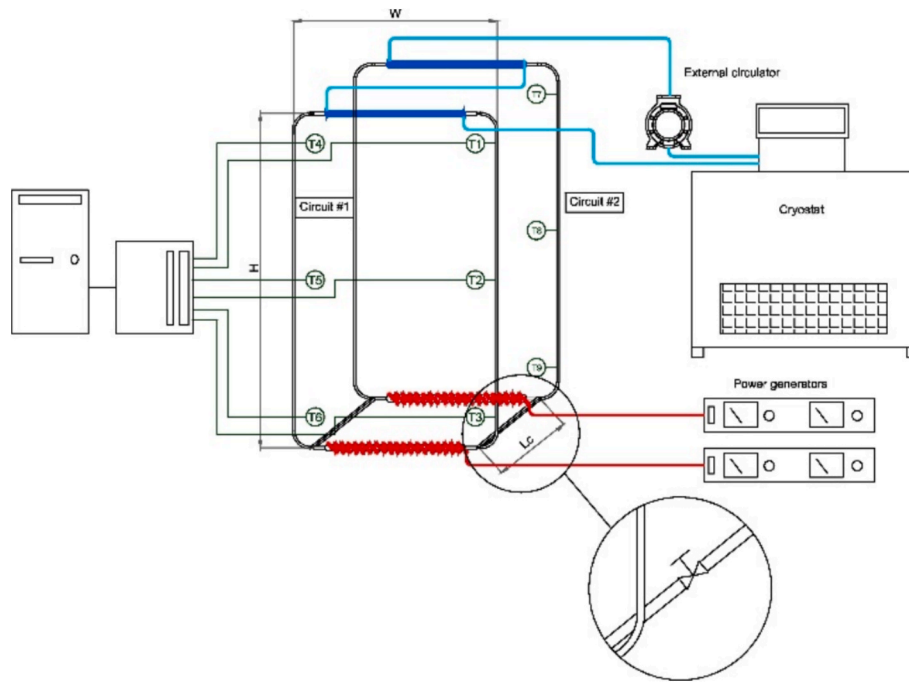


Fig. 40. Experimental setup sketch (only 2 parallel loops represented for simplicity, the real setup has 3 or 4 connected loops) [57]. Copyright © 2020 Elsevier Ltd.

reversal, and severe oscillations. From an application-oriented perspective, integrating numerical models with experimental studies and multiscale simulations (combining CFD with system codes) can significantly aid in optimizing NCL designs. This approach is particularly critical in applications where safety and rapid system response are paramount, such as nuclear reactors and emergency cooling systems. A deeper understanding of thermal–hydraulic interactions and stability boundaries is essential to developing more robust passive safety systems. Despite significant advancements in NCL technology, several research gaps remain unaddressed:

- Influence of environmental conditions: The impact of fluctuating ambient pressure and temperature on long-term NCL stability has not been fully explored.
- New loop geometries: Studies on multi-loop NCLs and integrated hybrid systems remain limited.
- Aerospace applications: The use of NCLs in spacecraft thermal management is an area with enormous potential. Given the energy limitations in spacecraft, CO₂-based NCLs could serve as efficient cooling solutions. However, the effects of microgravity on flow behavior need further investigation. Preliminary studies suggest that supercritical CO₂ loops may be a viable option for thermal control in spacecraft, but additional research is required to assess their long-term performance under extreme conditions.

Future research roadmap

To advance NCL research from case-specific studies to deployable engineering tools, we recommend the following research directions:

- Optimizing geometric design to reduce instabilities and improve efficiency in liquid metal- and molten salt-based systems.
- Investigating corrosion effects in liquid–metal and molten salt NCLs and developing advanced protective coatings.
- Utilizing hybrid nanofluids to improve heat transfer efficiency and minimize sedimentation issues.
- Exploring underrepresented fluids and micro-scale applications of NCLs in aerospace systems and electronics cooling.

- Integrating CFD models with AI-driven models as advanced hybrid modeling strategies to predict system behavior under critical conditions and improve real-time monitoring. Looking forward, efficient, safe, and sustainable NCLs are expected to be more significant in next-generation energy systems and space applications.

CRediT authorship contribution statement

M. Hashemi-Tilehnoee: Writing – review & editing, Writing – original draft, Supervision, Methodology, Formal analysis, Conceptualization. **M. Misale:** Writing – review & editing, Writing – original draft, Investigation, Conceptualization. **Seyyed Masoud Seyyedi:** Writing – original draft, Formal analysis. **E. Palomo del Barrio:** Writing – review & editing. **A. Marchitto:** Writing – review & editing, Formal analysis. **S. S. Rahim Hosseini:** Writing – original draft, Visualization, Investigation. **M. Sharifpur:** Writing – review & editing.

Declaration of competing interest

The authors declare that they have no known competing financial interests or personal relationships that could have appeared to influence the work reported in this paper.

Data availability

No data was used for the research described in the article.

References

- [1] M. Hashemi-Tilehnoee, N. Sahebi, A.S. Dogonchi, S.M. Seyyedi, S. Tashakor, Simulation of the dynamic behavior of a rectangular single-phase natural circulation vertical loop with asymmetric heater, *Int. J. Heat Mass Transf.*, 139 (2019), <https://doi.org/10.1016/j.ijheatmasstransfer.2019.05.076>.
- [2] J.B. Keller, Periodic oscillations in a model of thermal convection, *J. Fluid Mech.*, (1966), <https://doi.org/10.1017/S0022112066001423>.
- [3] P. Welander, On the oscillatory instability of a differentially heated fluid loop, *J. Fluid Mech.*, (1967), <https://doi.org/10.1017/S0022112067000606>.
- [4] K. Chen, On the oscillatory instability of closed-loop thermosyphons, *J. Heat Transfer* (1985), <https://doi.org/10.1115/1.3247510>.

- [5] P.K. Vijayan, Experimental observations on the general trends of the steady state and stability behaviour of single-phase natural circulation loops, *Nucl. Eng. Des.*, (2002), [https://doi.org/10.1016/S0029-5493\(02\)00047-X](https://doi.org/10.1016/S0029-5493(02)00047-X).
- [6] M. Misale, L. Tagliafico, TRANSIENT AND STABILITY BEHAVIOUR OF SINGLE-PHASE NATURAL CIRCULATION LOOPS, *Heat Technol.*, (1987).
- [7] Y. Zvirin, R. Greif, Transient behavior of natural circulation loops: Two vertical branches with point heat source and sink, *Int. J. Heat Mass Transf.*, (1979), [https://doi.org/10.1016/0017-9310\(79\)90053-X](https://doi.org/10.1016/0017-9310(79)90053-X).
- [8] D. Lu, X. Zhang, C. Guo, Stability analysis for single-phase liquid metal rectangular natural circulation loops, *Ann. Nucl. Energy* (2014), <https://doi.org/10.1016/j.anucene.2014.06.014>.
- [9] Y. Geng, X. Liu, X. Li, Y. Zhang, Numerical simulation of a toroidal single-phase natural circulation loop with a k-L- ω transitional turbulence model, *Nucl. Eng. Technol.*, (2024), <https://doi.org/10.1016/j.net.2023.09.030>.
- [10] F. Mascari, et al., OECD/NEA/CSNI state-of-the-art report on scaling in system thermal-hydraulics applications to nuclear reactor safety and design (The S-SOAR), *Nucl. Eng. Des.*, (2024), <https://doi.org/10.1016/j.nucengdes.2023.112750>.
- [11] F. D'Auria, Thermal-hydraulics of water cooled nuclear reactors, Woodhead Publishing (2017).
- [12] S.A. Hosseini, R. Akbari, A.S. Shirani, F. D'Auria, Analysis of the natural circulation flow map uncertainties in an integral small modular reactor, *Nucl. Eng. Des.*, (2021), <https://doi.org/10.1016/j.nucengdes.2021.111156>.
- [13] F. D'Auria, Y. Hassan, Challenges and concerns for development of nuclear thermal-hydraulics, *Nucl. Eng. Des.*, (2021), <https://doi.org/10.1016/j.nucengdes.2021.111074>.
- [14] A. Borgohain, et al., Natural circulation studies in a LBE loop for a wide range of temperature, *Nucl. Eng. Des.*, (2016), <https://doi.org/10.1016/j.nucengdes.2016.01.029>.
- [15] K.T. Agbevanu, S.K. Debrah, E.M. Arthur, E. Shitsi, "Liquid metal cooled fast reactor thermal hydraulic research development, A Review," (2023), <https://doi.org/10.1016/j.heliyon.2023.e16580>.
- [16] R. Roper, et al., "Molten salt for advanced energy applications, A Review," (2022), <https://doi.org/10.1016/j.anucene.2021.108924>.
- [17] F. D'Auria, G.M. Galassi, "Natural circulation situations relevant to nuclear power plants," *Proc. GCNEP-IAEA Course Nat. Circ. Phenom. Passiv. Saf. Syst. Adv. Water Cool. React.*, (2009).
- [18] M. Misale, P. Garibaldi, J.C. Passos, G.G. de Bitencourt, Experiments in a single-phase natural circulation mini-loop, *Exp. Therm. Fluid Sci.*, (2007), <https://doi.org/10.1016/j.expthermflusci.2006.11.004>.
- [19] S.M. Seyyedi, A.S. Dogonchi, M. Hashemi-Tilehnoee, Investigating the Orientation of the Heater and Cooler on the Performance of a Mini Natural Circulation Loop with Cu-Water Nanofluid, *Amirkabir J. Mech. Eng.*, 52 (11) (2019) 3203–3224, <https://doi.org/10.22060/mej.2019.16499.6407>.
- [20] S. Nakul, U.C. Arunachala, Stability and thermal analysis of a single-phase natural circulation looped parabolic trough receiver, *Sustain. Energy Technol. Assessm.* (2022), <https://doi.org/10.1016/j.seta.2022.102242>.
- [21] S. Nakul, U.C. Arunachala, P.K. Vijayan, Experimental and analytical study on the stability of a low aspect ratio single-phase natural circulation loop coupled to a parabolic trough collector, *Int. Commun. Heat Mass Transf.*, (2023), <https://doi.org/10.1016/j.icheatmasstransfer.2023.106751>.
- [22] T. Srivastava, D.N. Basu, Dynamic characterization of supercritical natural circulation loop under periodic excitation, *Int. J. Therm. Sci.*, (2024), <https://doi.org/10.1016/j.ijthermalsci.2023.108835>.
- [23] M. Misale, M. Froggeri, Influence of pressure drops on the behavior of a single-phase natural circulation loop: Preliminary results, *Int. Commun. Heat Mass Transf.*, (1999), [https://doi.org/10.1016/S00735-1933\(99\)00046-9](https://doi.org/10.1016/S00735-1933(99)00046-9).
- [24] W. Ambrosini, J.C. Ferreri, Prediction of stability of one-dimensional natural circulation with a low diffusion numerical scheme, *Ann. Nucl. Energy* (2003), [https://doi.org/10.1016/S0306-4549\(03\)00119-1](https://doi.org/10.1016/S0306-4549(03)00119-1).
- [25] S.K. Mousavian, M. Misale, F. D'Auria, M.A. Salehi, Transient and stability analysis in single-phase natural circulation, *Ann. Nucl. Energy* (2004), <https://doi.org/10.1016/j.anucene.2004.01.005>.
- [26] V. Chatoorgoon, A. Voodi, D. Fraser, The stability boundary for supercritical flow in natural convection loops: Part I: H₂O studies, *Nucl. Eng. Des.*, (2005), <https://doi.org/10.1016/j.nucengdes.2005.06.003>.
- [27] P.K. Vijayan, M. Sharma, D. Saha, Steady state and stability characteristics of single-phase natural circulation in a rectangular loop with different heater and cooler orientations, *Exp. Therm. Fluid Sci.*, (2007), <https://doi.org/10.1016/j.expthermflusci.2006.10.003>.
- [28] D.S. Pikhwal, W. Ambrosini, N. Forgone, P.K. Vijayan, D. Saha, J.C. Ferreri, Analysis of the unstable behaviour of a single-phase natural circulation loop with one-dimensional and computational fluid-dynamic models, *Ann. Nucl. Energy* (2007), <https://doi.org/10.1016/j.anucene.2007.01.012>.
- [29] F. Devia, M. Misale, Analysis of the effects of heat sink temperature on single-phase natural circulation loops behaviour, *Int. J. Therm. Sci.*, (2012), <https://doi.org/10.1016/j.ijthermalsci.2012.03.006>.
- [30] J.Y. Wang, T.J. Chuang, Y.M. Ferng, CFD investigating flow and heat transfer characteristics in a natural circulation loop, *Ann. Nucl. Energy* (2013), <https://doi.org/10.1016/j.anucene.2013.01.015>.
- [31] P. Naphade, A. Borgohain, R.T.K. Raj, N.K. Maheshwari, Experimental and CFD study on natural circulation phenomenon in lead bismuth eutectic loop, *Procedia Eng.* (2013), <https://doi.org/10.1016/j.proeng.2013.09.170>.
- [32] M. Sharma, P.K. Vijayan, D.S. Pikhwal, Y. Asako, Steady state and stability characteristics of natural circulation loops operating with carbon dioxide at supercritical pressures for open and closed loop boundary conditions, *Nucl. Eng. Des.*, (2013), <https://doi.org/10.1016/j.nucengdes.2013.07.023>.
- [33] S. Kang, K.S. Ha, H.T. Kim, J.H. Kim, I.C. Bang, An experimental study on natural convection heat transfer of liquid gallium in a rectangular loop, *Int. J. Heat Mass Transf.*, (2013), <https://doi.org/10.1016/j.ijheatmasstransfer.2013.07.026>.
- [34] D. Martelli, N. Forgone, G. Barone, and W. Ambrosini, "Validation of the coupled calculation between RELAP5 STH code and Ansys FLUENT CFD code," p. 23, 2014.
- [35] D. Lu, X. Zhang, C. Guo, A computing approach with the heat-loss model for the transient analysis of liquid metal natural circulation loop, *Sci. Technol. Nucl. Install.*, (2014), <https://doi.org/10.1155/2014/769346>.
- [36] A.K. Yadav, S. Bhattacharyya, M.R. Gopal, Optimum Operating Conditions for Subcritical/Supercritical Fluid-Based Natural Circulation Loops, *J. Heat Transfer* (2016), <https://doi.org/10.1115/1.4031921>.
- [37] J.Y. Kudariyawar, A.M. Vaidya, N.K. Maheshwari, P. Satyamurthy, Computational study of instabilities in a rectangular natural circulation loop using 3D CFD simulation, *Int. J. Therm. Sci.*, (2016), <https://doi.org/10.1016/j.ijthermalsci.2015.11.003>.
- [38] L. Luzzi, et al., Assessment of analytical and numerical models on experimental data for the study of single-phase natural circulation dynamics in a vertical loop, *Chem. Eng. Sci.*, (2017), <https://doi.org/10.1016/j.ces.2016.12.058>.
- [39] J.Y. Kudariyawar, A.K. Srivastava, A.M. Vaidya, N.K. Maheshwari, P. Satyamurthy, Computational and experimental investigation of steady state and transient characteristics of molten salt natural circulation loop, *Appl. Therm. Eng.*, (2016), <https://doi.org/10.1016/j.applthermaleng.2015.12.114>.
- [40] M. Krishnani, D.N. Basu, On the validity of Boussinesq approximation in transient simulation of single-phase natural circulation loops, *Int. J. Therm. Sci.*, (2016), <https://doi.org/10.1016/j.ijthermalsci.2016.03.004>.
- [41] A.K. Srivastava, J.Y. Kudariyawar, A. Borgohain, S.S. Jana, N.K. Maheshwari, P. K. Vijayan, Experimental and theoretical studies on the natural circulation behavior of molten salt loop, *Appl. Therm. Eng.*, (2016), <https://doi.org/10.1016/j.applthermaleng.2015.12.065>.
- [42] M.K.S. Sarkar, D.N. Basu, Working regime identification for natural circulation loops by comparative thermalhydraulic analyses with three fluids under identical operating conditions, *Nucl. Eng. Des.*, 293 (2015) 187–195, <https://doi.org/10.1016/j.nucengdes.2015.07.046>.
- [43] Y.H. Shin, et al., Experimental studies and computational benchmark on heavy liquid metal natural circulation in a full height-scale test loop for small modular reactors, *Nucl. Eng. Des.*, (2017), <https://doi.org/10.1016/j.nucengdes.2017.03.001>.
- [44] S. Nadella, A.K. Srivastava, N.K. Maheshwari, A semi-analytical model for linear stability analysis of rectangular natural circulation loops, *Chem. Eng. Sci.*, (2018), <https://doi.org/10.1016/j.ces.2018.08.034>.
- [45] C.C. Yue, et al., Flow characteristics of natural circulation in a lead-bismuth eutectic loop, *Nucl. Sci. Tech.*, (2017), <https://doi.org/10.1007/s41365-017-0187-x>.
- [46] S.T. Inampudi, B. Marthi, S. Sahoo, Entropy generation in water-based natural circulation loop, *J. Heat Transfer* (2018), <https://doi.org/10.1115/1.4039764>.
- [47] F.A. Braz Filho, G.B. Ribeiro, A.D. Caldeira, Fourier analysis of the RELAP5/3D adaptive time-stepping scheme on a natural circulation loop, *Ann. Nucl. Energy* (2018), <https://doi.org/10.1016/j.anucene.2017.11.018>.
- [48] A.K. Yadav, M. Ramgopal, S. Bhattacharyya, Transient analysis of subcritical/supercritical carbon dioxide based natural circulation loop with end heat exchangers: experimental study, *Heat Mass Transf. Und Stoffuebertragung* (2017), <https://doi.org/10.1007/s00231-017-2038-z>.
- [49] S.M. Seyyedi, N. Sahebi, A.S. Dogonchi, M. Hashemi-Tilehnoee, Numerical and experimental analysis of a rectangular single-phase natural circulation loop with asymmetric heater position, *Int. J. Heat Mass Transf.*, (2019), <https://doi.org/10.1016/j.ijheatmasstransfer.2018.11.030>.
- [50] A. Dass, S. Gedupudi, 1-D semi-analytical modeling and parametric study of a single phase rectangular Coupled Natural Circulation Loop, *Chem. Eng. Sci.*, (2019), <https://doi.org/10.1016/j.ces.2019.05.050>.
- [51] Z. Li, P. Gao, Y. Lin, Y. Zhang, P. Ji, C. Zou, Investigation on flow instability in a natural circulation loop with rod bundles, *Ann. Nucl. Energy* (2019), <https://doi.org/10.1016/j.anucene.2019.04.027>.
- [52] D.N. Basu, Dynamic frequency response of a single-phase natural circulation loop under an imposed sinusoidal excitation, *Ann. Nucl. Energy* (2019), <https://doi.org/10.1016/j.anucene.2019.06.050>.
- [53] R. Chouhan, A. Borgohain, A. K. Shrivastava, N. K. Maheshwari, P.K. Vijayan, "CFD analysis of molten fluoride salt natural circulation in a rectangular loop," in *Thorium—Energy for the Future*, 2019. doi: 10.1007/978-981-13-2658-5_36.
- [54] L. Liu, P. Peterson, D. Zhang, I. Johnson, S. Qiu, G.H. Su, Scaling and distortion analysis using a simple natural circulation loop for FHR development, *Appl. Therm. Eng.*, (2020), <https://doi.org/10.1016/j.applthermaleng.2019.114849>.
- [55] I. Thili, S.M. Seyyedi, A.S. Dogonchi, M. Hashemi-Tilehnoee, D.D. Ganji, Analysis of a single-phase natural circulation loop with hybrid-nanofluid, *Int. Commun. Heat Mass Transf.*, (2020), <https://doi.org/10.1016/j.icheatmasstransfer.2020.104498>.
- [56] G. Raveesh, R. Adarsh, S. Rupesh, Orifice enabled flow stabilization of natural circulation loop at lower inclinations, *Kerntechnik* (2020), <https://doi.org/10.3139/124.190088>.
- [57] M. Misale, J.A. Bocanegra, D. Borelli, A. Marchitto, Experimental analysis of four parallel single-phase natural circulation loops with small inner diameter, *Appl. Therm. Eng.*, (2020), <https://doi.org/10.1016/j.applthermaleng.2020.115739>.
- [58] T. Srivastava, P. Sutradhar, M.K.S. Sarkar, D.N. Basu, "Supercritical natural circulation loop: A technology for future reactor", *Handbook of Research on*

- Advancements in Supercritical Fluids Applications for Sustainable, Energy Syst. (2020), <https://doi.org/10.4018/978-1-7998-5796-9.ch009>.
- [59] D. Hariyanto, S. Permana, and Supriyadi, "Experimental and simulation approach of the loop geometry effect on the natural circulation system of the advanced nuclear reactor," *Int. J. Energy Res.*, (2021) <https://doi.org/10.1002/er.5903>.
- [60] E. Yun, B.G. Jeon, H.S. Park, Experimental study on a single-phase natural circulation loop and its steady-state solution, *Appl. Therm. Eng.*, (2020), <https://doi.org/10.1016/j.applthermaleng.2020.115190>.
- [61] A. Battistini, A. Cammi, S. Lorenzi, M. Colombo, M. Fairweather, Development of a CFD – LES model for the dynamic analysis of the DYNASTY natural circulation loop, *Chem. Eng. Sci.*, (2021), <https://doi.org/10.1016/j.ces.2021.116520>.
- [62] M. Misale, J.A. Bocanegra, A. Marchitto, Thermo-hydraulic performance of connected single-phase natural circulation loops characterized by two different inner diameters, *Int. Commun. Heat Mass Transf.*, (2021), <https://doi.org/10.1016/j.icheatmasstransfer.2021.105309>.
- [63] D.N. Elton, U.C. Arunachala, P.K. Vijayan, Stability enhancement in large diameter rectangular natural circulation loops using flow restrictors, *Int. Commun. Heat Mass Transf.*, (2021), <https://doi.org/10.1016/j.icheatmasstransfer.2021.105412>.
- [64] A. Dass, S. Gedupudi, Numerical investigation on the heat transfer coefficient jump in tilted single-phase natural circulation loop and coupled natural circulation loop, *Int. Commun. Heat Mass Transf.*, (2021), <https://doi.org/10.1016/j.icheatmasstransfer.2020.104920>.
- [65] B.S. Jinshah, R.K. Kottala, K.R. Balasubramanian, A. Francis, Experimental analysis of phase change material integrated single phase natural circulation loop, *Mater. Today Proc.* (2019), <https://doi.org/10.1016/j.matpr.2021.04.251>.
- [66] T.M. Schriener, M.S. El-Genk, Gas-lift enhanced natural circulation of alkali and heavy liquid metals for passive cooling of nuclear reactors, *Int. J. Multiph. Flow* (2021), <https://doi.org/10.1016/j.ijmultiphaseflow.2021.103783>.
- [67] D. Hariyanto, A. Waris, Supriyadi, Computational fluid dynamics analysis of the natural circulation system in vertical heater horizontal cooler (VHHC) molten salt loop, *J. Phys. Conf. Ser.* (2022), <https://doi.org/10.1088/1742-6596/2243/1/012057>.
- [68] A. Dass, S. Gedupudi, Stability analysis of a single phase rectangular coupled natural circulation loop system employing a Fourier series based 1-D model, *Chem. Eng. Sci.*, (2022), <https://doi.org/10.1016/j.ces.2021.116900>.
- [69] Q. Cai, F. D'Auria, K. Umminger, D. Bestion, J. Shan, Prioritizing pressure drop research in nuclear thermal hydraulics, *Prog. Nucl. Energy* (2022), <https://doi.org/10.1016/j.pnucene.2022.104358>.
- [70] Z. Gao, K. Qiao, J. Bai, Z. Wang, H. Liu, P. Li, Numerical investigation of natural circulation loop with supercritical CO₂ on the thermal control system of micro spacecrafts, *Int. J. Heat Mass Transf.*, (2023), <https://doi.org/10.1016/j.ijheatmasstransfer.2023.124661>.
- [71] M. Sahu, J. Sarkar, L. Chandra, Experimental study on energy-exergy performance of single-phase natural circulation loop using mono/hybrid nano-oils, *Int. J. Therm. Sci.*, (2023), <https://doi.org/10.1016/j.ijthermalsci.2023.108554>.
- [72] S.C. Bozkır, N. Çobanoğlu, S. Doğanay, Z.H. Karadeniz, E.B. Elçiöğlü, A. Turgut, Investigation of external magnetic field effect on the performance of ferrofluid-based single-phase natural circulation loops, *Therm. Sci. Eng. Prog.*, (2023), <https://doi.org/10.1016/j.tsep.2023.101921>.
- [73] J.A. Bocanegra, A. Marchitto, M. Misale, Study of a square single-phase natural circulation loop using the lattice boltzmann method, *Appl. Mech.*, (2023), <https://doi.org/10.3390/applmech4030048>.
- [74] P. Subramanian, A. Dass, S. Tiwari, S. Gedupudi, Fourier series-based modelling of the effects of thermal coupling on the transient dynamics of component loops in a coupled natural circulation loop, *Chem. Eng. Sci.*, 296 (December) (2024) 120176, <https://doi.org/10.1016/j.ces.2024.120176>.
- [75] G. Angelo, E. Angelo, N.L. Scuro, W.M. Torres, D.A. Andrade, Verification and validation of seven turbulence models for a natural circulation loop under transient conditions, *Ann. Nucl. Energy* 206 (May) (2024) 110612, <https://doi.org/10.1016/j.anucene.2024.110612>.
- [76] V. Boopalan, S. Kumar Arumugam, P. Rajesh Kanna, Effect of operating regimes on the heat transfer and buoyancy characteristics of supercritical CO₂ natural circulation loop - A numerical study, *Therm. Sci. Eng. Prog.*, 50 (January) (2024) 102579, <https://doi.org/10.1016/j.tsep.2024.102579>.
- [77] H. Li, et al., Natural circulation transient thermal-hydraulic analysis and corrosion precipitation study in a LBE flow loop, *Nucl. Eng. Des.*, (2024), <https://doi.org/10.1016/j.nucengdes.2024.112975>.
- [78] Y. Zvirin, A. Shitzer, G. Grossman, The natural circulation solar heater-models with linear and nonlinear temperature distributions, *Int. J. Heat Mass Transf.*, (1977), [https://doi.org/10.1016/0017-9310\(77\)90072-2](https://doi.org/10.1016/0017-9310(77)90072-2).
- [79] J.C. Chato, Natural convection flows in parallel-channel systems, *J. Heat Transfer* (1963), <https://doi.org/10.1115/1.3686122>.
- [80] P.K. Vijayan, H. Austregesilo, V. Teschendorff, Simulation of the unstable oscillatory behavior of single-phase natural circulation with repetitive flow reversals in a rectangular loop using the computer code athlet, *Nucl. Eng. Des.*, (1995), [https://doi.org/10.1016/0029-5493\(94\)00972-2](https://doi.org/10.1016/0029-5493(94)00972-2).
- [81] M. Misale, Overview on Single-Phase Natural Circulation Loops, *Proc. Intl. Conf. Adv. Mech. Autom. Eng.*, (2014).
- [82] K.R. Balasubramanian, B.S. Jinshah, K. Ravikumar, S. Divakar, Thermal and hydraulic characteristics of a parabolic trough collector based on an open natural circulation loop: The effect of fluctuations in solar irradiance, *Sustain. Energy Technol. Assessments* (2022), <https://doi.org/10.1016/j.seta.2022.102290>.
- [83] L. Chen, X.R. Zhang, H. Yamaguchi, Z.S. Liu, Effect of heat transfer on the instabilities and transitions of supercritical CO₂ flow in a natural circulation loop, *Int. J. Heat Mass Transf.*, (2010), <https://doi.org/10.1016/j.ijheatmasstransfer.2010.05.030>.
- [84] M. Misale, F. Devia, P. Garibaldi, Experiments with Al 20 3 nanofluid in a single-phase natural circulation mini-loop: Preliminary results, *Appl. Therm. Eng.*, 40 (2012) 64–70, <https://doi.org/10.1016/j.applthermaleng.2012.01.053>.
- [85] A.K. Yadav, M. Ram Gopal, S. Bhattacharyya, Transient analysis of subcritical/supercritical carbon dioxide based natural circulation loops with end heat exchangers: Numerical studies, *Int. J. Heat Mass Transf.*, (2014), <https://doi.org/10.1016/j.ijheatmasstransfer.2014.07.068>.
- [86] M. Misale, M. Frogheri, Stabilization of a single-phase natural circulation loop by pressure drops, *Exp. Therm. Fluid Sci.*, (2001), [https://doi.org/10.1016/S0894-1777\(01\)00075-9](https://doi.org/10.1016/S0894-1777(01)00075-9).
- [87] V. Chatoorgoon, Stability of supercritical fluid flow in a single-channel natural-convection loop, *Int. J. Heat Mass Transf.*, (2001), [https://doi.org/10.1016/S0017-9310\(00\)00218-0](https://doi.org/10.1016/S0017-9310(00)00218-0).
- [88] L. Cammarata, A. Fichera, A. Pagano, Stability maps for rectangular circulation loops, *Appl. Therm. Eng.*, (2003), [https://doi.org/10.1016/S1359-4311\(03\)00027-9](https://doi.org/10.1016/S1359-4311(03)00027-9).
- [89] V. Chatoorgoon and P. Upadhye, "Analytical studies of supercritical flow instability in natural convection loops," Avignon, Fr., 2005.
- [90] A.K. Nayak, M.R. Gartia, P.K. Vijayan, Nanofluids: A novel promising flow stabilizer in natural circulation systems, *AIChE J.*, (2009), <https://doi.org/10.1002/aic.11659>.
- [91] P.K. Jain, Rizwan-uddin, Numerical analysis of supercritical flow instabilities in a natural circulation loop, *Nucl. Eng. Des.* (2008), <https://doi.org/10.1016/j.nucengdes.2007.10.034>.
- [92] M. Misale, P. Garibaldi, L. Tarozzi, G.S. Barozzi, Influence of thermal boundary conditions on the dynamic behaviour of a rectangular single-phase natural circulation loop, *Int. J. Heat Fluid Flow* (2011), <https://doi.org/10.1016/j.ijheatfluidflow.2010.12.003>.
- [93] B.T. Swapnalee, P.K. Vijayan, A generalized flow equation for single phase natural circulation loops obeying multiple friction laws, *Int. J. Heat Mass Transf.*, (2011), <https://doi.org/10.1016/j.ijheatmasstransfer.2011.01.023>.
- [94] D.N. Basu, S. Bhattacharyya, P.K. Das, Performance comparison of rectangular and toroidal natural circulation loops under steady and transient conditions, *Int. J. Therm. Sci.*, (2012), <https://doi.org/10.1016/j.ijthermalsci.2012.02.011>.
- [95] M. Krishnani, D.N. Basu, Computational stability appraisal of rectangular natural circulation loop: Effect of loop inclination, *Ann. Nucl. Energy* (2017), <https://doi.org/10.1016/j.anucene.2017.04.012>.
- [96] S. Sadhu, M. Ramgopal, S. Bhattacharyya, Experimental studies on an air-cooled natural circulation loop based on supercritical carbon dioxide – Part A: Steady state operation, *Appl. Therm. Eng.*, (2018), <https://doi.org/10.1016/j.applthermaleng.2017.10.017>.
- [97] R. Saha, K. Ghosh, A. Mukhopadhyay, S. Sen, Dynamic characterization of a single phase square natural circulation loop, *Appl. Therm. Eng.*, (2018), <https://doi.org/10.1016/j.applthermaleng.2017.09.092>.
- [98] B. Deng, L. Chen, X. Zhang, L. Jin, The flow transition characteristics of supercritical CO₂ based closed natural circulation loop (NCL) system, *Ann. Nucl. Energy* (2019), <https://doi.org/10.1016/j.anucene.2019.04.032>.
- [99] H. Cheng, H. Lei, L. Zeng, C. Dai, Experimental investigation of single-phase natural circulation in a mini-loop driven by heating and cooling fluids, *Exp. Therm. Fluid Sci.*, (2019), <https://doi.org/10.1016/j.expthermfluidsci.2019.01.003>.
- [100] D.N. Elton, U.C. Arunachala, P.K. Vijayan, Investigations on the dependence of the stability threshold on different operating procedures in a single-phase rectangular natural circulation loop, *Int. J. Heat Mass Transf.*, (2020), <https://doi.org/10.1016/j.ijheatmasstransfer.2020.120264>.
- [101] T. Srivastava, D.N. Basu, Numerical characterization of heat transfer deterioration in supercritical natural circulation loop and role of loop inclination, *Nucl. Eng. Des.*, (2022), <https://doi.org/10.1016/j.nucengdes.2022.111704>.
- [102] A.K. Srivastava, N. Saikrishna, N.K. Maheshwari, Linear and Nonlinear Stability Analysis of Molten Salt Natural Circulation Loop, *J. Nucl. Eng. Radiat. Sci.*, (2023), <https://doi.org/10.1115/1.4063040>.
- [103] S. Nakul, A. U. C., "Computational and analytical study on the stability and utility aspects of single-phase natural circulation loop in parabolic trough collector," *Int. J. Therm. Sci.*, 2024, doi: 10.1016/j.ijthermalsci.2023.108817.
- [104] D.N. Basu, S. Bhattacharyya, P.K. Das, Effect of geometric parameters on steady-state performance of single-phase NCL with heat loss to ambient, *Int. J. Therm. Sci.*, (2008), <https://doi.org/10.1016/j.ijthermalsci.2007.11.010>.
- [105] M. Misale, "Experimental study on the influence of power steps on the thermohydraulic behavior of a natural circulation loop," 2016. doi: 10.1016/j.ijheatmasstransfer.2016.04.036.
- [106] J.A. Bocanegra, A. Marchitto, M. Misale, Parallel connected natural circulation loops using different working fluids: experimental results, *Journal of Physics: Conference Series* (2024), <https://doi.org/10.1088/1742-6596/2685/1/012072>.
- [107] V. Goyal, V. Hassija, V. Pandey, S. Singh, Non-linear dynamics of single phase rectangular natural circulation loop, *Prog. Nucl. Energy* (2020), <https://doi.org/10.1016/j.pnucene.2020.103530>.
- [108] A. Cammi, M. Misale, F. Devia, M.T. Cauzzi, A. Pini, L. Luzzi, Stability analysis by means of information entropy: Assessment of a novel method against natural circulation experimental data, *Chem. Eng. Sci.*, (2017), <https://doi.org/10.1016/j.ces.2017.03.036>.
- [109] T. Wahidi, R.A. Chandavar, A.K. Yadav, Stability enhancement of supercritical CO₂ based natural circulation loop using a modified Tesla valve, *J. Supercrit. Fluids* (2020), <https://doi.org/10.1016/j.supflu.2020.105020>.

- [110] H. Cheng, H. Lei, L. Zeng, C. Dai, Theoretical and experimental studies of heat transfer characteristics of a single-phase natural circulation mini-loop with end heat exchangers, *Int. J. Heat Mass Transf.*, (2019), <https://doi.org/10.1016/j.ijheatmasstransfer.2018.08.136>.
- [111] P. Garibaldi, M. Misale, Experiments in single-phase natural circulation miniloops with different working fluids and geometries, *J. Heat Transfer* (2008), <https://doi.org/10.1115/1.2948393>.
- [112] C. Dai, L. Zeng, H. Lei, Heat transfer enhancement based on single phase natural circulation loops, *Int. J. Heat Mass Transf.*, (2020), <https://doi.org/10.1016/j.ijheatmasstransfer.2020.119601>.
- [113] FAO, Carbon sequestration in dryland soils. 2004.
- [114] F. D'Auria, M. Lanfredini, V&V&C in nuclear reactor thermal-hydraulics, *Nucl. Eng. Des.*, (2019), <https://doi.org/10.1016/j.nucengdes.2019.110162>.
- [115] J.M. Blackburn, D.P. Long, A. Cabañas, J.J. Watkins, Deposition of conformal copper and nickel films from supercritical carbon dioxide, *Science* (80-), (2001), <https://doi.org/10.1126/science.1064148>.
- [116] F.C.V.N. Fourie, C.E. Schwarz, J.H. Knoetze, Phase equilibria of alcohols in supercritical fluids. Part I. the effect of the position of the hydroxyl group for linear C8 alcohols in supercritical carbon dioxide, *J. Supercrit. Fluids* (2008), <https://doi.org/10.1016/j.supflu.2008.07.001>.
- [117] V. Dostal, P. Hejzlar, M.J. Driscoll, The supercritical carbon dioxide power cycle: Comparison to other advanced power cycles, *Nucl. Technol.*, (2006), <https://doi.org/10.13182/NT06-A3734>.
- [118] H. Yamaguchi, X.R. Zhang, K. Fujima, Basic study on new cryogenic refrigeration using CO₂ solid-gas two phase flow, *Int. J. Refrig.*, (2008), <https://doi.org/10.1016/j.ijrefrig.2007.08.001>.
- [119] P. Neksa, H. Reksad, G.R. Zakeri, P.A. Schiefloe, CO₂-heat pump water heater: Characteristics, system design and experimental results, *Int. J. Refrig.*, (1998), [https://doi.org/10.1016/S0140-7007\(98\)00017-6](https://doi.org/10.1016/S0140-7007(98)00017-6).
- [120] V. Archana, A.M. Vaidya, P.K. Vijayan, Numerical modeling of supercritical CO₂ natural circulation loop, *Nucl. Eng. Des.*, 293 (2015), <https://doi.org/10.1016/j.nucengdes.2015.07.030>.
- [121] P. K. Vijayan et al., "Investigations on the effect of heater and cooler orientation on the steady state, transient and stability behaviour of single-phase natural circulation in a rectangular loop," 2002.
- [122] K. Kiran Kumar, M. Ram Gopal, Experimental studies on CO₂ based single and two-phase natural circulation loops, *Appl. Therm. Eng.*, 31 (16) (2011) 3437–3443, <https://doi.org/10.1016/j.applthermaleng.2011.06.029>.
- [123] F. Parisio, V. Vilarrasa, Sinking CO₂ in Supercritical Reservoirs, *Geophys. Res. Lett.*, (2020), <https://doi.org/10.1029/2020GL090456>.
- [124] B.T. Swapnalee, P.K. Vijayan, M. Sharma, D.S. Pilkhwal, Steady state flow and static instability of supercritical natural circulation loops, *Nucl. Eng. Des.*, (2012), <https://doi.org/10.1016/j.nucengdes.2012.01.002>.
- [125] Z. Guo, L. Rüpke, C. Tao, HydrothermalFoam v1.0: A 3-D hydrothermal transport model for natural submarine hydrothermal systems, *Geosci. Model Dev.*, (2020), <https://doi.org/10.5194/gmd-13-6547-2020>.
- [126] K. Kiran Kumar, M. Ram Gopal, Steady-state analysis of CO₂ based natural circulation loops with end heat exchangers, *Appl. Therm. Eng.*, (2009), <https://doi.org/10.1016/j.applthermaleng.2008.08.002>.
- [127] A.K. Yadav, M.R. Gopal, S. Bhattacharyya, CO₂ based natural circulation loops: new correlations for friction and heat transfer, *Int. J. Heat Mass Transf.*, 55 (17–18) (2012) 4621–4630.
- [128] S.K. Rai, P. Kumar, V. Panwar, Numerical analysis of influence of geometry and operating parameters on Ledinegg and dynamic instability on supercritical water natural circulation loop, *Nucl. Eng. Des.*, (2020), <https://doi.org/10.1016/j.nucengdes.2020.110830>.
- [129] F. Világi, et al., Leakage estimation of the high-pressure and high-temperature natural circulation helium loop, *Ann. Nucl. Energy* (2020), <https://doi.org/10.1016/j.anucene.2020.107584>.
- [130] M. Vach, B. Knížat, Mathematical model of unsteady flow in a natural circulation helium loop, *Appl. Therm. Eng.*, (2024), <https://doi.org/10.1016/j.applthermaleng.2023.121916>.
- [131] H. Furci, B. Baudouy, A. Four, Inhibition of premature transient boiling crisis induced by heat-load step pulses in a helium natural circulation loop by dynamic initial condition, *Int. J. Heat Mass Transf.*, (2018), <https://doi.org/10.1016/j.ijheatmasstransfer.2018.02.105>.
- [132] A.K. Srivastava, N. Saikrishna, N.K. Maheshwari, Steady state performance of molten salt natural circulation loop with different orientations of heater and cooler, *Appl. Therm. Eng.*, (2023), <https://doi.org/10.1016/j.applthermaleng.2022.119318>.
- [133] J. Reis, J. Seo, Y. Hassan, Consequences of molten salt solidification in a natural circulation flow visualization loop due to heater failure, *Nucl. Eng. Des.*, 424 (2024) 113278.
- [134] J.A. Choi, S.U.S. Eastman, Enhancing thermal conductivity of fluids with nanoparticles, *Am. Soc. Mech. Eng. Fluids Eng. Div. FED* (1995).
- [135] B. Sun, C. Peng, D. Yang, H. Li, Effect of the wick and the working medium on the thermal resistance of FPHP, *Front. Energy Res.*, (2018), <https://doi.org/10.3389/feng.2018.00037>.
- [136] A. M. Hussein, R. A. Bakar, and K. Kadrigama, "Erratum: Study of forced convection nanofluid heat transfer in the automotive cooling system. Case Stud. Therm. Eng. 16 (2014) 50-61 DOI: 10.1016/j.csite.2013.12.001." 2015. doi: 10.1016/j.csite.2015.03.005.
- [137] K.Y. Leong, R. Saidur, S.N. Kazi, A.H. Mamun, Performance investigation of an automotive car radiator operated with nanofluid-based coolants (nanofluid as a coolant in a radiator), *Appl. Therm. Eng.*, (2010), <https://doi.org/10.1016/j.applthermaleng.2010.07.019>.
- [138] W. Chen, C. Zou, X. Li, Application of large-scale prepared MWCNTs nanofluids in solar energy system as volumetric solar absorber, *Sol. Energy Mater. Sol. Cells* (2019), <https://doi.org/10.1016/j.solmat.2019.109931>.
- [139] A.K. Nayak, M.R. Gartia, P.K. Vijayan, Thermal-hydraulic characteristics of a single-phase natural circulation loop with water and Al₂O₃ nanofluids, *Nucl. Eng. Des.*, 239 (3) (2009) 526–540, <https://doi.org/10.1016/j.nucengdes.2008.11.014>.
- [140] C.J. Ho, Y.N. Chung, C.M. Lai, Thermal performance of Al₂O₃/water nanofluid in a natural circulation loop with a mini-channel heat sink and heat source, *Energy Convers. Manag.*, (2014), <https://doi.org/10.1016/j.enconman.2014.07.079>.
- [141] S. Doganay, A. Turgut, Enhanced effectiveness of nanofluid based natural circulation mini loop, *Appl. Therm. Eng.*, (2015), <https://doi.org/10.1016/j.applthermaleng.2014.10.083>.
- [142] H.D. Koca, S. Doganay, A. Turgut, Thermal characteristics and performance of Ag-water nanofluid: Application to natural circulation loops, *Energy Convers. Manag.*, (2017), <https://doi.org/10.1016/j.enconman.2016.12.058>.
- [143] S. Thomas, C.B. Sobhan, Stability and transient performance of vertical heater vertical cooler natural circulation loops with metal oxide nanoparticle suspensions, *Heat Transf. Eng.*, (2018), <https://doi.org/10.1080/01457632.2017.1338859>.
- [144] R.B. Bejjam, K. Kiran Kumar, K. Balasubramanian, Experimental studies on nanofluid-based rectangular natural circulation loop, *J. Therm. Sci. Eng. Appl.*, (2019), <https://doi.org/10.1115/1.4043760>.
- [145] Z. Ghorbanali, S. Talebi, Investigation of a nanofluid-based natural circulation loop, *Prog. Nucl. Energy* (2020), <https://doi.org/10.1016/j.pnucene.2020.103494>.
- [146] M. Sahu, J. Sarkar, L. Chandra, Steady-state and transient hydrothermal analyses of single-phase natural circulation loop using water-based tri-hybrid nanofluids, *AIChE J.*, 67 (6) (2021) 1–12, <https://doi.org/10.1002/aic.17179>.
- [147] M. Misale, J.A. Bocanegra, A. Marchitto, Long-term experimental study on gravitational sedimentation of water aluminum oxide nanofluid at different volumetric concentrations, *Int. J. Sediment Res.*, (2023), <https://doi.org/10.1016/j.ijsrc.2023.01.002>.
- [148] J.A. Bocanegra, A. Marchitto, M. Misale, "Nanofluids in solar collectors: a comprehensive review focused on its sedimentation," *Clean Technol. Environ. Policy* (2024) 1–32.
- [149] C.M. Alexander, J.C. Dabrowiak, J. Goodisman, Gravitational sedimentation of gold nanoparticles, *J. Colloid Interface Sci.*, (2013), <https://doi.org/10.1016/j.jcis.2013.01.005>.
- [150] S. Chakraborty, P.K. Panigrahi, "Stability of nanofluid, A Review," (2020), <https://doi.org/10.1016/j.applthermaleng.2020.115259>.
- [151] X. Liu, G. Chen, C. Su, Effects of material properties on sedimentation and aggregation of titanium dioxide nanoparticles of anatase and rutile in the aqueous phase, *J. Colloid Interface Sci.*, (2011), <https://doi.org/10.1016/j.jcis.2011.06.085>.
- [152] S. Chakraborty, An investigation on the long-term stability of TiO₂ nanofluid, *Mater. Today Proc.* (2019), <https://doi.org/10.1016/j.matpr.2019.03.032>.
- [153] H.T. Zhu, Y.S. Lin, Y.S. Yin, A novel one-step chemical method for preparation of copper nanofluids, *J. Colloid Interface Sci.*, (2004), <https://doi.org/10.1016/j.jcis.2004.04.026>.
- [154] S.A. Kumar, K.S. Meenakshi, B.R.V. Narashimhan, S. Srikanth, G. Arthanareeswaran, Synthesis and characterization of copper nanofluid by a novel one-step method, *Mater. Chem. Phys.*, (2009), <https://doi.org/10.1016/j.matchemphys.2008.07.027>.
- [155] J. Wang, G. Li, H. Zhu, J. Luo, B. Sundén, Experimental investigation on convective heat transfer of ferrofluids inside a pipe under various magnet orientations, *Int. J. Heat Mass Transf.*, (2019), <https://doi.org/10.1016/j.ijheatmasstransfer.2018.12.023>.
- [156] D. Zhen, J. Wang, Y. Pang, Z. Chen, B. Sundén, HEAT TRANSFER PERFORMANCE AND FRICTION FACTOR OF VARIOUS NANOFLOIDS IN A DOUBLE-TUBE COUNTER FLOW HEAT EXCHANGER, *Therm. Sci.*, (2020), <https://doi.org/10.2298/TSCI200323280Z>.
- [157] D. Zheng, J. Wang, Z. Chen, J. Baleta, B. Sundén, Performance analysis of a plate heat exchanger using various nanofluids, *Int. J. Heat Mass Transf.*, 158 (2020) 119993.
- [158] Z. Chen, D. Zheng, J. Wang, L. Chen, B. Sundén, Experimental investigation on heat transfer characteristics of various nanofluids in an indoor electric heater, *Renew. Energy* (2020), <https://doi.org/10.1016/j.renene.2019.09.036>.
- [159] J. Wang, Z. Zhai, D. Zheng, L. Yang, B. Sundén, Investigation of Heat Transfer Characteristics of Al₂O₃-Water Nanofluids in an Electric Heater, *Heat Transf. Eng.*, (2021), <https://doi.org/10.1080/01457632.2020.1818427>.
- [160] J. Wang, G. Li, T. Li, M. Zeng, B. Sundén, Effect of various surfactants on stability and thermophysical properties of nanofluids, *J. Therm. Anal. Calorim.*, 143 (2021) 4057–4070.
- [161] D. Zheng, J. Yang, J. Wang, S. Kabelac, B. Sundén, Analyses of thermal performance and pressure drop in a plate heat exchanger filled with ferrofluids under a magnetic field, *Fuel* (2021), <https://doi.org/10.1016/j.fuel.2021.120432>.
- [162] A.K. Nayak, P.P. Kulkarni, P.K. Vijayan, Study on the transient and stability behaviour of a boiling two-phase natural circulation loop with Al₂O₃ nanofluids, *Appl. Therm. Eng.*, (2011), <https://doi.org/10.1016/j.applthermaleng.2011.02.009>.
- [163] F. D. Auria, A. Lombardi-Costa, and A. Bousbia-Salah, "Joint ICTP-IAEA Course on Natural Circulation Phenomena and Passive Safety Systems in Advanced Water Cooled Reactors," 2010.

- [164] J.H. Song, Performance of a two-phase natural circulation in a rectangular loop, *Nucl. Eng. Des.*, (2012), <https://doi.org/10.1016/j.nucengdes.2012.01.006>.
- [165] N. Goudarzi, S. Talebi, Linear stability analysis of a double-channel two-phase natural circulation loop, *Prog. Nucl. Energy* (2013), <https://doi.org/10.1016/j.pnucene.2013.04.006>.
- [166] N. Goudarzi, S. Talebi, Improving performance of two-phase natural circulation loops by reducing of entropy generation, *Energy* (2015), <https://doi.org/10.1016/j.energy.2015.09.101>.
- [167] C. Peng, W. Zhuo, Y. Zan, J. Xu, X. Lu, Y. Huang, Investigation on Pressure Drop Oscillation in Two-Phase Natural Circulation system, *Hedongli Gongcheng/ Nuclear Power Eng.*, (2017), <https://doi.org/10.13832/j.jnpe.2017.04.0178>.
- [168] F. D'Auria, G.M. Galassi, Characterization of instabilities during two-phase natural circulation in typical PWR conditions, *Exp. Therm. Fluid Sci.*, (1990), [https://doi.org/10.1016/0894-1777\(90\)90081-H](https://doi.org/10.1016/0894-1777(90)90081-H).
- [169] D.D. Lisowski, O. Omotowa, M.A. Muci, A. Tokuhiko, M.H. Anderson, M. L. Corradini, Influences of boil-off on the behavior of a two-phase natural circulation loop, *Int. J. Multiph. Flow* (2014), <https://doi.org/10.1016/j.ijmultiphaseflow.2013.12.005>.
- [170] D. Franken, Z. Ahmed, S. Eckels, S. Eckels, H. Bindra, Impact of dissolved salts on two-phase flow and boiling heat transfer in a natural circulation loop, *Chem. Eng. Sci.*, (2019), <https://doi.org/10.1016/j.ces.2019.05.046>.
- [171] A. Li, Y. Chen, Y. Rao, K. Ouyang, Research on characteristic of flow instability in a two-phase natural circulation loop with parallel once-through steam generators, *Int. J. Adv. Nucl. React. Des. Technol.*, 5 (4) (2023) 189–199, <https://doi.org/10.1016/j.jandt.2024.05.003>.
- [172] Z. Abbati, J. Chen, K. Cheng, F. Zhao, F. Niu, S. Tan, An experimental study of two-phase flow instability in a multi-loop natural circulation system, *Ann. Nucl. Energy* (2020), <https://doi.org/10.1016/j.anucene.2019.107269>.
- [173] S.T. Lim, K.M. Kim, H. Kim, D.W. Jerng, H.S. Ahn, Experimental investigation of two-phase natural circulation loop as passive containment cooling system, *Nucl. Eng. Technol.*, (2021), <https://doi.org/10.1016/j.net.2021.07.004>.
- [174] K.N.V. Adinarayana, P. Mangarjuna Rao, S.M. Ali, Analysis of coupled two-phase natural circulation loops by developing HEM and DFM based numerical models, *Int. J. Therm. Sci.*, (2023), <https://doi.org/10.1016/j.ijthermalsci.2023.108584>.
- [175] A. Mangal, V. Jain, A.K. Nayak, Capability of the RELAP5 code to simulate natural circulation behavior in test facilities, *Prog. Nucl. Energy* (2012), <https://doi.org/10.1016/j.pnucene.2012.06.005>.
- [176] N. Kumar, J.B. Doshi, P.K. Vijayan, Investigations on the role of mixed convection and wall friction factor in single-phase natural circulation loop dynamics, *Ann. Nucl. Energy* (2011), <https://doi.org/10.1016/j.anucene.2011.06.004>.
- [177] R.K. Shah, A.L. London, F.M. White, Laminar Flow Forced Convection in Ducts, *J. Fluids Eng.*, (1980), <https://doi.org/10.1115/1.3240677>.
- [178] R. K. Shah, "Thermal entry length solutions for the circular tube and parallel plates," *Proc. 3rd Natl. heat mass Transf. Conf.*, vol. Vol. 1. De, 1975.
- [179] R. Siegel, E.M. Sparrow, T.M. Hallman, Steady laminar heat transfer in a circular tube with prescribed wall heat flux, *Appl. Sci. Res. Sect. A* (1958), <https://doi.org/10.1007/BF03184999>.
- [180] J.P. Meyer, M. Everts, Single-phase mixed convection of developing and fully developed flow in smooth horizontal circular tubes in the laminar and transitional flow regimes, *Int. J. Heat Mass Transf.*, (2018), <https://doi.org/10.1016/j.ijheatmasstransfer.2017.10.070>.
- [181] J.A. Bocanegra, M. Misale, Lattice Boltzmann model of a square natural circulation loop with small inner diameter: working fluid effects, *J. Phys. Conf. Ser.* (2023), <https://doi.org/10.1088/1742-6596/2509/1/012007>.
- [182] J. Latt, et al., Palabos: parallel lattice Boltzmann solver, *Comput. Math. with Appl.*, 81 (2021) 334–350.